

Computed Tomography (CT)

Editors:

Kyle D. Wood, MD

Authors:

Aditya Bagrodia, MD; Juan Javier-DesLoges, MD, MS

Last Updated:

Tuesday, February 21, 2023

Keywords:

Hounsfield units, Bosniak classification

1. Technical Considerations

Computed tomography (CT) has become one of the most important and widespread tools used in urologic practice. As in the case of conventional radiographs, CT imaging takes advantage of the attenuation of x-ray photons as they pass through various body tissues. Tomography is the formation of images by serial sectioning through the use of a penetrating wave. In the case of CT, images of internal structures are created by recording the passage of x-rays as they pass through thin slices of body tissue. A computer then reconstructs cross-sectional images of the body on the basis of the differential transmission of the x-rays as they pass through internal body structures.

Godfrey Hounsfield began developing the first modern CT scanner in 1967. The first clinical CT was installed in England in 1971.¹ The 1979 Nobel Prize in Medicine and Physiology was awarded to Allan M. Cormack and Sir Godfrey Hounsfield for the development of CT.² Although basic principles remain the same, significant advances over the past 40 years have resulted in the development of multi-detector CT devices, improving soft tissue detail and allowing the possibility of rapid 3-D reconstruction of internal structures.³

1.1 Components of the CT scanner

1.1.1 X-ray Tube

A collimated x-ray beam is generated on one side of the patient, and the amount of transmitted radiation is measured by a detector placed on the opposite side of the x-ray beam.

These measurements are then repeated systematically, while a series of exposures from different projections is made as the x-ray beam rotates around the patient. Data collected by the detectors is reconstructed by computerized algorithms to result in a viewable image. X-ray tube voltages used in CT scanners range from 80 to 140 kV and tube currents can range up to 1000 mA. Currents are modulated as the tube rotates around the patient, increasing when the path length is increased (as in a lateral abdominal projection) and decreasing when the path length is decreased (as in an AP

projection).

As with conventional radiographic images, **the basis for CT images is the attenuation of x-ray photons as they pass through the patient.** In CT, a computer reconstructs a cross-sectional image of the body from measurements of x-ray transmission through thin slices of body tissue. A narrow, collimated x-ray beam is generated on one side of the patient and the transmitted radiation is measured by detectors on the opposite side. This is repeated many times as the x-ray beam rotates about the patient creating a series of exposures from different projections.⁴ Dual source CT uses two different x-ray energies produced from a rapidly alternating single tube or from two separate x-ray tubes. Different images are produced from the attenuation values generated with low- and high-energy x-rays. The information from these two images can then be combined using a subtraction algorithm. Applications for dual-energy CT include angiography and lung perfusion studies.⁵ It has also been proposed to be used for stone density assessment and renal mass characterization.

1.1.2 Detectors

The x-ray tube is rigidly attached to an x-ray detector located on the opposite side of the patient. The x-ray tube and detector scan across the subject, sweeping the beam through each axial slice. First-generation single-slice CT scanners had a single detector array, with each array containing approximately 250 individual detectors arranged in an axial plane. Newer scanners have 750 detectors or more per array.

1.1.3 Rotating Gantry

The x-ray tube and the x-ray detectors are housed in the donut shaped part of the scanner called the gantry. Slip-ring technology permits continuous rotation of the x-ray tube and detectors within the gantry. They are circular electrical conductive rings that use an antenna to wirelessly transmit radio waves to a receiver. Prior to this innovation, the scanner would have to alternate rotations to unwind the cables in the gantry.⁶ **The time for a complete rotation of the x-ray tube ranges from 0.3 to 2.0 seconds.** Since the 1970s, the rotation time has decreased from approximately 300 seconds to 0.3 seconds. **Increasing the speed of gantry rotation combined with an increasing number of detector arrays has decreased the acquisition time from 135 seconds per image in 1972 to more than 200 images per second in 2012.**

1.2 Image Reconstruction

As described above, CT creates an image of the body from measurements of attenuation collected from multiple projections around an anatomic slice of tissue. A cross-sectional view of a layer of the body is divided into many tiny blocks (**pixels**) from which a reconstructed image is displayed. A pixel, or **picture element**, is a two-dimensional representation of the amount of radiation absorbed for that location. It is a single value of attenuation (expressed visually in grayscale) that is derived from the average of all tissue densities within the corresponding voxel. The pixel size is determined by dividing the field of view by the matrix size. The typical field of view for a body scan is 40 cm. The

typical matrix size used in CT is 512 rows by 512 columns. Therefore, each pixel is approximately 0.8 mm on a side (40 cm divided by 512).³

The gray scale of each pixel on CT is a function of the amount of radiation absorbed at that point, which is termed an attenuation value, expressed in **Hounsfield units (HU)**. A voxel, or volume element, is a three-dimensional element determined by the product of pixel size and slice thickness. Several imaging variables are adjusted to allow adequate, detailed image resolution, while minimizing the time on the scanner and limiting exposure to radiation. The variable application of pitch, beam collimation, detector size, and tube voltage are used by the radiologist and imaging technologist for ideal image requisition.⁷

1.3 Hounsfield units

The value for each pixel is called a Hounsfield unit (HU) or CT number. The attenuation value assigned to each pixel is based on a reference scale for which the density of distilled water at standard temperature and pressure is defined as 0 HU. Air is assigned the value of -1000 HU and +1000 HU is assigned to dense cortical bone (though bone can range from +400 to +1000). The attenuation of lung from -600 to -400, fat ranges from -100 to -60, that of blood from +30 to +45 and soft tissue from +40 to +80.⁸ Some kidney stones can have HU > 1000.⁴

1.4 Window Width and Level

The operator can adjust the appearance of the image by selecting the number of shades of gray (**window width**) as well as the shade of gray corresponding to the middle shade within the scale (**window level**).⁴ By changing window width and window level, image contrast can be optimized for evaluating structures of various densities (lung, bone, kidney, etc.). HU above the chosen range are displayed as white and those below the range are displayed as black.

1.5 Pitch

Pitch is defined as the ratio between the distance the table travels during one gantry rotation and the width of the x-ray beam. Typically, the pitch varies between 0.7 and 1.5.⁹ If the pitch is equal to 1 - the table travel equals the beam width - there is uniform coverage with no gaps. If the pitch is less than one, then the table travel is less than the beam width and there is overlap in radiation coverage. Therefore, there is better resolution but higher patient dose. If the pitch is greater than one, then the table travel is greater than the beam width and there are gaps in coverage.⁶ In this situation there is decreased patient dose, but lower resolution.

1.6 3D Reconstruction



Figure 1: Normal coronal reconstruction during excretory phase of CTIVP. Bone windows are used to better visualize the collecting structures.

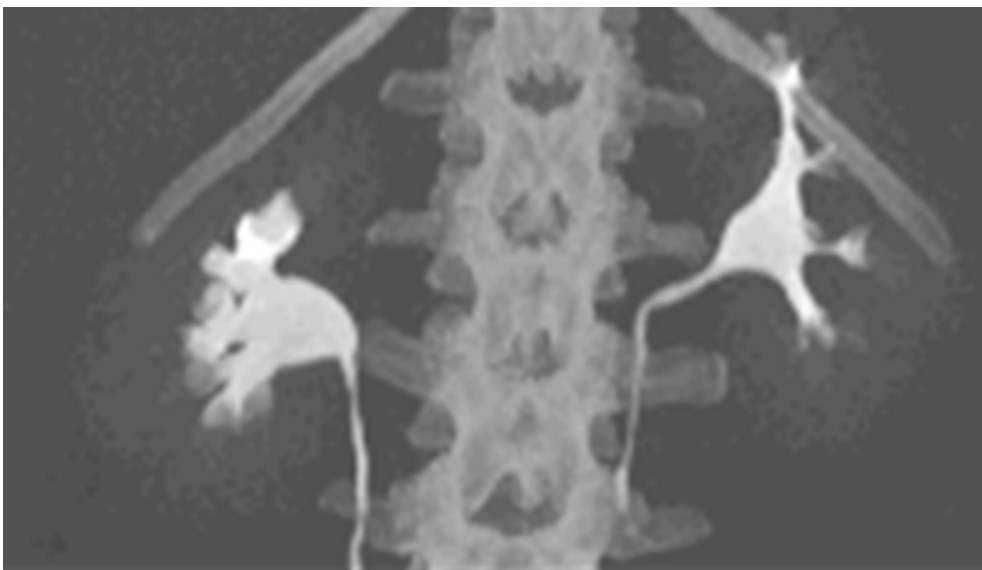


Figure 2: Normal coronal maximum intensity projection showing excretory calyceal opacification phase

Multiplanar reconstruction or reformatting (MPR) is a technique used to create new images in planes orthogonal to that of the original scanned volume (typically sagittal and coronal cross-sections). This method of reordering voxels - in planes other than the one originally acquired during the scan - forms the basis for other 3D reconstructive techniques. Since data on the entire volume of the scanned object is obtained, it is even possible to obtain images in oblique or curved planes.

Shaded surface display (SSD) is an imaging modality that uses differences between the density of

the surface to be mapped and surrounding tissues to create a 3D contour of the object being studied. A threshold attenuation value is chosen corresponding to the boundary between the object and its surrounding tissues. Voxels at this interface are selected and then connected to map the surface of the object. A virtual light source is used to create contrast and shading.¹⁰ Surface rendering is also the basis for virtual endoscopy. Voxels at the edge of a tubular structure like the colon, airway or blood vessels are identified and the remaining voxels are subtracted out. Specific algorithms are then used to create a virtual colonoscopy, bronchoscopy or angiogram that can be navigated by the user.¹¹

Another technique called **maximum intensity projection** displays the pixels of greatest intensity along individual x-ray paths (**Figure 2**). It is useful for the depiction of bone and contrast-filled blood vessels where there is a large difference between the attenuation of these structures and the surrounding tissues. MIP is useful for CT angiography and has also been used for CT urography.¹¹ A similar technique called minimum intensity projection selects the minimum attenuation value along the x-ray path. This is useful for delineating structures filled with lower attenuation material such as bile ducts, the pancreatic duct or the bronchial tree.¹²

Volume rendering is distinct from other 3D techniques in that the entire set of CT data is used to generate images. From any viewing angle, a weighted sum of the attenuation values of all voxels along that line is calculated. Each voxel is assigned an opacity level that determines its relative contribution to the sum.¹³ Unlike SSD and MIP, which use only a small fraction of the available data, 3D volume rendering does not distort structures in the reconstructed planes. As a result, detailed anatomic relationships are preserved and procedures such as partial nephrectomy and donor nephrectomy can be performed with more accuracy and fewer complications.¹⁴

1.7 Types of CT Scanners

Initial **single-slice** machines would rotate the x-ray source and detectors around a stationary object. Following a complete rotation, the object would be moved along its axis, and the next rotation started. Newer machines permitted continuous rotation with the object to be imaged slowly and smoothly slid through the x-ray ring. These are called **helical or spiral CT** machines.² A subsequent development was **multi-detector CT (MDCT)**. Instead of a single row of detectors, MDCT uses multiple rows of detectors capturing multiple cross-sections simultaneously. In the late 1990s, four-slice MDCT was introduced into clinical practice. It produces four images per rotation of the x-ray tube. The early 2000s brought the advent of successively more detector arrays. MDCT with 64 arrays are in common use today and even 320-row scanners are used for certain applications.

1.8 Dual Modality (PET-CT)

Nuclear medicine applications such as positron emission tomography (PET) often lack anatomic detail. **Coregistration of PET with another imaging modality like CT allows for better localization of lesions**. Instead of x-rays produced by an x-ray tube, PET uses rings of detectors that absorb photons produced by injected radiopharmaceuticals. In the case of PET/CT the most

commonly used radionuclide is ^{18}F in the form of the radiopharmaceutical fluorodeoxyglucose (FDG). The patient passes through a gantry that houses both PET and CT imaging systems. While CT images are created, regions of increased radiopharmaceutical uptake are recorded by the PET scanner. Unfortunately, many radiopharmaceuticals are concentrated in the urine, rendering them ineffective for urologic applications. Other agents, such as ^{11}C -choline, have low urinary excretion and may be more useful for assessment of prostate cancer.¹⁵

1.9 Artifact

By definition, an **artifact** is a discrepancy between the attenuation coefficients of the reconstructed image and those of the object being imaged.¹⁶ Several different types of artifacts can degrade CT image quality. Artifacts can be caused by patient factors (e.g. patient movement or presence of metallic implants), errors in scanner calibration, or even effects such as beam hardening which occur as a result of the same physical properties that make CT scanning possible. In a study of almost 7200 CT scans performed during a one-year period at a single institution, 432 scans (6%) had to be repeated due to the presence of a major artifact.¹⁷

1.10 Motion

Motion artifacts are caused when the patient moves, either voluntarily or involuntarily. Patient motion often results in a streak artifact or shading artifact. Motion artifact can be reduced by decreasing scan time or by asking patients to hold their breath for the duration of the scan. In some cases, sedation may be necessary. Scanner settings can be adjusted as well. Overscanning is a technique in which additional measurements are taken at the beginning and end of a 360° rotation. Data from these repeated images are averaged with the initial ones. Cardiac gating can help to minimize the artifacts created by the rapid motion of the heart.¹⁸

1.11 Beam Hardening

When x-ray photons pass through dense tissue, lower energy x-rays are absorbed while higher energy x-rays are able to pass through the object. This **preferential attenuation of the lower energy photons results in an upward shift of the average energy reaching the detectors, and thus, an artificial underestimation of the attenuation coefficient for that region**. Beam hardening can result in dark streaks or shadowing.¹⁹

1.12 Partial-Volume Averaging

This artifact results from the assumption that each voxel is homogenous in composition. If a voxel contains tissues of different densities, then an average is taken to obtain one attenuation coefficient. The volume-averaging phenomenon can be corrected for by using thinner slices. This makes voxels smaller and decreases the heterogeneity of a given volume. Viewing the affected region in another projection can also rule out potential partial volume artifacts.¹⁶

2. Adverse Effects

The International Commission on Radiological Protection (ICRP) provides periodic recommendations on radiation exposure protection for radiation workers, patients and members of the general public. Occupational radiation dose limits in the US are set by the National Council on Radiation Protection and Measurements (NCRP). **The legal effective dose limit for any single year is 50 mSv, though both the ICRP and NCRP recommend a dose limit of 20 mSv per year, averaged over 5 years.** This excludes any medical procedures the worker might undergo and natural background radiation.²⁰ While the gray (Gy) and sievert (Sv) both express the amount of radiation energy absorbed per kilogram of mass, the sievert specifically refers to the biological equivalent dose absorbed by human tissue.

The objective of radiation protection is to reduce the risk of cumulative exposure to ionizing radiation. Increased radiation exposure leads to a higher risk of cancer, acquiring genetic defects and developing tissue-specific problems such as cataracts. Furthermore, radiation exposure during pregnancy can have teratogenic effects on the fetus.²¹ Radiation workers only receive significant exposure when they are standing close to the patient (patient scatter) or the x-ray source (leakage radiation). Personnel monitoring devices must be worn to ensure that individuals stay below the dose limit and to monitor an institution's radiation safety practices.

Lead aprons are a very good protective barrier for radiation workers. A typical lead apron is constructed from lead-impregnated vinyl and weighs about 10 pounds. It has 0.5 mm of lead equivalents and attenuates at least 90% of x-rays. Lead aprons must be stored properly (avoiding folding) and tested annually with fluoroscopy to check for cracks, though there is little consensus on what criteria should be used for discarding unsuitable lead aprons.^{22,23} In addition to lead aprons, operators should wear: a neck shield to reduce the dose to the thyroid, **leaded glasses** to decrease the risk of developing cataracts and **leaded gloves** if the hands are placed directly into the x-ray beam. Operators should **avoid being in the room unless it is necessary to perform the given study.** If the operator must be present (as is the case for many fluoroscopy studies), **distance from the radiation source should be maximized and fluoroscopy time minimized.** Despite the emphasis placed on radiation safety, a recent survey demonstrated that the use of protective equipment and radiation monitoring devices was insufficient among urology residents and fellows.²⁴

Room shielding is another factor that must be considered for operator protection. Radiation barriers are designed with attention to the following: **the amount of time the machine is in use, the distance from the x-ray source to the operator, the proportion of time that the energy source is directed towards the operator and the fraction of time that an operator is present behind the barrier .**

3. Pregnancy

3.1 Pregnant Radiation Workers

The ICRP recommends a limit of **1 mSv of exposure from the declaration of pregnancy by a radiation worker until the birth of the child.**²⁵ The NCRP, however, sets that limit at **0.5 mSv per**

month, or a total of 5 mSv for the duration of the pregnancy.²⁶ Nevertheless, the average amount of background radiation that a person is exposed to is **3 mSv per year, while the exposure to a fetus is 0.5-1.0 mSv over the course of a normal gestation.**²⁷ Pregnant radiation workers are recommended to wear a dosimeter on the abdomen underneath their lead aprons in order to monitor the fetal radiation dose. **Double-thickness lead aprons** are available for pregnant workers. These have been shown to significantly decrease the under-lead radiation dose, though the absolute benefit is small and may not be necessary for all workers.²⁸ Despite the importance of this topic, written guidelines and national consensus statements on this topic are lacking.²⁹

3.2 Pregnant Patients

According to the consensus statements from major national and international organizations, the risk of deterministic effects (e.g. miscarriage or teratogenic effects) appears to be **negligible in fetuses exposed to radiation levels at or below a threshold of 50 mGy (50 mSv).**^{30,31,32,33} Nevertheless, experts emphasize that deterministic effects (a cutoff value exists; severity depends on dose) should not be confused with stochastic effects (a cutoff value does not exist; probability, but not severity, depends on dose).³⁴ In the stochastic model, there is a cumulative increase in the lifetime probability of developing cancer based on total absorbed radiation dose and, by definition, there is no safe threshold value.³⁵ Thus, many studies stress the **ALARA principle (As Low As Reasonably Achievable)**, advocating no more radiation exposure than is necessary to come to a satisfactory diagnosis.³⁶ One recent study found that the average fetal radiation dose from a CT scan of the abdomen and pelvis was approximately 25 mGy, and only one scan of the 86 exceeded the 50-mGy threshold.³⁷ Another study, investigating a total of 435 abdominopelvic CT scans, showed that average to be approximately 17 mGy. This study also demonstrated a 90% increase in the use of such CT scans in pregnant women from the years 1997-2001 to 2002-2006.³⁸ A low dose stone protocol CT scan has become a useful imaging modality for pregnant patients with suspected nephrolithiasis (for whom renal ultrasonography has been inconclusive). This type of CT delivers a lower average fetal radiation dose (approximately 10 mGy) because the tube current can be decreased and the pitch increased when looking for **high-contrast kidney stones**. Furthermore, once the patient thickness exceeds 25 cm (which would be very common in the second and third trimester), a four-view IVP actually delivers more radiation to the fetus.³⁹

In accordance with the guidelines from the **American College of Obstetricians and Gynecologists (ACOG)**, with few exceptions, radiation from a CT scan or nuclear medicine is at a dose much lower than the exposure that would be associated with fetal harm.⁴⁰ Therefore, if these studies are needed and more readily available, they should not be withheld from a pregnant patient.

4. Children

The use of CT in the evaluation of pediatric patients has **increased** considerably over the last 20 years.⁴¹ Furthermore, children are **more sensitive** than adults to the same radiation dose and have a longer lifespan to develop radiation-induced cancers.³³ One study estimated that of the 600,000

abdominal and head CT scans performed annually in the US on children under the age of 15, 500 would lead to a cancer death.⁴² Another study found a similar projection: the 4 million pediatric CT scans performed annually in the US would result in 4870 future cancers. This study also demonstrated that the lifetime risk of developing a solid organ tumors or leukemia was **greatest for female patients and younger patients.**⁴¹

Applying the ALARA principle is especially important in the pediatric population. The clinician should confirm that the CT scan is necessary and consider alternative imaging modalities such as US and MRI. The region of coverage and the number of phases (pre- and post-contrast scans) should be limited appropriately. **The individual CT settings should be adjusted based on indication and the size of the child.** Areas that are especially radiation sensitive such as thyroid, breast and gonads should be shielded when possible.⁴³ In one of the studies mentioned above, it was estimated that reducing the highest quartile of radiation doses down to the median level would prevent 2090 (43%) of these radiation-related cancers.⁴¹ Furthermore, it has been suggested that up to one third of CT scans are not medically necessary.⁴⁴ Eliminating these unnecessary scans would further reduce the number of cancers by 930 (19%), resulting in a 62% total reduction in radiation-attributable cancers by combining these two strategies.

5. Iodinated Contrast Agents

Pioneering work on the first iodinated contrast agents (ICAs) was done in the late 1920s and early 1930s. Moses Swick, a urologist, is credited with developing the first iodinated contrast agent for intravenous urography, though several others were working on similar agents at that time.⁴⁵ ICAs were then introduced into clinical practice in the 1950s. Since that time they have become the most widely used class of contrast agents in the world. These agents share a **common functional group – a tri-iodinated benzene ring.** The relatively large size of the iodine atoms, held in close proximity to the other iodine atoms by the benzene ring, makes ICAs very effective attenuators of x-rays.⁴⁶ ICAs come in 4 varieties: ionic monomer, ionic dimer, nonionic monomer, and nonionic dimer. **Ionic monomeric ICAs**, such as diatrizoate (Hypaque), consist of one tri-iodinated benzene ring with a carboxylate group substituent providing the ionic charge to the compound. **Ionic dimeric agents**, such as ioxaglate (Hexabrix), consist of two tri-iodinated benzene rings linked by an organic functional group. These also contain at least one carboxylate group substituted on one of the benzene rings. **Nonionic monomeric ICAs**, such as isohexol (Omnipaque), contain one iodinated benzene ring without a charged carboxylate group. **Nonionic dimers**, such as iodixanol (Visipaque), contain two tri-iodinated benzene rings linked by an organic functional group with no carboxylate group substituent. Ionic agents can disrupt the electric potential of cell membranes, which accounts for their **relatively higher toxicity** compared to nonionic agents. Ionic monomers also provide the weakest x-ray attenuation and must, therefore, be administered in a concentration that is significantly higher (1500-2400 mOsm/L) than that of blood (280-290 mOsm/L). It is for this reason that ionic monomers are also referred to as **high-osmolarity contrast agents**. Ionic dimers and nonionic monomers are considered **low-osmolarity agents** with an osmolarity ranging from 290 mOsm/L to

860 mOsm/L. Nonionic dimers are iso-osmolar with blood.⁴⁶

Contrast agents that do not contain iodine have been investigated.⁴⁷ Of the non-iodinated compounds that have been explored, **gadolinium-based agents** seem to hold the most promise. Several studies have investigated their use for angiography in patients for whom ICAs were absolutely contraindicated.⁴⁸ The images obtained with these agents seemed to be adequate, though the operator is limited to a much smaller concentration and total deliverable volume than with ICAs.⁴⁹

5.1 Idiosyncratic (allergic-like) Reactions

Although the vast majority of adverse reactions to ICAs are mild and self-limiting, they are fairly common - with some studies showing rates as high as 15%. **Lower osmolarity ICAs have a much better safety profile (approximately 3% rate of adverse reactions)**, but clinicians must still be aware of the risks involved in studies that use iodinated contrast.⁵⁰ There are several factors that can predispose an individual to severe contrast reactions. Patients with **asthma** have a 6-fold increased risk with low-osmolarity ICAs and a 10-fold increased risk with high-osmolarity agents. Individuals with a **history of adverse reaction to ICAs** have a 5-fold risk and those with atopy/allergy have a 3-fold risk.⁵¹ Shellfish allergy does not seem to confer any more risk than other food allergies. Iodine itself cannot be an allergen – it is a ubiquitous element and is essential for life.⁵² Individuals who are allergic to shellfish are often reacting to a class of muscle proteins called **tropomyosins**, and not iodine. These are found in crustaceans and mollusks, but not scaled fish.⁵³

Acute reactions to contrast agents occur within one hour of use. The severity of these reactions can range from mild (pain at the injection site, nausea, rash) to severe (bronchospasm, laryngeal edema and hypotension). In one large Japanese study, severe acute reactions occurred about five times more frequently after the administration of ionic, high-osmolarity agents than with a low-osmolarity or iso-osmolar agent (0.22% versus 0.04%).⁵⁴ A review of several large studies found that the rate of severe reactions ranged from 0.02% to 0.5%.⁵²

Although exceedingly rare, deaths have occurred from administration of ICAs as well. One large series reported four deaths in 300,000 patients who underwent intravenous urography over a 20-year period (0.0013%).⁵⁵ A systematic review of the literature found a similarly low range of 0.0006-0.006%.⁵²

As with oral administration of contrast media, contrast reactions via direct injection (into the bladder, ureter or renal collecting system) have been reported, though are extremely rare.⁵⁶

The first step in treatment of contrast reactions is to **prevent** them from occurring in the first place. Employing other imaging modalities (US, MRI or non-contrast CT) is obviously the safest way to do this. If ICAs must be used, ionic monomeric (high-osmolarity) agents should be avoided in patients with any of the above risk factors (asthma, atopy, history of contrast allergy). As mild reactions are often self-limiting, treatment is centered on symptom management: **administration of antiemetics for nausea and vomiting, corticosteroids and antihistamines for rash and pruritus, IV fluids and possibly mild vasopressors for hypotension, and atropine for hypotension with**

bradycardia (vagal reaction). For patients with a severe acute reaction, management is the same as a cardiopulmonary arrest – **maintain airway, breathing and circulation.**⁴⁶ **Epinephrine** should be administered and is considered the treatment of choice (whether these reactions are anaphylactic or anaphylactoid).⁵⁷

Patients at risk for acute contrast reactions may be **pretreated with corticosteroids**. One study found no significant difference in the rate of acute reaction with oral administration of a single dose of 32 mg of methylprednisolone 2 hours prior to injection of the ICA.⁵⁸ However, another study demonstrated a significant reduction (1.7% versus 4.9% for placebo) in the overall rate of acute contrast reactions with two doses of 32 mg of methylprednisolone (one given 6-24 hours prior to contrast injection and another given 2 hours prior).⁵⁹ As a result of these and similar findings, many institutions now give at least two pretreatment doses of corticosteroids separated by several hours, with or without the administration of antihistamines.^{59,60}

Delayed reactions to ICAs can also occur. These reactions take place between one hour and one week after administration of the contrast agent. Symptoms are similar to an acute reaction and can include nausea, vomiting, diarrhea and hypotension, however cutaneous symptoms (pruritic rash or urticaria) are the most frequent finding. Delayed contrast reactions are often milder than acute reactions, but are fairly common with one study reporting rates as high as 14.3% (compared to 2.5% reported in the non-contrast arm control arm).⁶¹ While acute reactions are more likely to occur with ionic monomers, delayed reactions are approximately 3 times more likely with iso-osmolar agents (nonionic dimers) than with nonionic monomers or ionic dimers.⁶² In addition to the use of a nonionic dimer contrast agent, risk factors for this type of reaction include: **prior reaction to an ICA, concurrent treatment with interleukin 2, and possibly sun exposure.**^{61,63}

5.2 Nephrotoxicity

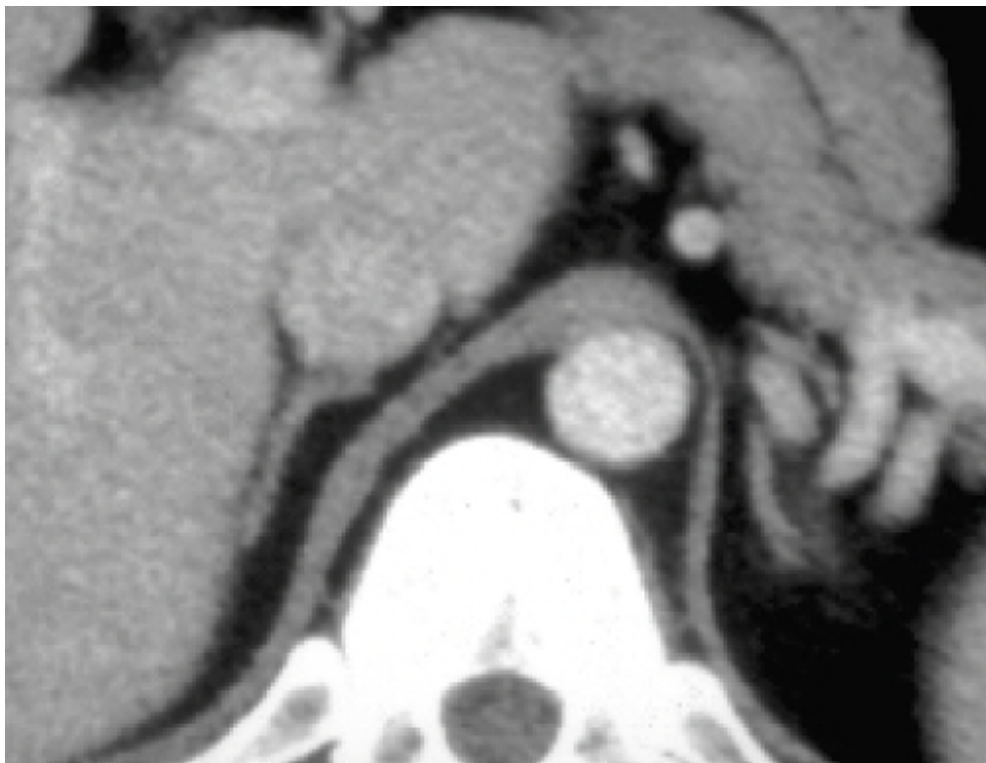
Contrast-associated nephropathy (CAN) is defined as a greater than 25% increase in serum creatinine within 3 days of administration of an ICA (once other possible etiologies have been ruled out). **Preexisting renal impairment** carries the greatest risk for development of CAN. In one study looking at patients undergoing angiographic procedures, the risk of post-contrast creatinine elevation was 2%, 10% and 62% for patients with a baseline creatinine of less than or equal to 1.2 mg/dL, 1.3 to 1.9 mg/dL and greater than or equal to 2.0 mg/dL, respectively.⁶⁴ Other risk factors include **higher patient age and comorbidities such as diabetes and hypertension** that predispose an individual to poor renal function. Conditions that result in diminished cardiac output such as **dehydration, severe hemodynamic instability, CHF, or a recent MI** can cause CAN as well. Administration of **nephrotoxic drugs** such as aminoglycosides or drugs that affect renal perfusion such as NSAIDs or ACE inhibitors also increase the risk of developing CAN.⁶⁵ High osmolarity agents (ionic monomers) seem to be the most nephrotoxic.⁵¹ However, it is unclear if low osmolarity agents or iso-osmolar agents confer the greater risk to renal function.⁶⁶ The risk of CAN also appears to be proportional to the administered volume of the ICA.⁶⁷ One study showed a 12% increase in the likelihood of nephropathy per each additional 100 mL of contrast used.⁶⁸ Nevertheless, it is important to note that

the vast majority of studies investigating CAN involve intra-arterial contrast administration. A link between intravenous contrast administration and CAN has not been clearly demonstrated.⁶⁹

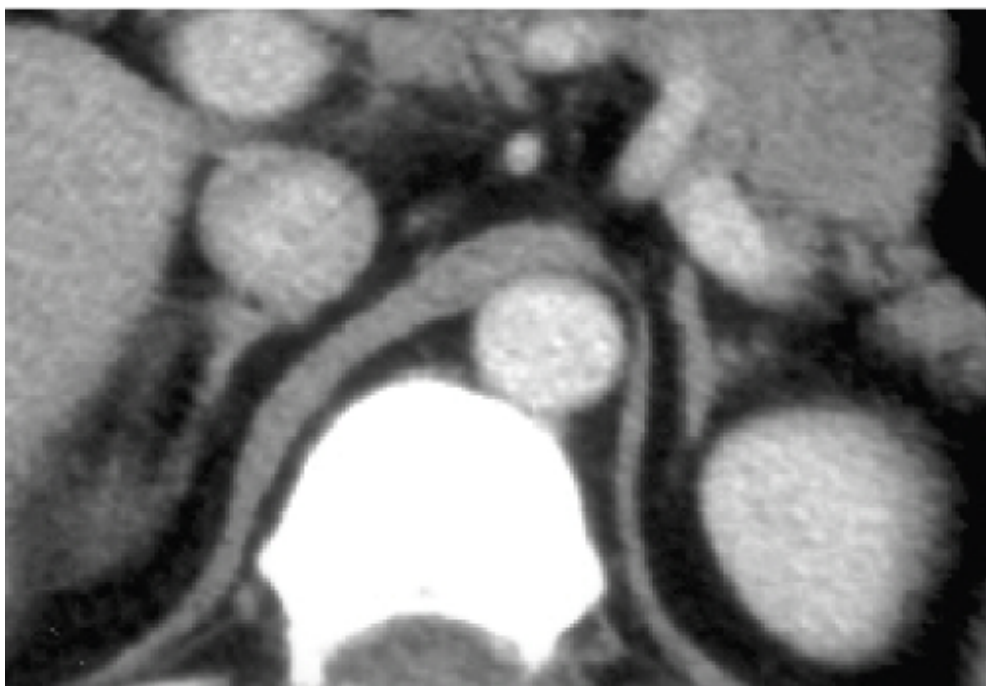
The use of hydration to avoid CAN is controversial and there is no conclusive evidence to support that prophylactic intravenous fluid administration is effective in preventing CAN. In a recent study published in the Lancet in 2017, in a randomized trial 660 patients with CKD Stage IIIa or IIIb CKD were assigned to prophylactic intravenous isotonic saline or no fluids. Prophylactic volume expansion did not reduce the incidence of acute kidney injury (2.7% vs 2.6%).⁷⁰ In a second randomized trial published in 2014, evaluating 139 patients with mild to moderate CKD, patients were randomized to sodium bicarbonate and no fluids, and the incidence of AKI was not statistically significant AKI.⁷¹

Use of N-acetylcysteine as prophylaxis against CAN has shown mixed results.⁷² A 2004 meta-analysis showed no clear benefit to its use,⁷³ while a 2009 meta-analysis demonstrated a benefit to high-dose N-acetylcysteine administration.⁷⁴ Although no clear guideline exists, most experts agree that N-acetylcysteine use is warranted since it is safe, inexpensive and may reduce the risk of CAN.^{46,72}

6. Clinical Applications



3A



3B

Figure 3: Normal coronal reconstruction during excretory phase of CTIVP. Bone windows are used to better visualize the collecting structures.

1/ 24/ 2001

3/26/ 2001

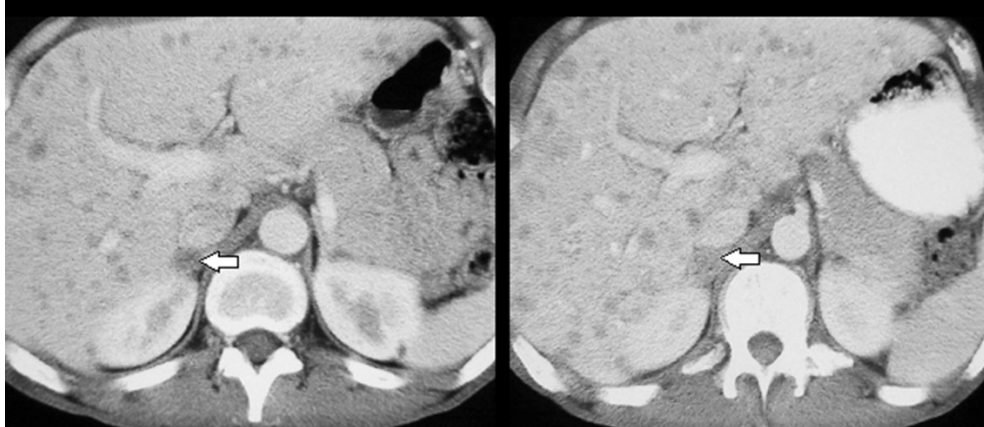


Figure 4: Enlarging right adrenal metastatic lesion (white arrows) over 2 month time interval. Diffuse hepatic metastases also present

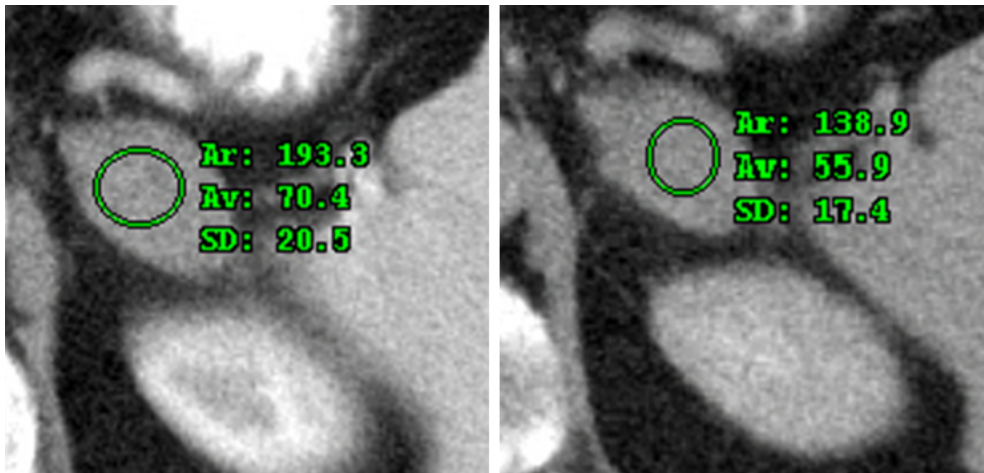


Figure 5: Metastatic left adrenal lesion from lung primary. Washout is well below 50 % on 15 minute delayed image

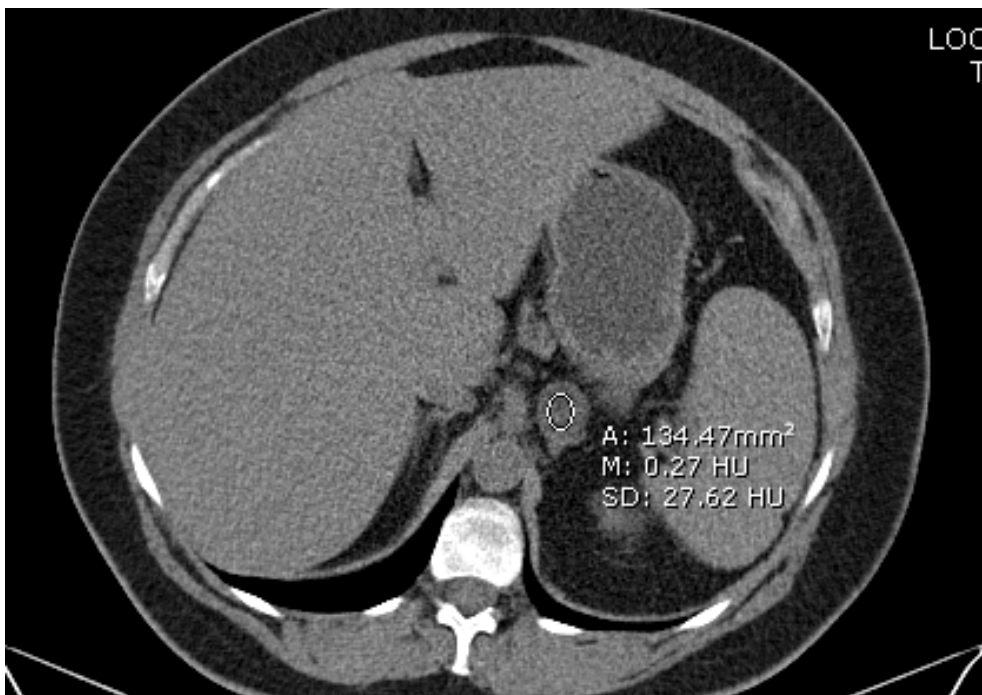


Figure 6: Cortical adrenal adenoma measures essentially 0 HU
noncontrast, diagnostic for a benign adenoma



Figure 7: A. Normal appearing, but functionally hyperplastic
adrenal glands in patient with Cushings as evidenced by the
excessive mediastinal fat on the chest CT (star) B

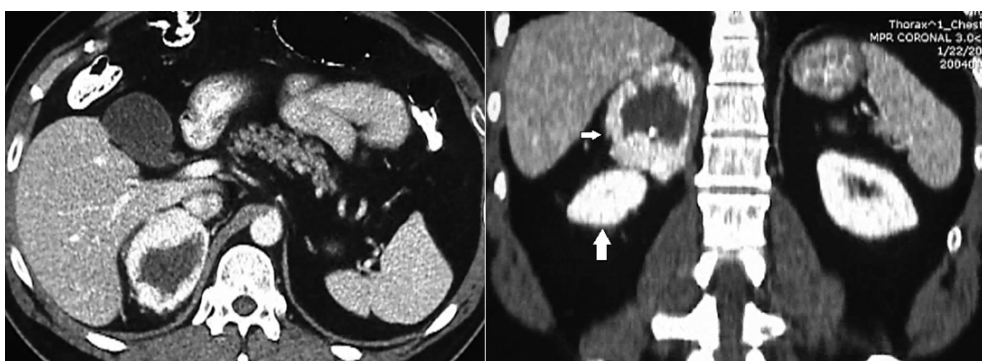


Figure 8: Axial and coronal reconstruction of large partially necrotic
right adrenal pheochromocytoma. Coronal images better define
the separation of right kidney (large arrow) and adrenal
pheochromocytoma (small arrow)

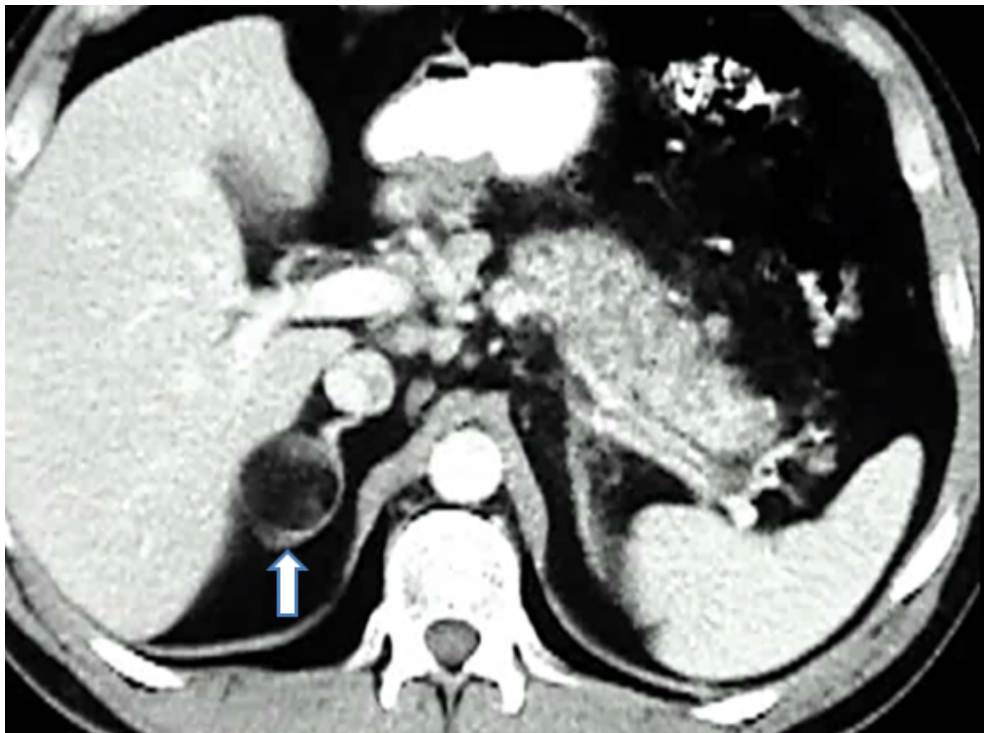


Figure 9: Classic right adrenal myelolipoma (arrow) with dark gross fat essentially black and similar to retroperitoneal fat on enhanced CT



Figure 10: Adrenal pseudocyst secondary to hemorrhage during pregnancy. Lesion is indistinguishable from malignancy on CT, but resolved on follow up imaging.

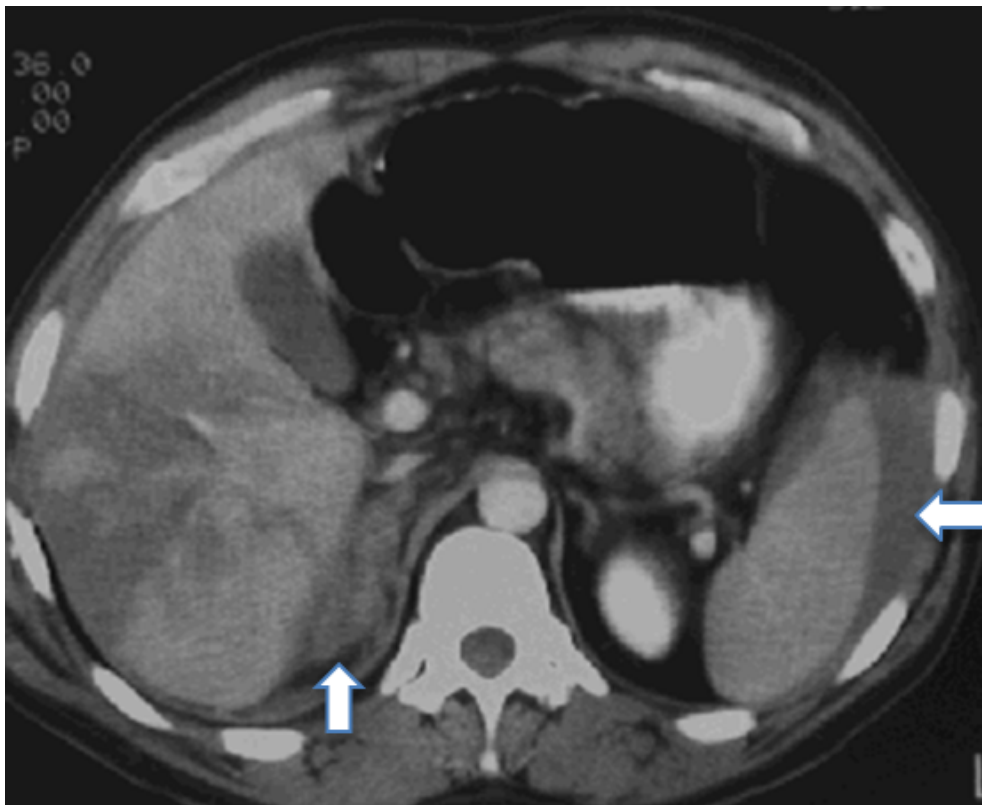


Figure 11: Traumatic adrenal hemorrhage with heterogeneous enlargement of right adrenal (vertical arrow). Hepatic injury and free fluid around spleen (horizontal arrow) also present

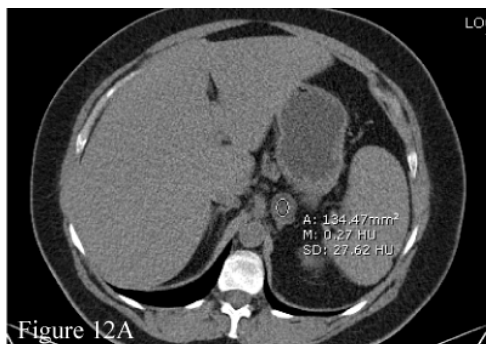


Figure 12A



Figure 12B

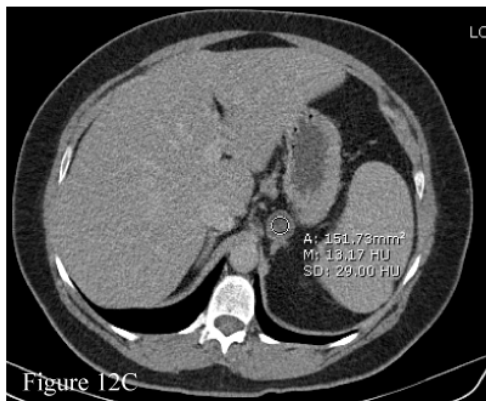


Figure 12C

Figure 12A, 12B and 12C: Adrenal study with unenhanced HU of “0”, enhanced HU 45 and 15 min delayed HU of 10. Relative washout is 71% and absolute washout is 71%. They are the same

as the unenhanced value was 0. In this case the unenhanced HU of 0 was diagnostic of benign lipid rich adenoma and the full adrenal protocol was not needed.

6.1 ADRENAL

6.1.1 Anatomy

The adrenal glands are generally imaged by CT in three clinical scenarios: 1) when hormone excess is suggestive of a functional adrenal mass, 2) in the setting of suspicion of metastatic disease to the adrenal glands, and 3) when adrenal lesions are found incidentally on imaging studies performed for other reasons. Although additional imaging modalities may be employed to determine the nature of an adrenal mass, CT remains a very important tool for assessment of these lesions.¹⁹

The adrenal glands are located in the retroperitoneum within Gerota's fascia and the perirenal fat. Each adrenal gland is enclosed within a fibrous capsule and is composed of a cortex and medulla. Directly beneath the capsule is the cortex, which contains three zones: the zona glomerulosa, the zona fasciculata, and the zona reticularis. The function of the zona glomerulosa is the production of mineralocorticoids, predominantly aldosterone. Beneath the zona glomerulosa is the zona fasciculata, which produces glucocorticoids such as cortisol. The inner layer of the cortex, the **zona reticularis**, produces sex steroids - adrenal estrogens and androgens such as dehydroepiandrosterone and androstenedione. The adrenal medulla contains chromaffin cells that are responsible for synthesis of epinephrine and norepinephrine.⁷⁵

The right adrenal gland is usually pyramidal in shape, while the left is more crescent-shaped. The right adrenal gland lies posterolateral to the IVC between the right crus of the diaphragm and underneath the liver. The medial aspect of the right adrenal can be retrocaval (**Figure 3**).

The left adrenal gland is lateral to the aorta, posterior to the body of the pancreas and the splenic vessels, and anterior to the diaphragm. The left adrenal gland is often more elongated than the right adrenal gland and will lie in a more superomedial position relative to the kidney. This places the gland closer to the left renal hilum, an important relationship to remember during dissection.¹⁹

The right adrenal vein enters the IVC posterolaterally, while the left adrenal vein enters the left renal vein from a cranial direction. Accessory adrenal veins are present in 5-10% of individuals and drain into the right renal vein, the right hepatic vein or the inferior phrenic vein.⁷⁶ The arterial blood supply is variable but generally receives contributions from the inferior phrenic artery (superior adrenal artery), aorta (middle adrenal artery) and renal artery (inferior adrenal artery). The main adrenal arteries then divide to form a subcapsular plexus. From this plexus some branches continue directly to the medulla, while others supply the cortex. On the venous side, medullary veins join to form the **main adrenal vein**. The lymphatic drainage of the adrenal glands is primarily through the paracaval lymph nodes on the right and the para-aortic lymph nodes on the left. The autonomic innervation of the adrenal glands is predominantly via preganglionic sympathetic fibers off the sympathetic trunk (leading directly to the chromaffin cells of the adrenal medulla). Postganglionic fibers originating from

the splanchnic ganglia provide innervation to the adrenal cortex. Parasympathetic innervation to the adrenal gland is not well defined.

6.1.2 Congenital Absence and Congenital Hypoplasia

Congenital absence or hypoplasia of the adrenal glands is very rare. Although it has only been described in limited case reports and case series, the existence of this entity has led to the discovery of several genes essential for gonadal and adrenal development. Genetic analyses of patients with X-linked adrenal hypoplasia congenita (AHC) have led to the discovery of mutations in DAX1 (Dosage-sensitive sex reversal-Adrenal hypoplasia congenita critical region on the X chromosome gene 1) and SF1 (steroidogenic factor 1), a downstream target of DAX1.⁷⁷ Patients with X-linked AHC have been shown to have small bilateral adrenal glands on CT.^{78,79}

6.1.3 Congenital Adrenal Hyperplasia

Congenital adrenal hyperplasia (CAH) is far more common than congenital hypoplasia or congenital absence of the adrenal glands. It occurs between 1 in 5,000 and 1 in 15,000 births.⁸⁰ The vast majority of cases of CAH result from a deficiency of 21-hydroxylase, though CAH can be caused by a defect in 11-hydroxylase, 17-hydroxylase, the cholesterol side chain cleavage enzyme, or 3 β -hydroxysteroid dehydrogenase. The resultant decrease in cortisol and the increase in ACTH enhances formation of adrenal steroids proximal to the enzymatic defect. This, in turn, causes a secondary increase in the formation of testosterone. **Because CAH is usually diagnosed soon after birth, there is little role for CT imaging.** Smaller CT imaging studies of patients with untreated or under-treated CAH have demonstrated **diffuse or nodular enlargement of the adrenals, with preservation of normal adrenal shape.**⁸¹ However, one study of older patients with CAH (mean age 28), demonstrated CT evidence of hyperplasia in only 40% of cases.⁸² Other reports have shown that individuals with CAH may develop neoplasm-like growths in the adrenal glands. These lesions may or may not regress with subsequent treatment of the underlying condition.

6.1.4 Adrenocortical Carcinoma

Adrenocortical carcinoma (ACC) is very rare with an incidence of approximately 1 per million. ACC has a bimodal age distribution that peaks in children in the first decade of life and adults in the fourth to fifth decades of life (with a slight female predominance). The majority of ACCs are sporadic and unilateral, however, several hereditary disorders are associated with an increased risk for ACC, including Li-Fraumeni syndrome and Beckwith-Wiedemann syndrome. Adrenal hyperfunction has been associated with 50-79% of adult ACC and up to 90% of pediatric cases.

CT findings of ACC include irregular borders and large size (average size 10-12 cm, with over 90% greater than 5cm). Central necrosis and irregular calcifications are commonly observed, and focal areas of fat are also occasionally reported. Noncontrast CT demonstrates increased attenuation compared to adenomas (39 HU versus 8 HU). Postcontrast CT demonstrates nodular regions of enhancement with central hypoperfusion and delayed washout. Tumor thrombus in the renal vein or IVC is frequently seen, as is direct invasion into adjacent structures. Metastases to regional lymph

nodes, lung, liver and bone are common at presentation.^{83,84}

6.1.5 Neuroblastoma

Neuroblastoma is the most common extracranial solid tumor of childhood, accounting for 8-10% of all childhood cancers. A recent review showed a median age at diagnosis of 19 months: 89% of patients were younger than 5 years, and 98% were diagnosed by age 10. Neuroblastoma arises from cells of the neural crest that form the adrenal medulla and sympathetic ganglia. Thus, tumors may occur anywhere along the sympathetic chain within the neck, chest, retroperitoneum, pelvis, or in the adrenal gland. Primary tumors arise in the adrenal gland in 50% of cases, retroperitoneal sympathetic ganglia in 30%, and in cervical and thoracic ganglia in the remaining 20%.

Children with a large abdominal mass will invariably undergo CT imaging. These studies play an important role in the evaluation of neuroblastoma. Imaging provides more information about the **local extent of the primary tumors** and can help guide management. CT findings, such as stippled calcifications are suggestive, though not diagnostic of neuroblastoma. Invasion of the renal parenchyma is not common, but it can be detected by CT as well. **In a study comparing CT imaging characteristics of neuroblastoma to Wilms tumor - the second most common extracranial solid tumor of childhood - encasement of vessels, spinal canal invasion or a paravertebral mass were more suggestive of neuroblastoma.**^{85,86,87,88,89}

6.1.6 Metastatic Tumors

Metastases to the adrenals are common in patients with solid organ malignancies. One large autopsy study found adrenal metastases in 27% of patients with epithelial malignancies (**Figure 4**). The most commonly cited primary tumors are **non-small carcinoma of the lung, breast adenocarcinoma and melanoma, though many others have been reported including colorectal, renal, stomach, esophagus and liver**. On CT, these lesions tend to be heterogeneous in appearance and lobulated in shape with less well-defined borders. Similar to ACC, the larger the mass the more likely it is to be malignant. Metastatic lesions can also demonstrate cystic changes with thick, irregular, contrast-enhancing walls. Metastases less than 3 cm in size are more often homogeneous, round and well defined and, thus, difficult to differentiate from benign adenomas (**Figure 5**).⁹⁰

6.1.7 Cortical Adenoma

Adenomas of the adrenal gland are benign, usually non-hypersecretory and fairly common. A review of several large autopsy series demonstrated an overall frequency of 6%. **Most adrenal masses are discovered on imaging obtained for other indications and the vast majority of these are ultimately proven to be adenomas** (**Figure 6**). Several studies looking at the prevalence of adrenal masses found incidentally on CT showed a similar prevalence of approximately 4-5%. In a review of several large series of incidental adrenal masses, 89% were clinically determined to be adenomas, and 93% of the adenomas showed no evidence of metabolic activity. On CT, adrenal adenomas are round, sharply defined, homogeneous and usually smaller than 3 cm.⁹¹

6.1.8 Cortical Hyperplasia

Adrenal hyperplasia is often associated with adrenal hormone hyperfunction. **Though the adrenal glands maintain their usual shape, they are often uniformly enlarged with limb thickness exceeding 10 mm. A multinodular growth pattern is also sometimes observed, which can be similar in appearance to multiple small metastases.** Biochemical hyperfunction may also be associated with a normal imaging appearance of the adrenals. The majority of patients with Cushing's syndrome (~70%) have bilateral adrenal hyperplasia, while only 20% of those with primary hyperaldosteronism (Conn's syndrome) demonstrate this finding (**Figure 7**).⁹⁰

6.1.9 Pheochromocytoma

Pheochromocytoma is a catecholamine-secreting tumor that arises from the chromaffin cells of the adrenal gland. It is estimated that this entity comprises approximately 5% of incidentally discovered adrenal masses. Most pheochromocytomas are benign, unilateral, arise in the adrenal medulla and are not associated with a hereditary syndrome. However, the classic "Rule of 10s" (10% malignant, 10% bilateral, 10% extra-adrenal, 10% familial, and 10% pediatric), while useful as a memorization tool, is **not very accurate or reliable**.

Approximately 5% of sporadic cases of pheochromocytoma turn out to be malignant and the rate in hereditary syndromes is only substantially higher in neurofibromatosis type 1 (~11%) and familial paraganglioma syndrome type 4 (30-50%). The malignancy rate is also higher (about 30%) for patients with extra-adrenal disease. Approximately 25% of pheochromocytomas are extra-adrenal (in which case they are referred to as paragangliomas). Paragangliomas can arise in the head, neck, chest, abdomen, pelvis and bladder. They can also be located at the aortic bifurcation or at the base of the inferior mesenteric artery, a region of chromaffin cells known as the organ of Zuckerkandl. Approximately 30% of pheochromocytomas are related to a hereditary syndrome. In fact, 66 patients out of a group of 271 (24%) with non-syndromic pheochromocytoma were later found to have a germ-line mutation that predisposed them to the disease. Finally, in a large registry of patients with symptomatic pheochromocytoma and paraganglioma, approximately 9% were diagnosed before the age of 18.

Pheochromocytomas on cross-sectional imaging are round, **well circumscribed and homogeneous**. Cystic change, central necrosis and calcifications may be present in some cases. Attenuation values on unenhanced CT are typically greater than 10 HU due to their vascularity and low lipid content. One study demonstrated a mean unenhanced attenuation of 35 HU, with no pheochromocytoma having an attenuation value less than 10 HU (range 17-59 HU). This study also showed no difference in CT findings for incidental versus symptomatic pheochromocytomas. Pheochromocytomas enhance avidly, with one study demonstrating significantly higher enhancement in the arterial phase when compared to adenomas. Most pheochromocytomas (~70%) can be differentiated from lipid-poor adenomas based on lower washout percentages. There are no known CT findings that predict malignancy in pheochromocytoma (**Figure 8**).^{92,93,94,95,96}

6.1.10 Ganglioneuroma

Ganglioneuroma is a rare, benign tumor that arises from neuroectodermal cells and consists of Schwann cells, ganglion cells and nerve fibers. These tumors can arise in the adrenal gland, the posterior mediastinum or retroperitoneum. In the largest reported series of adrenal ganglioneuromas (27 cases), median patient age was 31 years and median tumor size was 8 cm. On CT, these lesions are homogeneous in appearance and well circumscribed. Stippled calcifications are found in 30-40% of cases. In the series mentioned above, the median attenuation on unenhanced CT was 33 HU, 40 HU on post-contrast venous phase and 67 HU on delayed post-contrast phase.⁹⁷

6.1.11 Myelolipoma

Myelolipoma is a relatively uncommon benign tumor consisting of mature fat and bone marrow elements. Although most frequently found in the adrenal gland, myelolipoma can be found in the perirenal retroperitoneum and the presacral region. These tumors are often found incidentally - one large study showed 6% of incidentally discovered adrenal masses to be myelolipoma. They are not associated with endocrine abnormalities. CT usually demonstrates a predominance of fat (-100 to -80 HU) and smaller areas of higher density myeloid tissue (20-30 HU) (**Figure 9**).⁹⁸

6.1.12 Adrenal Cysts and Pseudocysts

Adrenal cysts are sharply marginated, homogeneous, thin-walled fluid-filled masses that do not enhance. **Cysts contain simple fluid (< 20 HU), but may have higher attenuation material inside or thin peripheral calcifications if hemorrhage has occurred.** While true cysts are lined with endothelial (and occasionally epithelial) cells, pseudocysts have fibrous walls without a cellular lining. Pseudocysts typically contain higher density fluid but also do not enhance. While the majority of pseudocysts are unilocular (81%) and have calcifications (74%), true cysts present with these attributes in about half of cases (**Figure 10**).⁹⁹

6.1.13 Adrenal Atrophy

On CT, adrenal atrophy appears as a shriveled iso-attenuating structure that maintains the adreniform shape. Atrophy can result from autoimmune adrenalitis, adrenal hemorrhage, and in the later stages of adrenal tuberculosis.

6.1.14 Tuberculosis

Adrenal tuberculosis (TB) is seen in approximately 6% of active tuberculosis cases. The adrenal gland is the fifth most common site of extrapulmonary TB after liver, spleen, kidney and bone. The lesions are usually **bilateral**, with series reporting rates between 69% and 91%. As granuloma formation and caseous necrosis occur, the glands initially become enlarged. Later in the disease process, **atrophy occurs with development of fibrosis and calcifications. Calcifications are seen in the majority of adrenal TB cases, but less than 10% of adrenal tumors.** Tuberculosis can ultimately cause necrosis of the adrenal gland, which manifests as Addison's disease once 90% of the adrenal tissue is destroyed. On CT, adrenal TB presents with a low attenuation center and peripheral enhancement; calcifications are often observed. Rarely, CT will demonstrate atrophic

adrenal glands as a result of adrenal TB.^{100,101,102}

6.1.15 Amyloidosis

Other infiltrative diseases, such as amyloidosis, sarcoidosis, and hemochromatosis may also affect the function of the adrenals. The amyloidoses are a group of diseases in which insoluble proteinaceous material is deposited in the extracellular spaces of various organs and tissues. This process is associated with eventual organ dysfunction, ranging from mild diseases to severe involvement leading to death. Amyloid deposition at endocrine sites has been demonstrated in several case series. Endocrine dysfunction due to infiltration of the thyroid, testes and adrenals has been described more frequently than in the parathyroid, pancreas, pituitary and ovaries. Amyloidosis of the adrenals is often described in autopsy series, since extensive accumulation of amyloid is necessary before symptomatic primary adrenal insufficiency occurs.

Although clinically significant adrenal failure is rare, studies have shown that patients with amyloidosis have a lower cortisol response with ACTH stimulation. Furthermore, in an analysis of 374 patients with amyloidosis, 41% had evidence of adrenal amyloid deposition on a nuclear medicine study. Thus, it is **recommended that patients with systemic amyloidosis undergo evaluation of adrenal reserve with the ACTH stimulation test**. On CT, the adrenal glands may demonstrate calcification, but this has only been described in limited case reports.^{103,104}

6.1.16 Fungal Infections

Fungal infections of the adrenal gland have been described in several case reports. One such report describes a patient who was ultimately diagnosed with Cryptococcus infection of both adrenal glands. The CT scan demonstrated **bilateral adrenal masses with central necrosis**. The authors note that most cases of adrenal Cryptococcus infection are accompanied by meningoencephalitis. Infection of the adrenals by Histoplasma species has also been described. A recent review of the literature found 242 cases of adrenal histoplasmosis spanning a 40-year period. Imaging characteristics include **marked enlargement of the affected adrenal that maintains the normal morphologic contour of the gland**. Similar to tuberculosis, necrotizing granulomas and caseous nodules can be observed. These granulomas may ultimately calcify. Adrenal infections with other organisms including Blastomyces, Pneumocystis carinii, and *Coccidioides* have also been described.^{105,106,107}

6.1.17 Adrenal Hemorrhage

Adrenal hemorrhage is **fairly common in neonates**. It is estimated to occur in ~1-2% of healthy infants and is associated with **birth trauma, hypoxia, prolonged labor and septicemia**. In older children and adults, adrenal hemorrhage is caused by trauma, coagulopathy or tumor (**Figure 11**). Unenhanced CT often demonstrates a round or oval hyperdense mass (50-90 HU) and peri-adrenal fat stranding is common. Traumatic adrenal hemorrhage is more common on the right side, perhaps due to compression between the liver and spine or because the right adrenal vein drains directly into the IVC and is thus more susceptible to changes in venous pressure. Evolution of the hemorrhage

leads to a decrease in size and density, which may eventually result in adrenal atrophy or formation of a pseudocyst. As described above, pseudocysts have central areas of hypoattenuation and often demonstrate peripheral calcifications.¹⁰⁸

6.1.18 Incidental Adrenal Masses

The malignancy rate of adrenal lesions is directly related to their size. It has been estimated that 4% to 5% of tumors less than 4 cm, 10% of tumors 4 to 6 cm, and 25% of tumors greater than 6 cm are adrenocortical carcinomas. In a series of over 1000 incidentally detected adrenal masses a 4-cm cutoff resulted in a high sensitivity (93%) with acceptable specificity (42%) for detecting malignancy. **Thus, in otherwise healthy individuals with acceptable perioperative risks, most experts recommend 4 cm as the cutoff diameter that warrants resection.** Furthermore, several studies have demonstrated that CT tends to underestimate the size of adrenal lesions by 15-20%, further supporting the rationale for using a 4-cm cutoff.¹⁰⁹

The majority of benign lesions do not grow substantially. In one study, only 7.4% of incidentally discovered adrenal masses grew greater than 5 mm during the two-year follow-up period. Studies with longer follow-up show that a higher percentage of lesions do increase in size, but in no more than 25% of cases. Lesions that are not resected should be reimaged at 6, 12, and 24 months to confirm slow or absent growth. Nevertheless, even for lesions that demonstrate significant growth (> 1 cm), and are ultimately resected, the malignancy rate is very low.^{110,111}

6.1.19 CT Washout

On non-contrast CT, adenomas will often demonstrate a density less than that of normal liver. This is because of their high lipid content (approximately 70% of adrenal adenomas are characterized as lipid-rich). **A mean attenuation value less than 10 HU is strongly suggestive of a benign adenoma with specificities approaching 100%.**¹¹²

However, the approximately 30% of lipid-poor adenomas (also known as atypical or indeterminate adenomas) will not be correctly categorized as benign using this method.¹¹³ Contrast washout is useful for further characterization of these masses, as washout tends to be more rapid (higher percentage) in adenomas than in other adrenal lesions. **A higher relative percentage washout (greater than 40%) or a higher absolute percentage washout (greater than 60%) is indicative of a benign adenoma.** Immediate (1-minute) and delayed (15-minute) post-contrast attenuation values are used to calculate the percentage of enhancement washout.¹¹⁴ Enhancement washout is defined as the difference between the immediate post-contrast attenuation and the delayed post-contrast attenuation.¹¹⁵ Relative percentage enhancement washout is defined as the enhancement washout divided by the immediate attenuation:

$$\text{Relative percentage washout} = [(immediate - delayed)/immediate] \times 100\%$$

The calculation for the absolute percentage enhancement washout includes a pre-contrast attenuation value:

$$\text{Absolute percentage washout} = [(immediate - delayed)/(immediate - precontrast)] \times 100\%$$

6.1.20 Adrenal Biopsy

Although adrenal biopsy has been shown to be diagnostically accurate, experts argue that most adrenal biopsies are unnecessary. First, modern imaging techniques coupled with clinical information provides a high degree of diagnostic accuracy. Second, the biopsy results rarely change management. Third, while complications are relatively rare, the risks of this procedure seem to outweigh the benefits in many cases. Additionally, some authors feel that biopsy may potentially make future laparoscopic adrenalectomy more difficult. It is recommended that adrenal biopsy only be pursued once appropriate radiographic and clinical diagnostic modalities have been explored, and only if the biopsy result will potentially change the management course. Furthermore, biopsy is not indicated if the tumor is metabolically active, if ACC is strongly suspected (due to concern for needle-tract seeding), or if pheochromocytoma has not been ruled out (due to the possibility of causing a hypertensive crisis). **Thus, the only clinical scenario in which adrenal mass biopsy maintains a significant role is in the setting of metastatic disease or a mass of unclear significance.** For patients with other primary malignancies, which may have recurred in the adrenal gland, biopsy results may alter the treatment plan.^{116,117,118}

7. Kidney

CT scanning constitutes an essential part of the evaluation of renal and urothelial pathology. CT allows for the simultaneous ability to image the renal vasculature, parenchyma and collecting system and when used appropriately can deliver a wealth of information to the urologist. **A comprehensive evaluation of the kidney and urothelial tract involves an unenhanced scan, followed by an enhanced scan of the abdomen and pelvis and a delayed excretory phase to evaluate the collecting system.** Unenhanced scans allow for the imaging of renal calculi as well as to obtain pre-contrast attenuation measurements of the renal parenchyma that may be compared to post contrast images (**Figure 13**). An early, enhanced phase (25 seconds) allows for the imaging of the vascular system, (**Figure 14**) while imaging at 90-180 seconds allows for imaging of the renal parenchyma. These are commonly referred to as arterial and nephrogenic phases respectively. (**Figure 15**) Delayed images at approximately 3-5 minutes (excretory phase; see **Figure 16**) will adequately image the renal collecting system, while the bladder is more adequately seen on 20 minute images.⁴

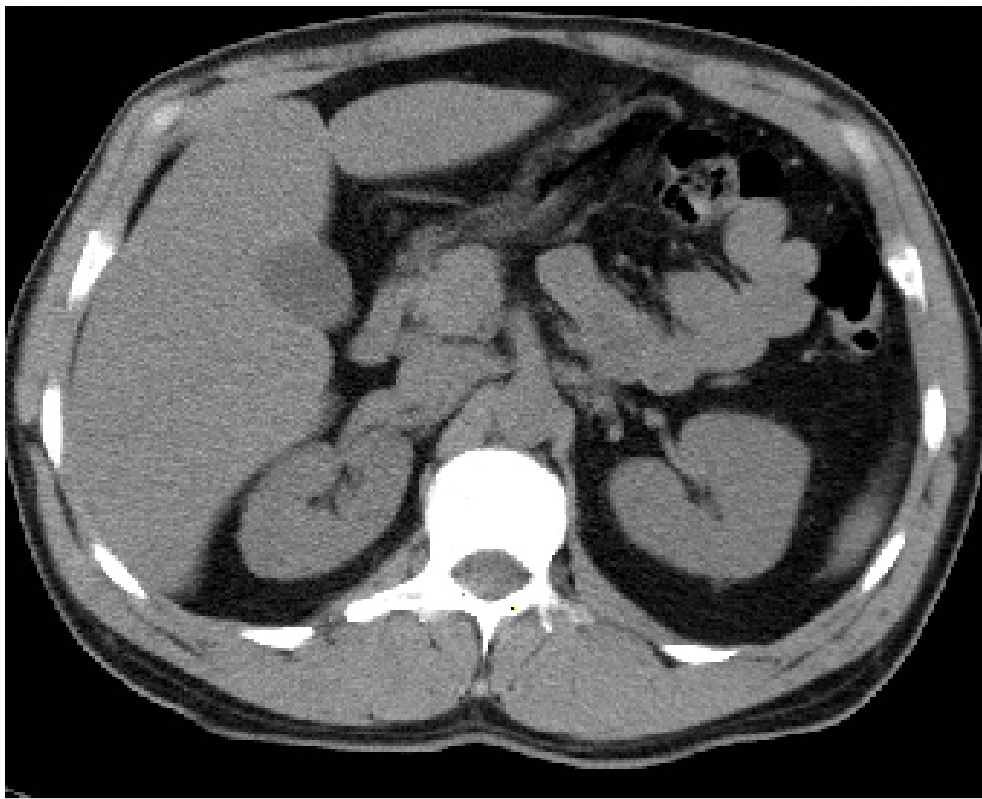


Figure 13: Normal unenhanced axial renal image showing no stones or hydronephrosis

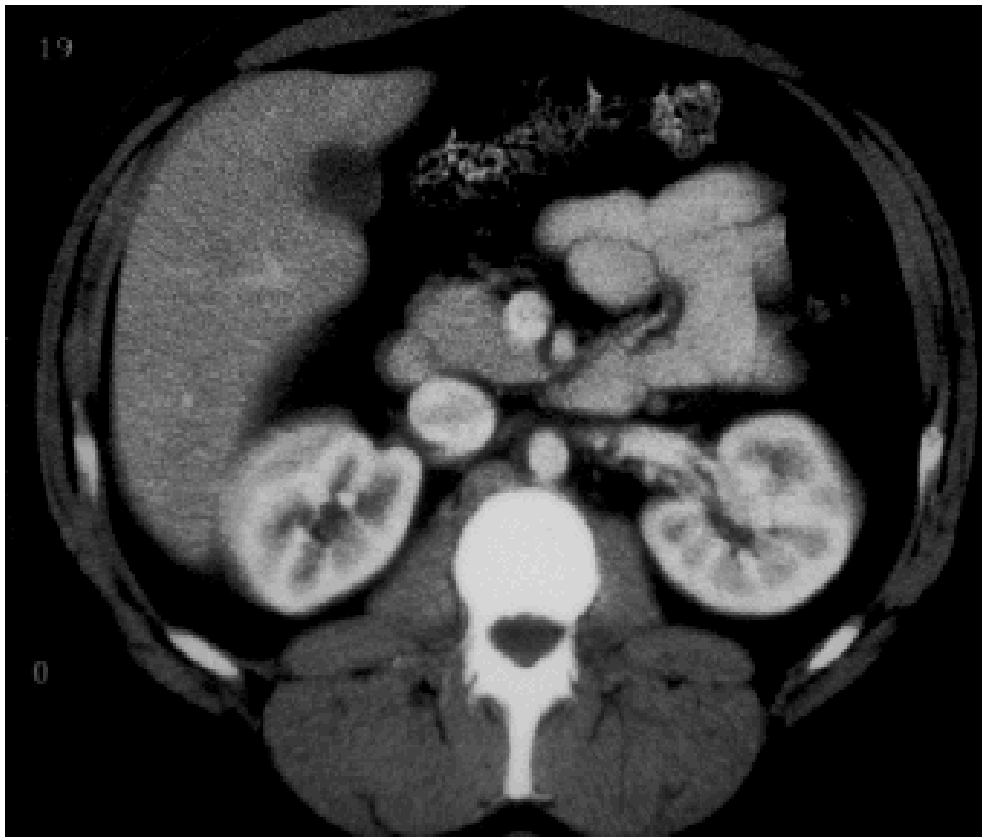


Figure 14: Normal early nephrogram phase showing cortico-medullary distinction

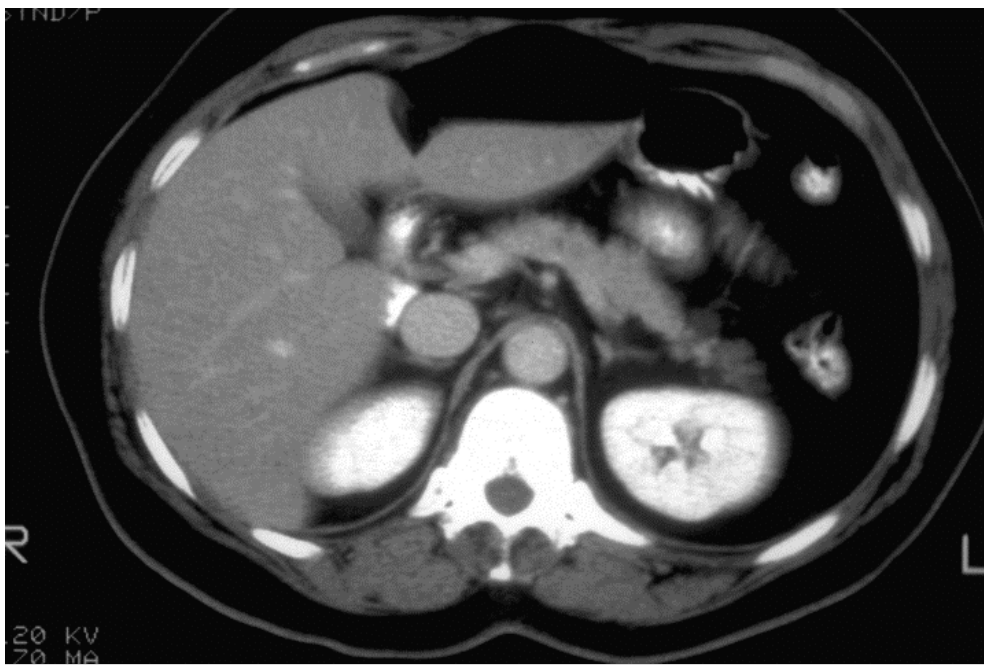


Figure 15: Nephrogenic phase shows homogeneous nephrogram

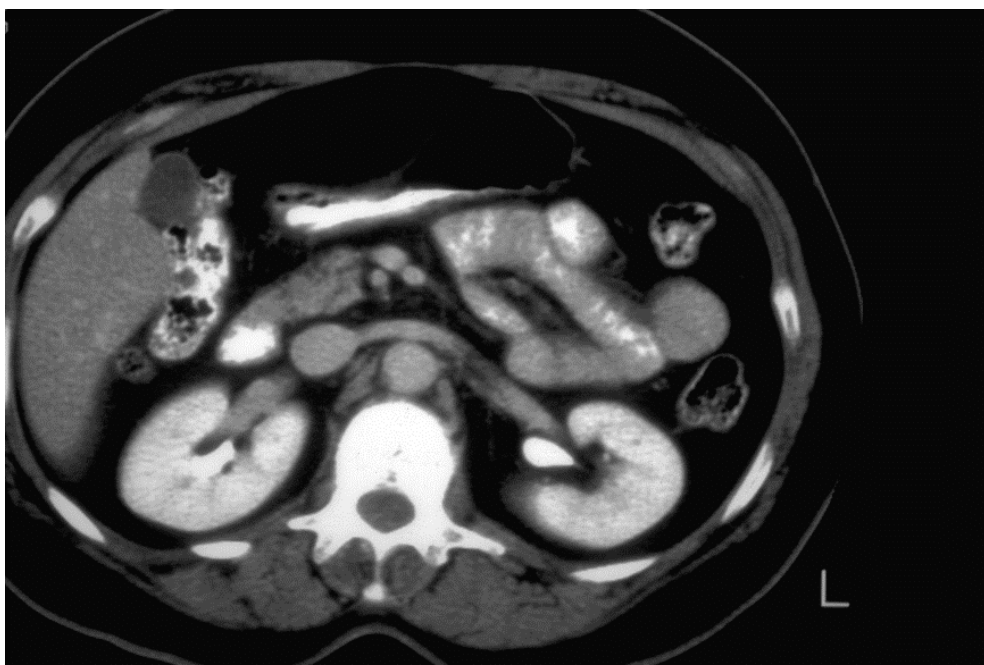


Figure 16: Excretory phase with filling of calyces and renal pelvis using soft tissue windows

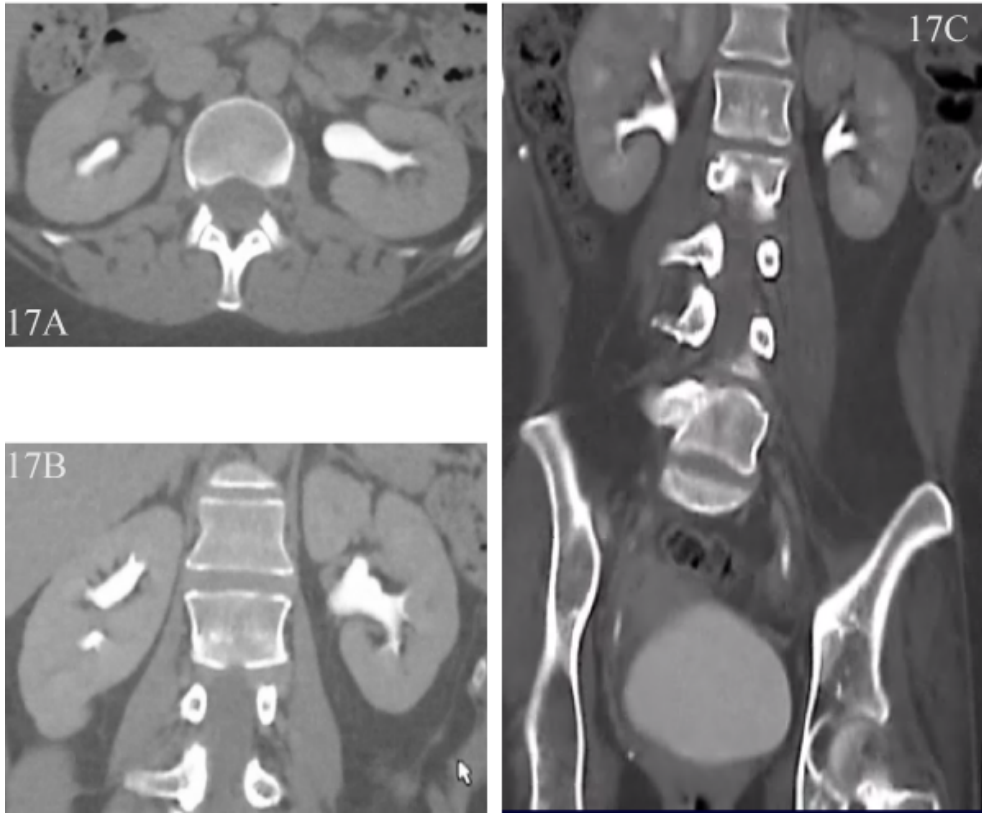


Figure 17: Axial images A and coronal reconstructions during excretory phase B. Bone windows are used to better visualize the collecting structures. Delayed coronal reconstructions below C visualize the entire collecting system

7.1 Imaging of Renal Vasculature

Vascular pathology such as renal artery aneurysms, renal artery stenosis, congenitally aberrant vessels, and A-V malformations are all adequately imaged during the arterial phase. **3D reconstruction** is also extremely helpful and allows for the construction of an angiogram. **CT angiography is considered the standard evaluation for the renal transplant donor.** CT angiography also detects **renal artery stenosis** with a high degree of accuracy. The sensitivity and specificity in detecting stenosis of 50% or more is approximately 90% and 97%, respectively.^{119,120,121}

Aneurysms may be seen on unenhanced images if they are calcified. After contrast administration the degree of enhancement will vary depending on the amount of thrombosis within the aneurysm. An arteriovenous fistula is an abnormal communication between the arterial and the venous circulations that bypasses the capillary bed. Early and delayed phase imaging should be obtained as they enhance during the arterial phase and wash out quickly. Renal emboli produce acute ischemia to the entire kidney or a segment depending upon which artery involved. CT typically demonstrates an area of decreased or no enhancement that corresponds to the area of the affected parenchyma. This is usually wedge shaped unless the entire kidney is involved. An embolus of the main renal artery will lead to an increase in renal size due to edema and no enhancement within the

parenchyma. There is usually some degree of capsular enhancement however due to flow within capsular vessels.¹²²

7.2 Imaging of the Renal Parenchyma

7.2.1 Anomalies of Renal Structure

Common congenital anomalies of renal structure include **renal ectopia, hypoplasia, horseshoe kidney, and rotational anomalies**. These anomalies are frequently associated with aberrant renal vessels and thus CT is a useful modality in identifying these vessels prior to any surgical intervention. Imaging findings in patients with a horseshoe kidney include (1) an abnormal axis for each kidney with the lower poles more medially located than the upper poles, (2) the kidneys lie in a more caudad position, and (3) a bilateral malrotation with the renal pelves in an anterior position so that the lower calyces are projected in a more medial position than the proximal ureter.¹²³

7.2.2 Renal Masses

A renal mass is characterized as either a simple or complex cyst or a solid mass. While simple cysts are easily identified on ultrasonography, **CT is useful in assessing wall thickness, the presence of septations, cyst density, calcifications and areas of enhancement**. Simple cysts have a density similar to water (5-20HU) and do not enhance. The walls of a simple cyst should be imperceptible and without septations. By definition, any cyst that does not fulfill the criteria of a simple cyst is labeled as complex.¹²⁴

In 1986, **Bosniak published criteria to stratify CT features of complex renal cysts (Table 1)**. Category I lesions are simple cysts while category II lesions are hyperdense with attenuation of greater than 20 HU (typically 60-80). They do not enhance, have no wall thickening, and are less than 3cm. Both category I and II lesions are benign and have no malignant potential. Category IIF are slightly more complex and may contain thin septations with perceived enhancement or slight calcifications within the septae or wall. While the risk of malignancy in this category is low, it is not zero and thus these lesions require further follow up. Category III lesions are more complex. They may be multiloculated and contain thickened septa with measurable enhancement. The risk of malignancy approaches 50%. Category IV lesions contain all of the features of type III cysts along with the presence of distinct enhancing soft tissue components. These are almost always malignant!^{125,126}

Table 1. Bosniak classification of renal cysts.

Category	Characteristics	Risk of Malignancy
I	Density similar to water (5-20 HU) Non enhancing Imperceptible walls	0%
II	Hyperdense (>20HU, typically 60-80) Non enhancing No wall thickening	0%
IIIF	Non enhancing May contain thin septations or slight calcification	Extremely Low
III	Maybe multiloculated Thickened septae with enhancement	Up to 50%
IV	Presence of distinct enhancing soft tissue component	Nearly 100%

The vast majority of solid renal masses that enhance more than 20 HU are malignant and should be managed accordingly per AUA Small Renal Mass guidelines with either surveillance with or without biopsy, ablation (if appropriate), or **surgery**.¹²⁷ Angiomyolipomas (AML) are an exception to this as they are benign. Any amount of fat on CT is diagnostic for AMLs. A multiphasic CT is the most useful for the evaluation of a solid mass. The unenhanced images are useful to measure enhancement after contrast as well as evaluate for the presence of any calcifications. The arterial phase delineates the arterial anatomy and assists in surgical planning while the nephrogenic phase helps to characterize the degree of enhancement as well as evaluate the renal vein for the presence of any filling defects. Delayed images are particularly useful in helping to differentiate central masses from urothelial lesions. CT is also useful for localizing renal masses for the purposes of cryoablation or diagnostic biopsy. ¹²⁸



Figure 18: Bosniak I simple cyst measuring water density, sharply marginated from kidney with imperceptible wall and no complicating features such as calcification or septa.

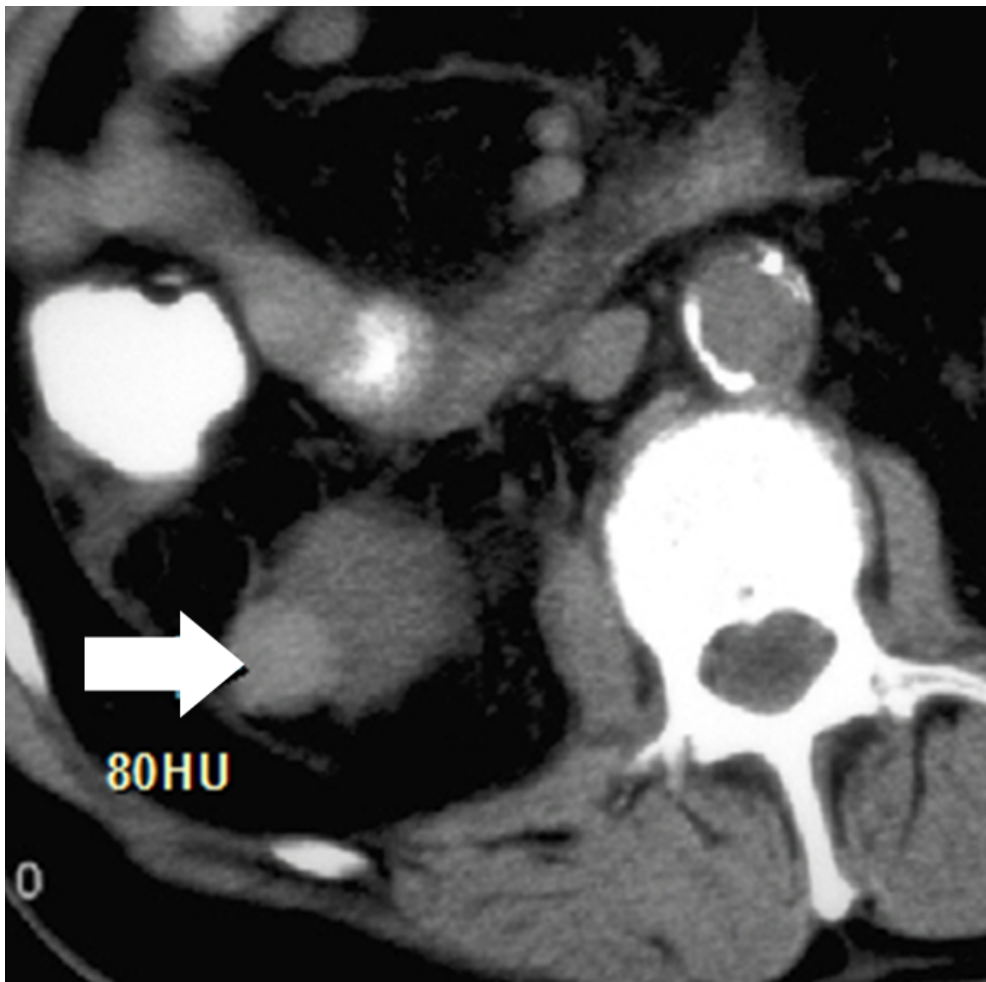


Figure 19: Bosniak II high density cyst on unenhanced scan

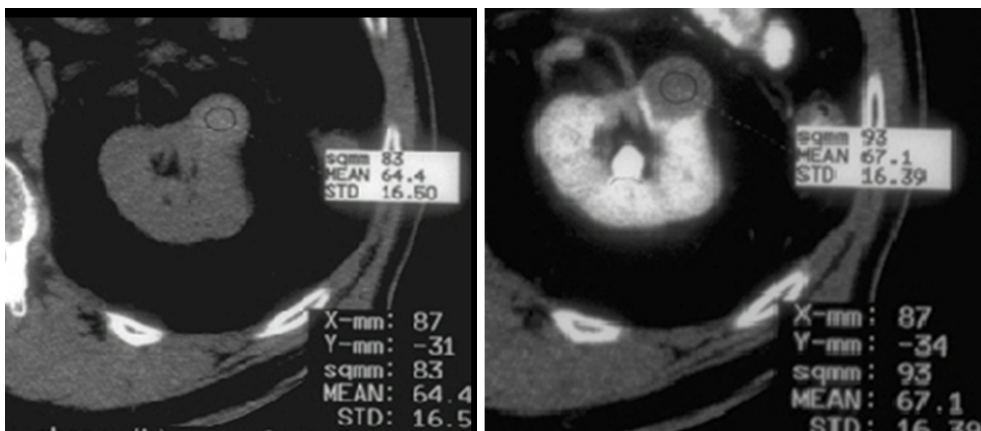


Figure 20: Bosniak II high density cyst measuring 64 HU unenhanced and 67 HU post contrast indicating no enhancement



Figure 21: Bosniak IIF lesion with thick calcification, but no enhancement. Follow up over several years showed no change

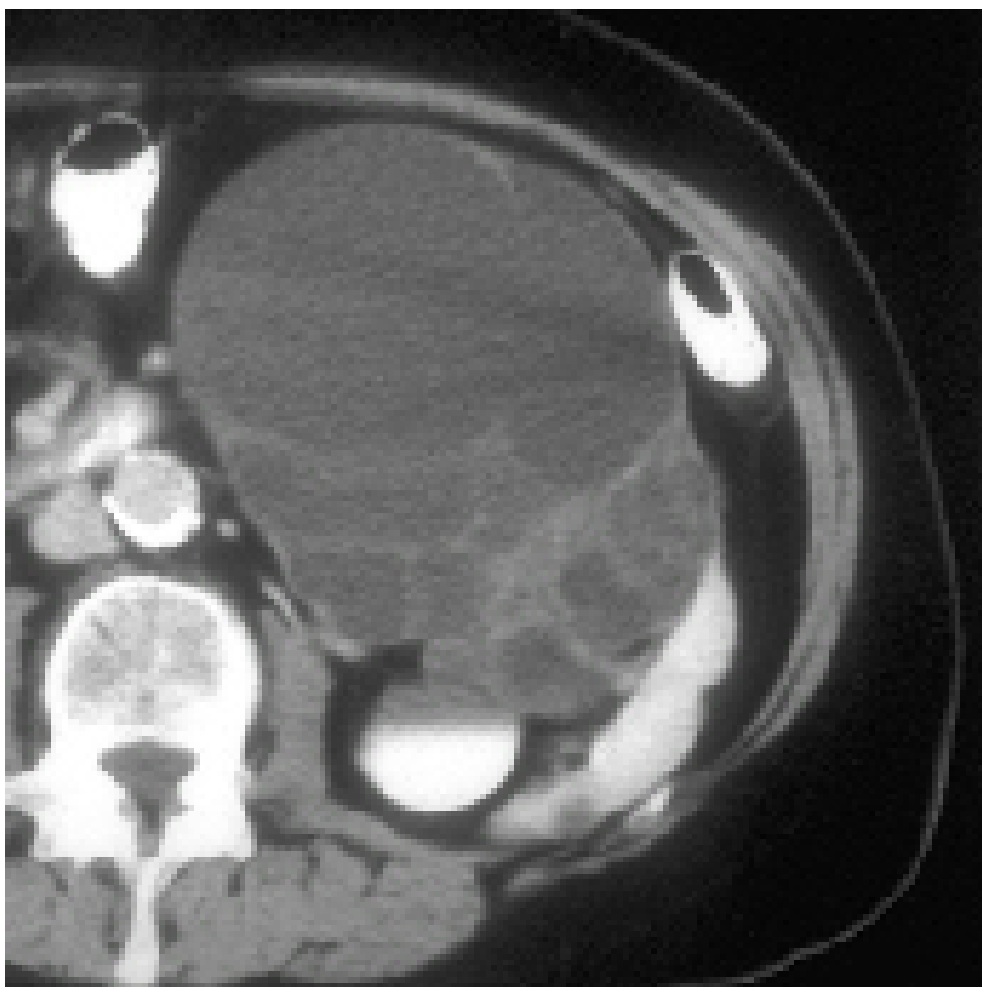


Figure 22: Large multilocular cyst with thick septations is a Bosniak III lesion. Benign at surgery

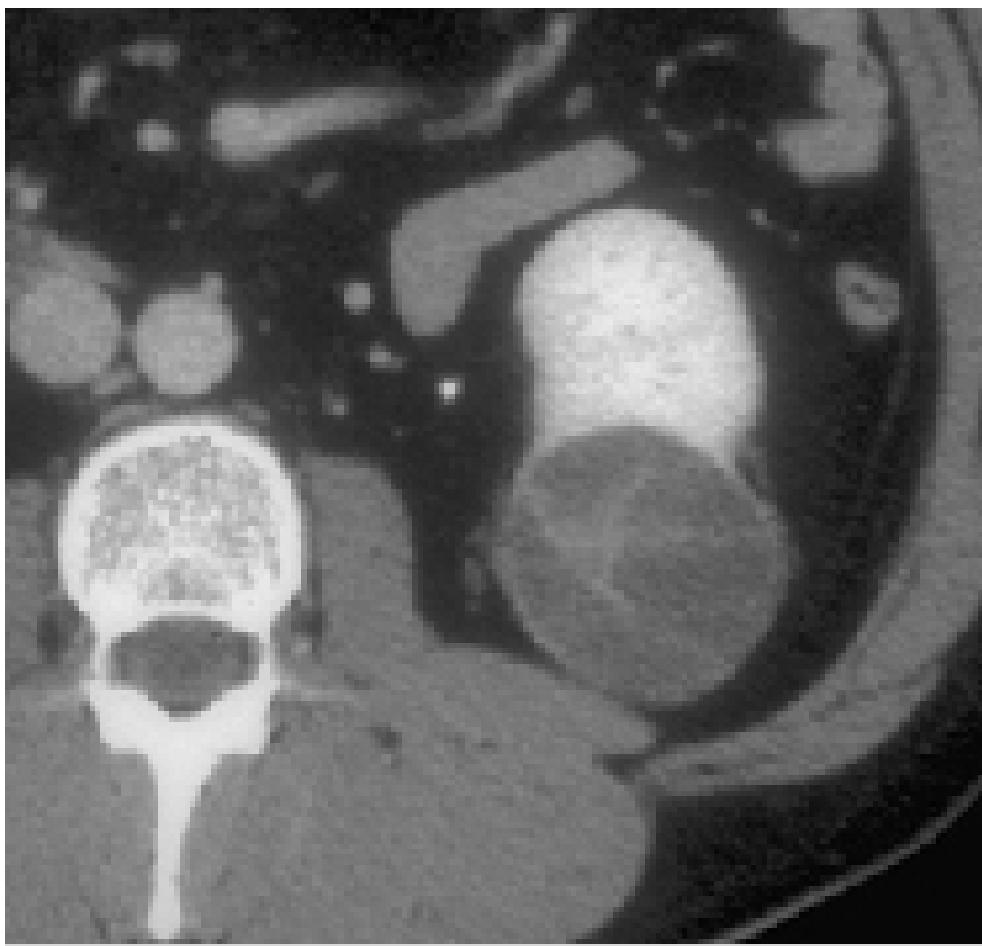


Figure 23: Similar appearing multilocular cyst with thick septations proved to be Renal Cell Carcinoma showing the difficulty in evaluating multilocular cysts.

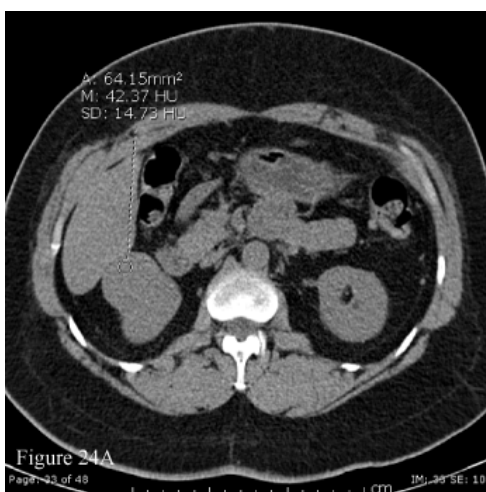


Figure 24A

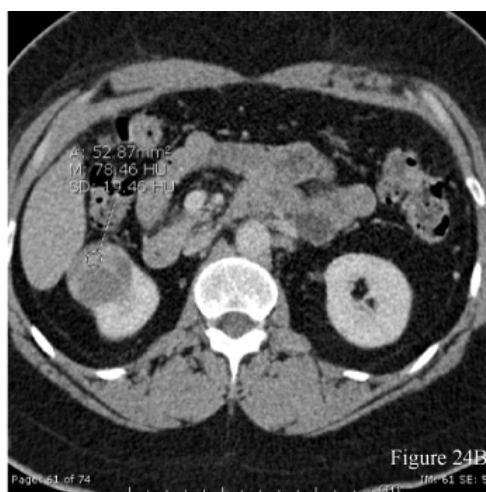
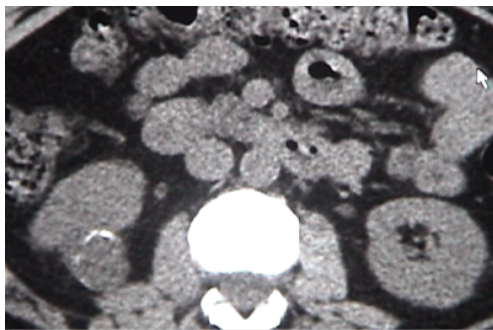
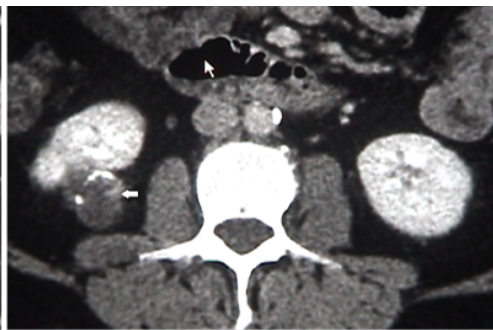


Figure 24B

Figure 24A and 24B: Septated cystic lesion with enhancing septa and nodular enhancement (ROI 42HU pre and 78HU post contrast) is Bosniak IV and was RCC at surgery.



25A



25B

Figure 25A and 25B: Right Bosniak IV lesion has thick calcification, but it is the small enhancing nodule (arrow) along the medial aspect of the lesion which makes it a class IV lesion. RCC at surgery.

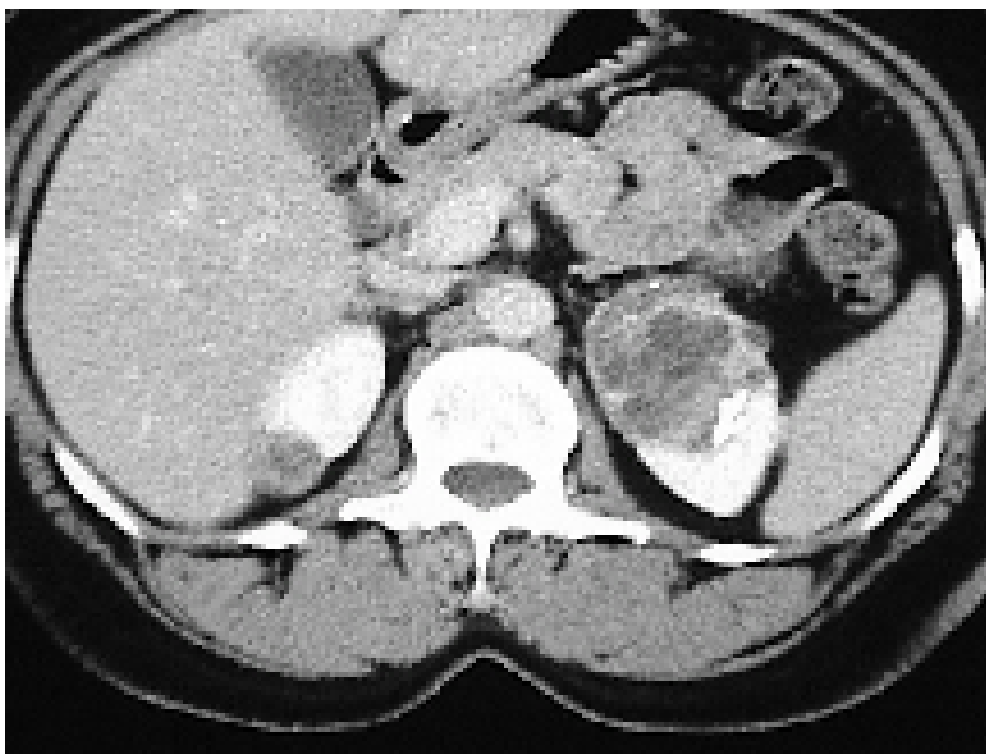


Figure 26: Large multilocular cyst with thick septations is a Bosniak III lesion. Benign at surgery



Figure 27: Similar appearing multilocular cyst with thick septations proved to be Renal Cell Carcinoma showing the difficulty in evaluating multilocular cysts.

7.2.3 Infections

CT imaging provides excellent anatomic detail when evaluating patients with suspected renal infections. Imaging provides useful anatomic information that may help elicit the underlying causes of an infection such as calculi or obstruction. **Contrast enhancement is necessary when evaluating patients with presumed pyelonephritis.** The classic CT findings in pyelonephritis include **renal enlargement, bulging in renal contour, wedge shaped zones of decreased enhancement radiating from the papillae to the cortex, and finally perinephric stranding or edema** (**Figure 27**). CT is the imaging study of choice for the diagnosis of an acute renal abscess. The rounded mass is usually a low-attenuation (10 to 20 HU) and does not enhance with contrast administration. The walls of the abscess are typically thick and irregular with some degree of enhancement. The presence of gas (less than -150U) within the abscess is diagnostic of an abscess. (**Figure 28**) The abscess may or may not extend into the perinephric space. (**Figure 29**)¹²⁹

Xanthogranulomatous pyelonephritis is thought to be the result of a chronic obstructive purulent infection. The classic findings on CT include an **enlarged poorly functioning kidney with a maintained reniform shape**. There is usually a central calculus or multiple calculi. Dilated calyces typically appear as multiple hypodense masses with surrounding hyperemia. (**Figure 30**)

Emphysematous pyelonephritis is an unusual variant of pyelonephritis whereby gas producing bacteria invade the renal parenchyma. This typically occurs in immunocompromised patients. CT images typically reveal diffuse infiltration with gas throughout the renal parenchyma; viewing the kidney in lung windows may provide further clarification regarding extent of air.¹³⁰

Other uncommon renal infections include tuberculosis and fungal infections. Depending on the stage

of the disease, renal tuberculosis is characterized by parenchymal calcifications and scarring, papillary necrosis, infundibular strictures or complete non function (autonephrectomy). **Infundibular stenosis or obstruction** is a hallmark of the disease and may be visualized on excretory images. Fungal infections usually develop in immunocompromised patients. This may lead to parenchymal infection, abscess formation, papillary necrosis, and the formation of fungal balls within the collecting system. CT may reveal an enlarged kidney with areas with inhomogenous nephrograms. Delayed images may reveal fungal balls that present as filling defects.^{129,131}

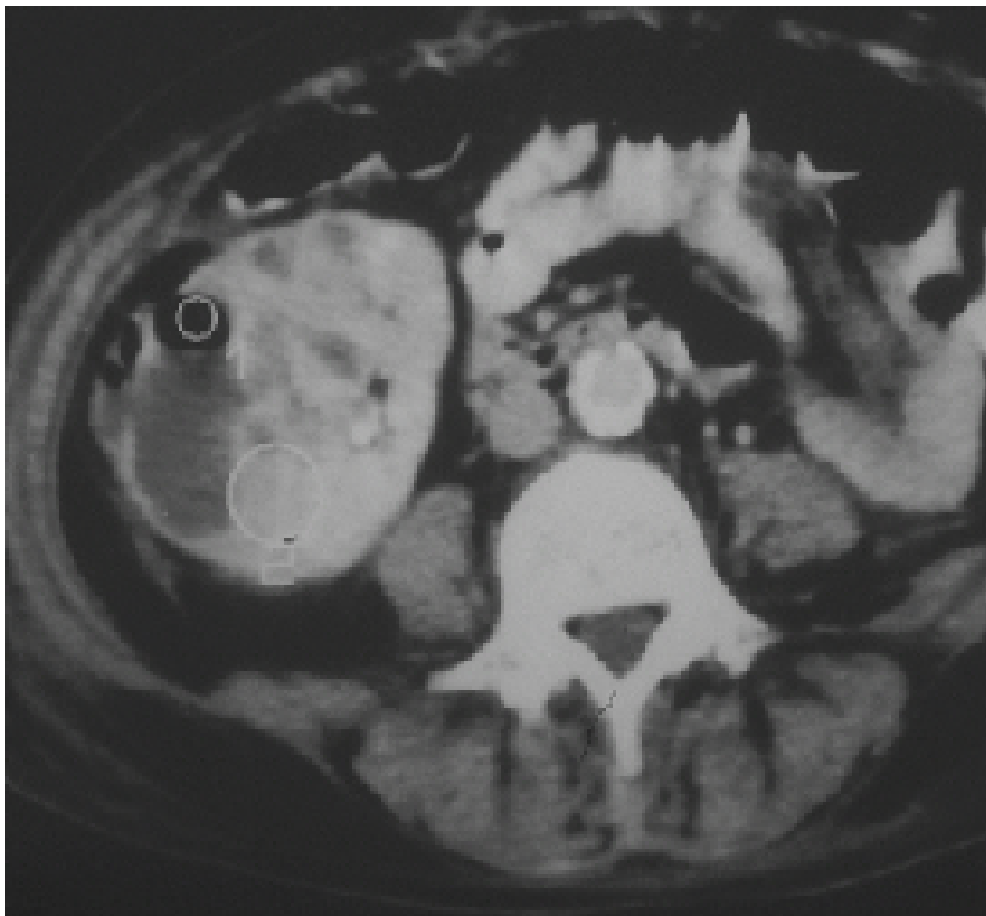


Figure 28: Air (small ROI) in a renal mass indicating renal abscess.



Figure 29: Perinephric abscess (arrow) with no obvious renal origin.

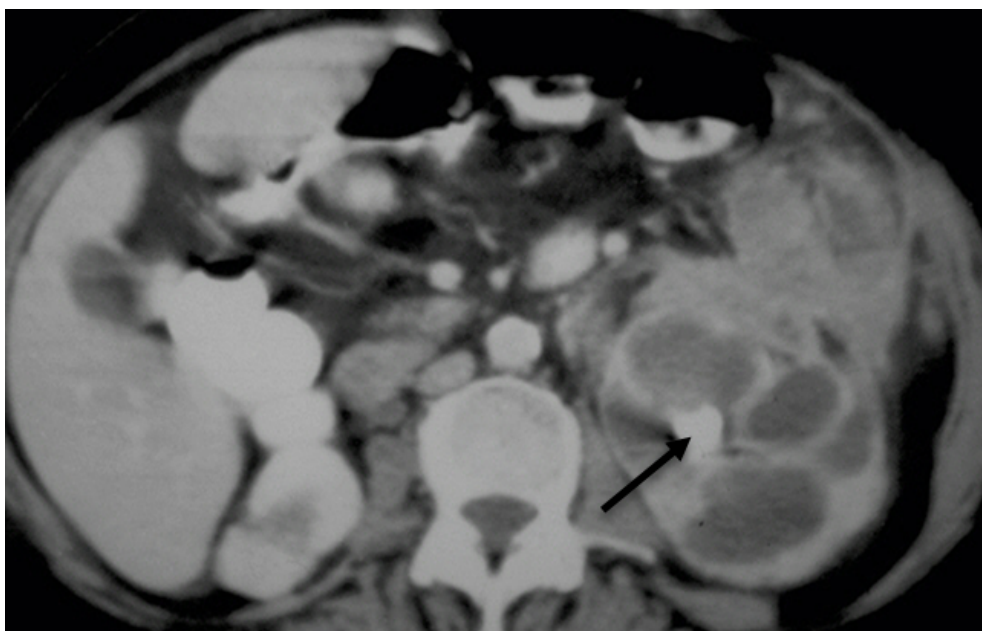


Figure 30: Xanthogranulomatous pyelonephritis left kidney with central calculus (arrow) and multiple hypodense areas producing the so called "Bear Paw" sign.

7.2.4 Renal Trauma

Blunt renal trauma represents a unique type of parenchymal pathology that requires rapid imaging. CT scanning is ideal for imaging suspected cases of renal trauma as it can accurately and rapidly assess the severity of injury as well as image other organs. Indications for CT imaging in suspected

renal trauma **include gross hematuria or microscopic hematuria in a child or hemodynamically unstable adult.** A typical protocol includes a cortico-medullary phase at 60-90 seconds after contrast injection and a 3-5 min delayed scan if the first run reveals evidence of parenchymal injury. Grade I trauma (renal contusion) is characterized by a focal area of decreased enhancement relative to the surrounding parenchyma. Lacerations appear as hypo-attenuated linear areas within the parenchyma. Grade II lacerations are less than 1cm while grade III are more than 1cm. Contrast extravasation signifies injury to the collecting system (grade IV). Thrombosis of the renal artery (grade IV) will lead to lack of enhancement within the entire kidney while a segmental thrombosis will produce a corresponding area of infarction. Grade V injuries include a shattered kidney or complete disruption of the renal hilum (**Table 2**).^{132,133}

Table 2 Renal Trauma Grading

Grade	CT Characteristics
I	Renal Contusion (focal area of decreased enhancement)
II	Laceration <1cm not involving the collecting system
III	Laceration >1cm not involving the collecting system
IV	Injury involving collecting system Injury to renal artery or vein (not both)
V	Shattered kidney Disruption of renal hilum

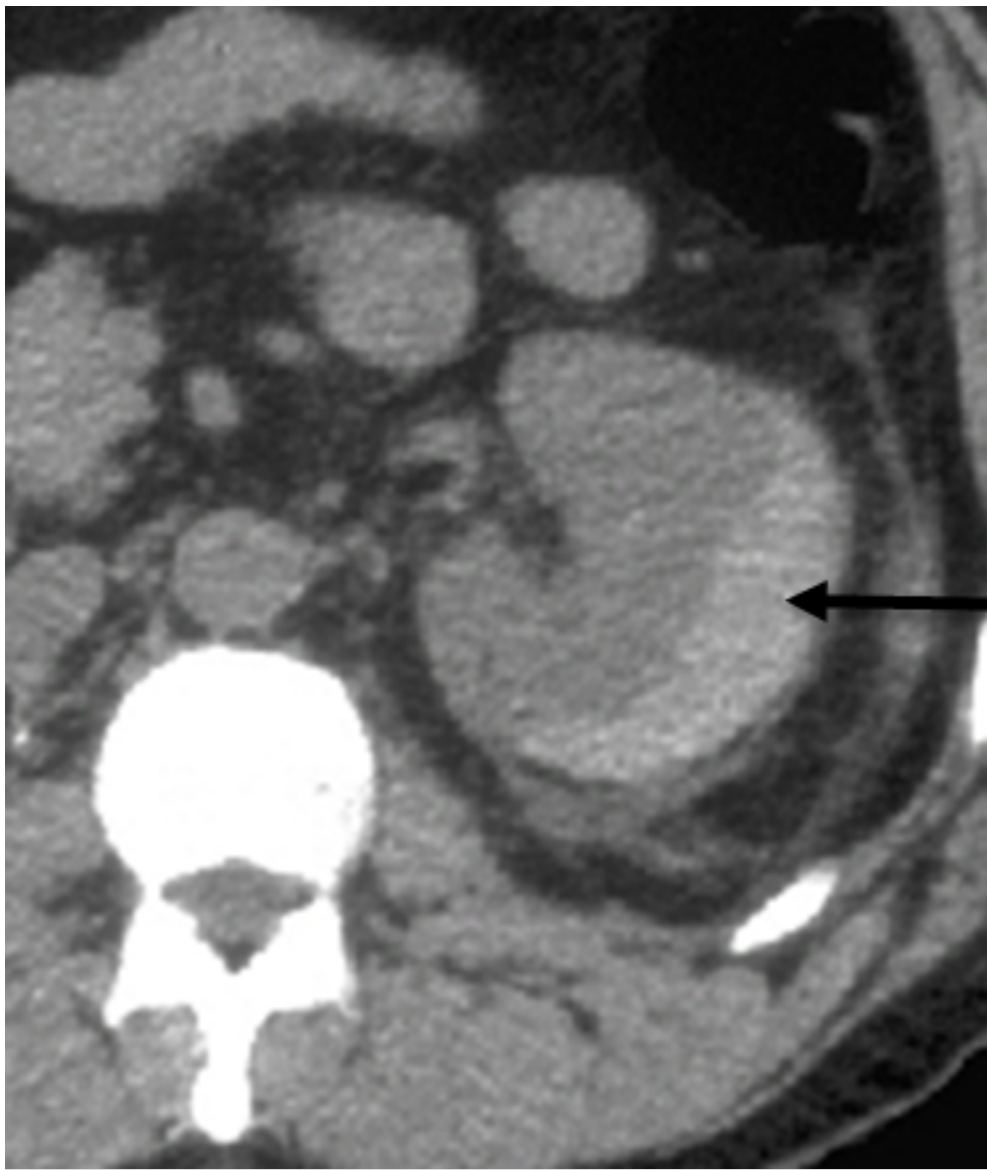


Figure 31: Acute left renal subcapsular hematoma with crescent shaped high attenuation fresh blood (arrow) compressing the lower density renal parenchyma- Grade I injury



Figure 32: Small focal anterior renal infarct (arrow) Grade I



Figure 33: Anterior right renal laceration >1cm (arrow) Grade III

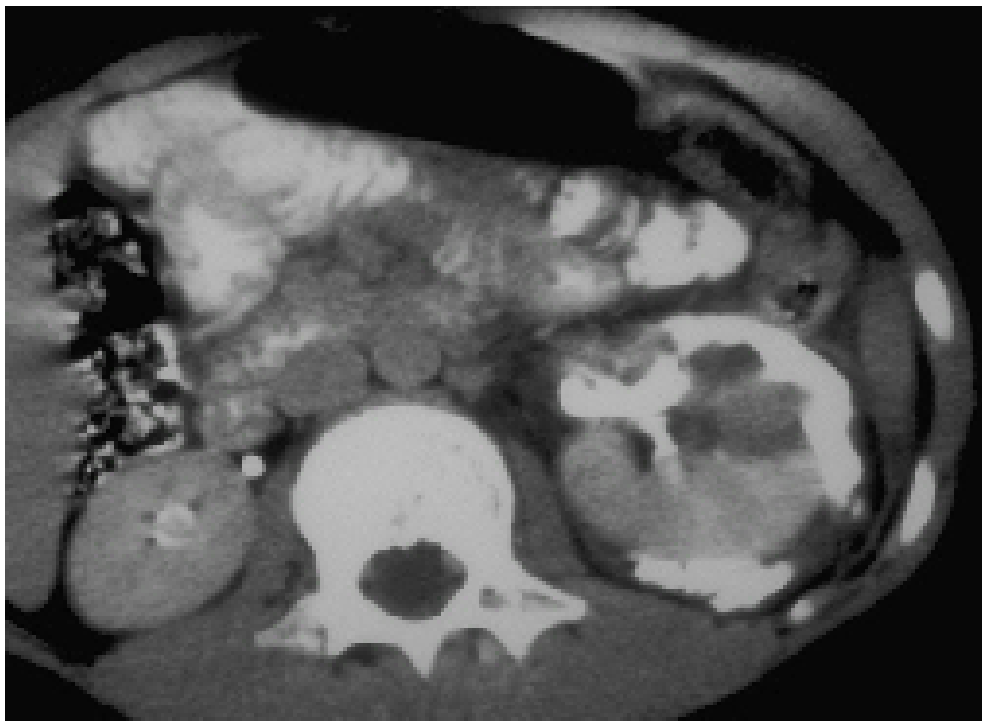


Figure 34: Laceration involving the left kidney collecting system with gross extravasation of contrast Grade IV

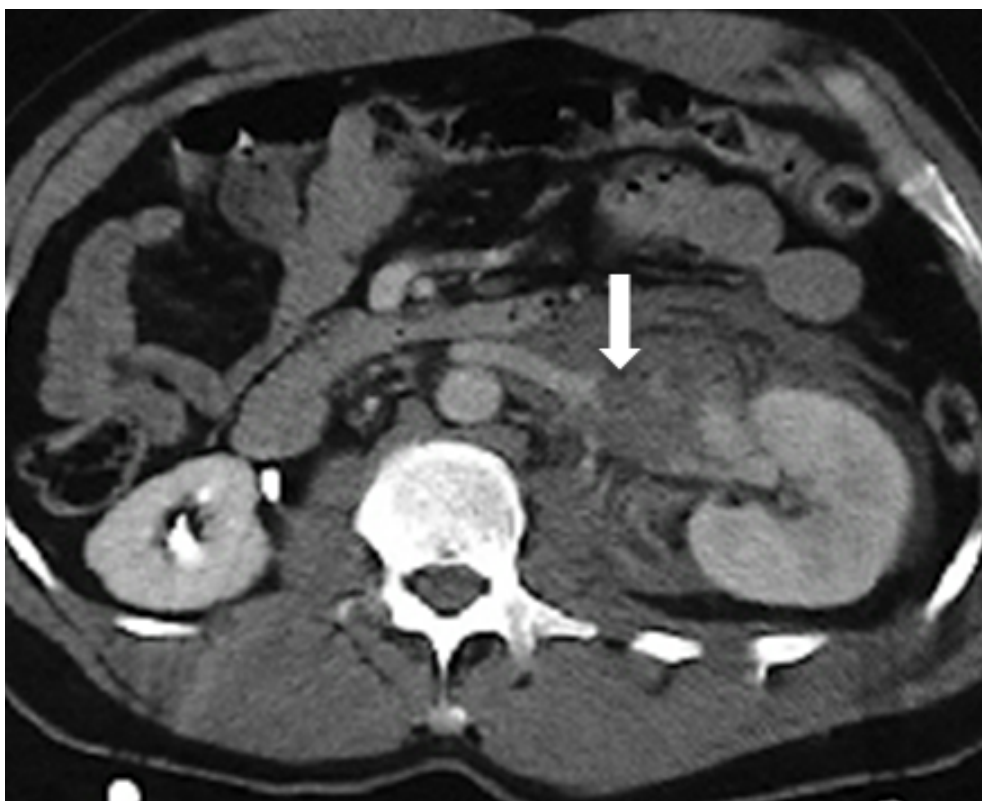


Figure 35: Localized renal vein injury (arrow) with large hematoma Grade IV



Figure 36: Shattered left kidney with hematoma Grade V

7.2.5 Imaging of the Renal Collecting system

Delayed images during the excretory phase of CT imaging allow for high resolution images of the urothelial tract. 3D reconstruction also allows for the construction of a “**CT Urogram**” that gives detailed anatomic information about the entire collecting system. (**Figure 37**) The numerous congenital anomalies of the upper collecting system such as calyceal diverticulae, extra renal and bifid pelvis, complete duplication, and ureteropelvic junction obstruction are all easily identified on delayed images. Hydronephrosis from UPJ obstruction is either the result of an intrinsic defect of the ureteropelvic junction or an external compression such as a crossing vessel. CT imaging allows for the delineation of both the collecting system as well the evaluation of the presence of crossing vessels. (**Figure 38**) The awareness of the presence of crossing vessels is extremely important when considering approaches to surgical repair. Arterial and excretory contrast enhance images should therefore be obtained when evaluating a patient with a suspected UPJ obstruction. Findings suggestive of UPJ obstruction include: 1- rotation of the kidney with the hilum facing anteriorly and the upper pole pointing laterally. 2- Absence of perinephric stranding. 3- Asymmetry of the rate and degree of corticomedullary and ureteropelvic opacification. 4- Cortical thinning. 5- Hydronephrosis of the extrarenal collecting system more than the intrarenal portion. ^{123,130}

CT has become the diagnostic **modality of choice for the evaluation of renal colic**. (**Figure 39**) All stones have attenuation values higher than that of surrounding tissue structures and thus they can all be visualized on non-contrast imaging, obviating the need for contrast administration. Stones appear as areas of high attenuation within the collecting system. Secondary signs that may be helpful in determining whether an area of calcification lies within the urothelial tract include ureteral edema around the stone (rim sign), a dilated ureter or pelvis above the stone (signifying obstruction), or inflammatory changes around the perinephric fat (**Figure 40** and **Figure 41**). The degree of

attenuation of calculus may help in differentiating uric acid stones from other types of calculi. **Uric acid stones have an attenuation range between 150-500HU while other calculi have ranges higher than 500HU.** There is however enough overlap that an absolute diagnosis of stone composition cannot be made. Different models of CT scanners may also yield different attenuation values for the same stone.^{129,134,135,136} Masses within the collecting system include urothelial malignancies, benign polyps, fungal balls, and foreign bodies. These are visualized with very high sensitivity and typically appear as filling defects during the excretory phase.



Figure 37: Coronal reconstruction from CTIVP showing left upper pole fillings defect which proved to be blood clot

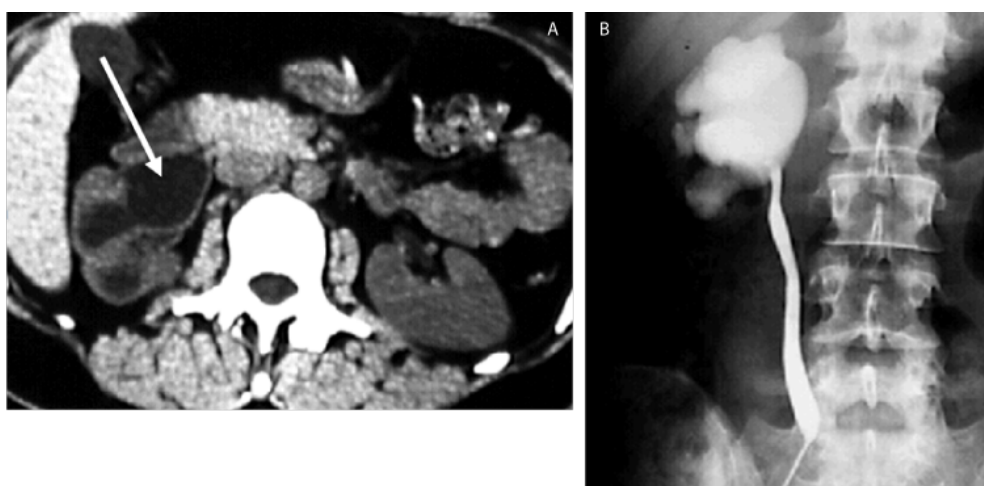


Figure 38A and 38B: Hydronephrosis on CT (arrow) and retrograde pyelogram secondary to UPJ obstruction.

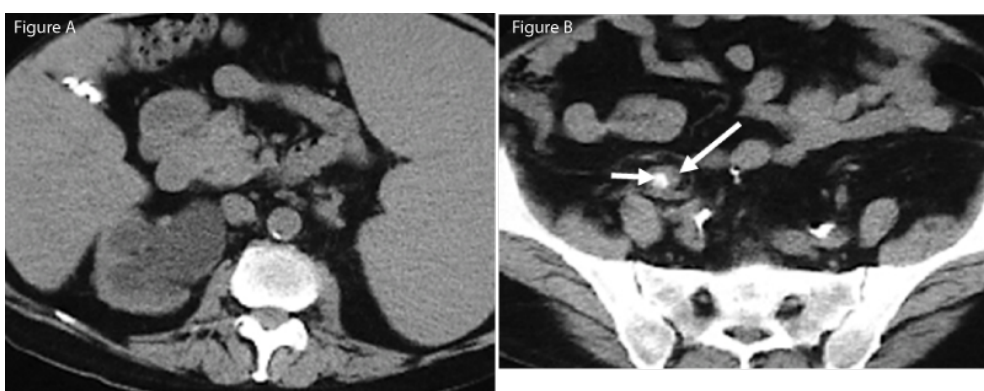


Figure 39A and 39B. Non contrast stone protocol CT

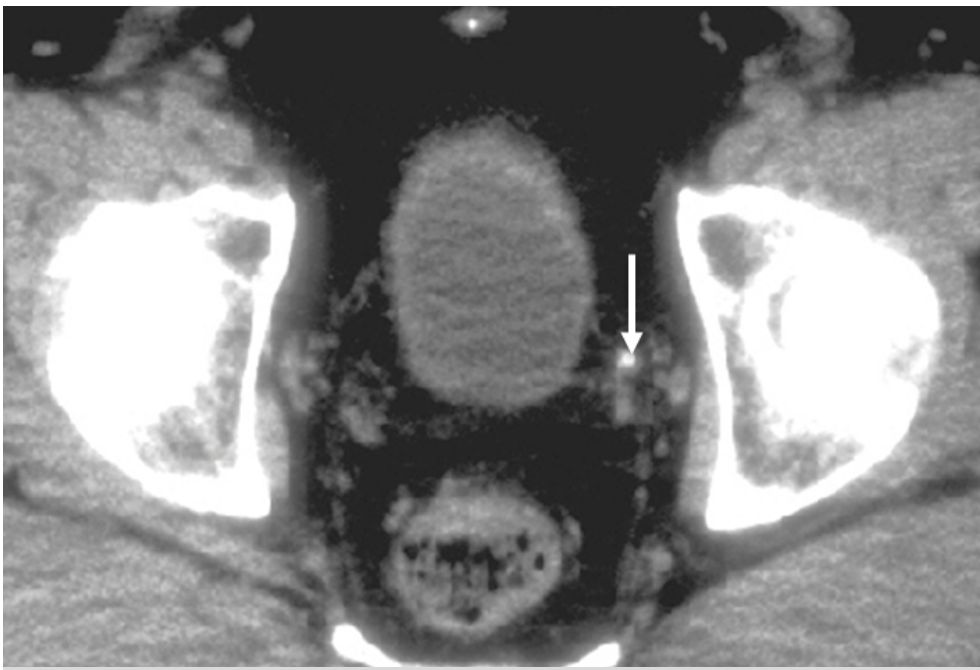


Figure 40: Non contrast CT showing distal ureteral stone with edematous ureter ie. rim sign (arrow)

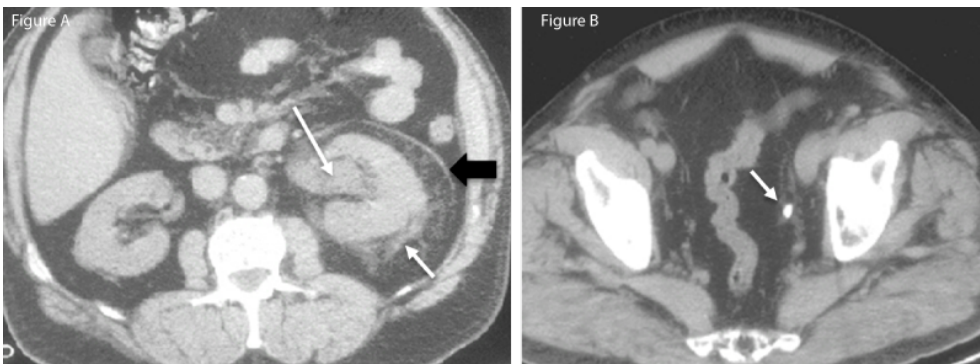


Figure 41A and 41 B: Non contrast CT A shows hydronephrosis (long white arrow), perinephric stranding (short white arrow) and thickening of Gerota's fascia (black arrow) due to a distal ureteral stone (arrow) shown in B

7.2.6 Retroperitoneal Urologic Pathology

The retroperitoneum is a potential space and is commonly the site of hemorrhage, fluid collections, adenopathy and fibrosis. **Hemorrhage** in the retroperitoneum may be the result of trauma or from the spontaneous rupture of a vessel (**Figure 42**). The most common cause of non-traumatic hemorrhage is a ruptured abdominal aortic aneurysm. The likelihood of spontaneous bleeding increases significantly with aneurysms greater than 5cm in diameter. Other common causes of spontaneous bleeding include rupture of a renal neoplasm or renal artery aneurysm. Diseases of the

adrenal gland, most commonly primary or secondary malignancies, may also spontaneously rupture. In 5-15% of cases the source of retroperitoneal hemorrhage may not be identified. **Acute hemorrhage is seen as an accumulation of fluid with an attenuation measuring 40 to 60 Hounsfield units.** The attenuation of the hematoma decreases over time, approaching water density during the final stages of resolution.¹²²

Extravasated urine (urinoma) is typically the result of a postoperative urine leak, renal injury or spontaneous fornecal rupture from obstruction. Urine collections will measure attenuation similar to that of water. Delayed cuts after contrast may demonstrate the presence of contrast outside of the collecting system.

Retroperitoneal adenopathy is typically the result of metastatic disease. Common malignancies include testicular cancer (**Figure 43**), lymphoma, renal cell carcinoma, and urothelial malignancies (**Figure 44**). **A retroperitoneal lymph node is considered enlarged if it is greater than 10mm in the short axis. When imaging patients with testicular cancer, a cutoff of 6-7mm is frequently considered to be abnormal.**

Primary retroperitoneal tumors are extremely rare. Benign tumors include lipomas, myelolipomas and nerve sheath tumors. Liposarcomas are the most common malignant primary retroperitoneal tumors and will appear as well defined fatty masses that may be difficult to differentiate from lipomas. They also may contain non fatty components which may suggest dedifferentiation.¹³⁷ Leiomyosarcomas arise from the walls of blood vessels, usually the middle third of the IVC. They typically appear as large masses with variable areas of necrosis (**Figure 45**).

Retroperitoneal fibrosis is a proliferation of fibrotic tissue that is usually around the lower abdominal aorta and common iliac vessels. The etiology is idiopathic in the majority of cases however it may result from radiation therapy, malignancy, drugs, and retroperitoneal hemorrhage. The desmoplastic reaction may entrap the ureters and lead to renal obstruction (**Figure 46**). The fibrotic plaques appear on CT as areas of low attenuation (30-50HU). The plaques usually do not displace the aorta. The degree of enhancement of the plaque after contrast varies and depends on the amount of fibrotic activity within the plaque. A biopsy is often required to rule out a malignant process.



Figure 42: Massive retroperitoneal bleed (white star) displacing the left kidney (white arrow) anteriorly. The bleed is relatively high density consistent with recent bleed. Metalic density (black arrow) in kidney is an embolization coil.



Figure 43: Metastatic low density retroperitoneal lymph nodes (white arrow) secondary to embryonal cell testis cancer

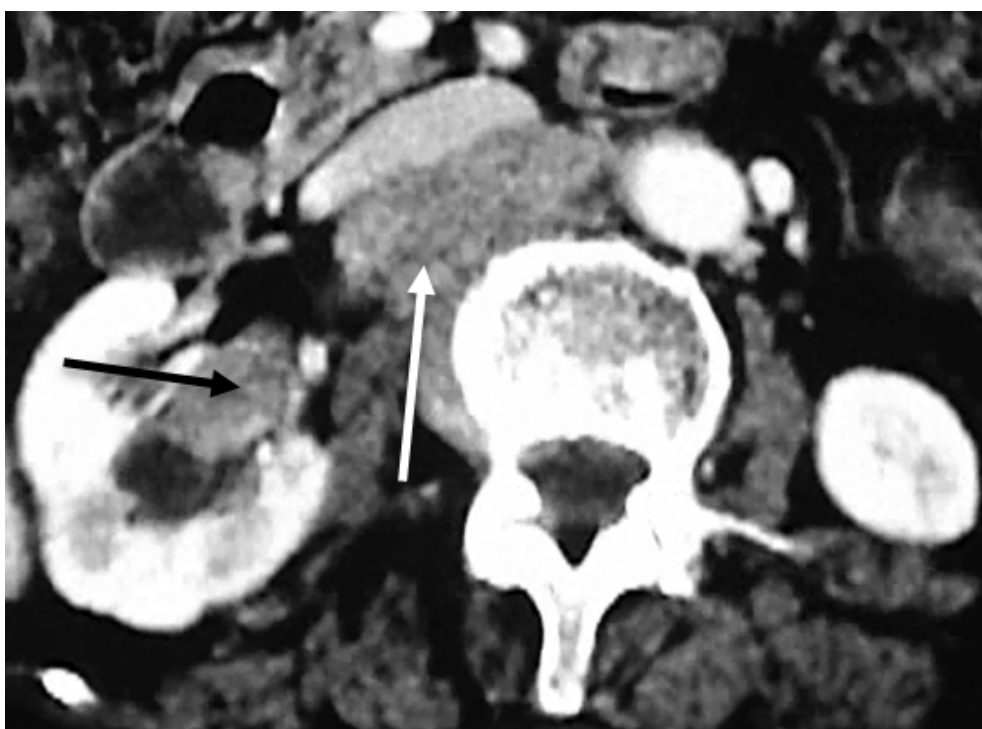


Figure 44: Axial CT with enhancement shows solid tissue in the right renal pelvis (black arrow) representing TCC as well as metastatic retroperitoneal adenopathy (white arrow) posterior to the IVC.



Figure 45: Large right retroperitoneal mass represents malignant transformation of a dermoid, Note the fat-fluid level (white arrow) in the anterior portion of the lesion



Figure 46: Coronal reconstruction from a CTIVP shows soft tissue (black arrow) encasing the right ureter in a patient with retroperitoneal fibrosis. The ureter is not significantly displaced medially as often seen in retroperitoneal fibrosis

8. Urinary Bladder

Imaging of the bladder by CT is useful in identifying pathologies of both the bladder wall as well as the lumen. **Bladder distension by contrast is key to the adequate visualization of the bladder.** Disorders of the bladder wall include congenital, infectious, neoplastic, and inflammatory etiologies.

8.1 Congenital Abnormalities

Congenital abnormalities of the bladder wall include congenital diverticulae, bladder duplication, exstrophy, and urachal abnormalities. Congenital diverticulae usually lie in close relationship to the ureteral orifice. The diverticulum may distort the ureteral orifice and lead to reflux (hutch diverticulum). Images on CT will typically reveal a contrast filled cavity lateral to the ureteral orifice. The urachus represents the obliterated allantois to the umbilical cord. Failure of the cord to completely obliterate may lead to a urachal sinus, diverticulum or cyst depending on what part of the allantois remains patent. A diverticulum of the dome of the bladder at the midline should raise

suspicion. Cysts may occasionally become infected and appear as an abscess in the midline with areas of variable attenuation depending on the amount of necrosis. ¹²³

8.2 Bladder Wall Pathology

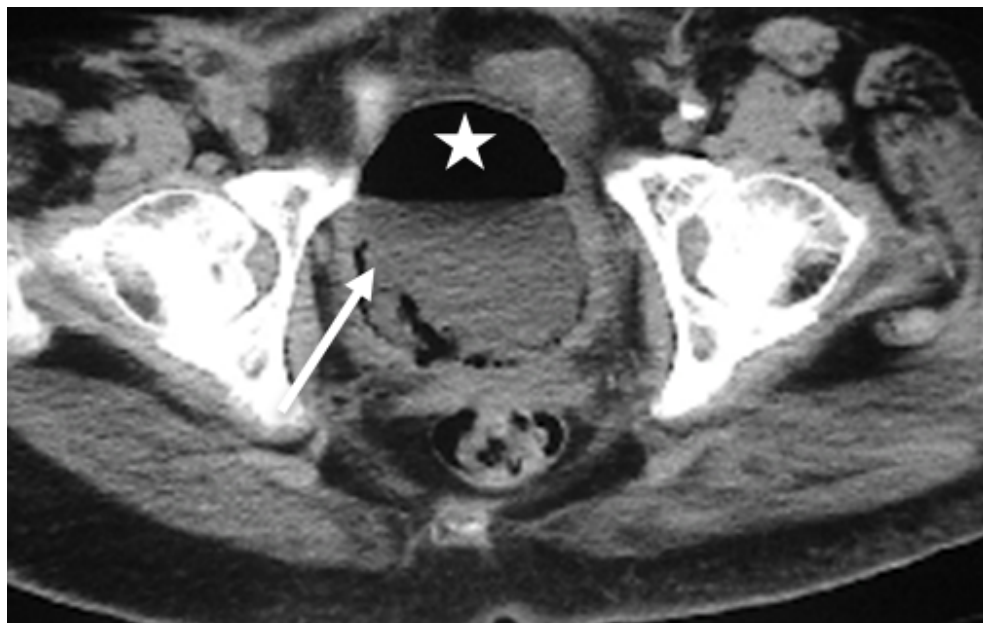


Figure 47: Pelvic CT showing gas within the bladder wall (white arrow) as well as the bladder lumen (white star) is diagnostic of emphysematous cystitis

8.2.1 Infections

Infections of the bladder wall (cystitis) invariably lead to some degree of bladder wall thickening and edema. Edema tends to appear as thickening of the wall with slightly decreased attenuation compared to the surrounding soft tissue. It is not possible to differentiate the acute edema that arises from acute cystitis from noninfectious causes of edema. Chronic cystitis however may lead to a decreased bladder capacity or thickening of the muscular wall, which may be appreciated, on CT. Emphysematous cystitis is a rare type of infection secondary to gas producing bacteria. Gas produced may migrate into the bladder wall and is commonly associated with immuno-compromised patients. Gas within the mural wall of the bladder on CT is diagnostic. ¹³⁸ Gas within the bladder lumen itself also raises the possibility of a fistula from the bladder to either the vagina or the bowel. This may arise secondary to inflammatory such as Crohn's disease or diverticulitis. Malignancy or iatrogenic trauma are also possibilities that should be considered. CT is highly sensitive for the detection of gas within the lumen. The visualization of contrast from the bladder into the bowel is diagnostic, however this is only seen in 50% of patients (**Figure 47**).^{132,139}

8.2.2 Other Causes of Bladder Wall Pathology

Calcifications of the bladder wall may occur secondary to infections such as schistosomiasis or tuberculosis. Other etiologies include radiation cystitis, amyloidosis, and cyclophosphamide cystitis.

Non contrast images will reveal areas of increased attenuation within the bladder wall.

Diffuse thickening of the bladder wall is commonly secondary to BPH in men but may also be a sign of neurogenic bladder or malignancy. Bladder diverticulae may also be seen in the setting of chronic obstruction in adults. They tend to be multiple and appear on delayed cuts as thin walled fluid filled sacs protruding from the bladder. Stones within the diverticulae may be seen on unenhanced images.

8.2.3 Bladder Cancer

Malignancies of the bladder wall have a wide variety of clinical presentation. This varies from subtle thickening of the bladder wall to large masses extending extravesically. CT is quite sensitive for the detection of bladder masses (**Figure 48**). They typically appear as an area of mural thickening. Smaller papillary masses may appear as filling defects within a contrast filled bladder. Larger masses may be seen to extend outside of the bladder. Small mucosal lesions and carcinoma in situ however can be easily missed on CT. CT is therefore an adjunct, not a replacement, to cystoscopy. **It is not sensitive enough to detect muscle wall invasion However, perivesical stranding may be suggestive of T3 disease, which may be also be caused by edema or post endoscopic resection inflammatory changes as well.** Hydronephrosis may also indicate intramural ureteral obstruction and extravesical extent of disease. While CT is not useful for ascertaining histologic subtypes, masses seen at the anterior aspect of the bladder extending extravesically should raise concern for urachal remnant adenocarcinomas (**Figure 50**).¹⁴⁰

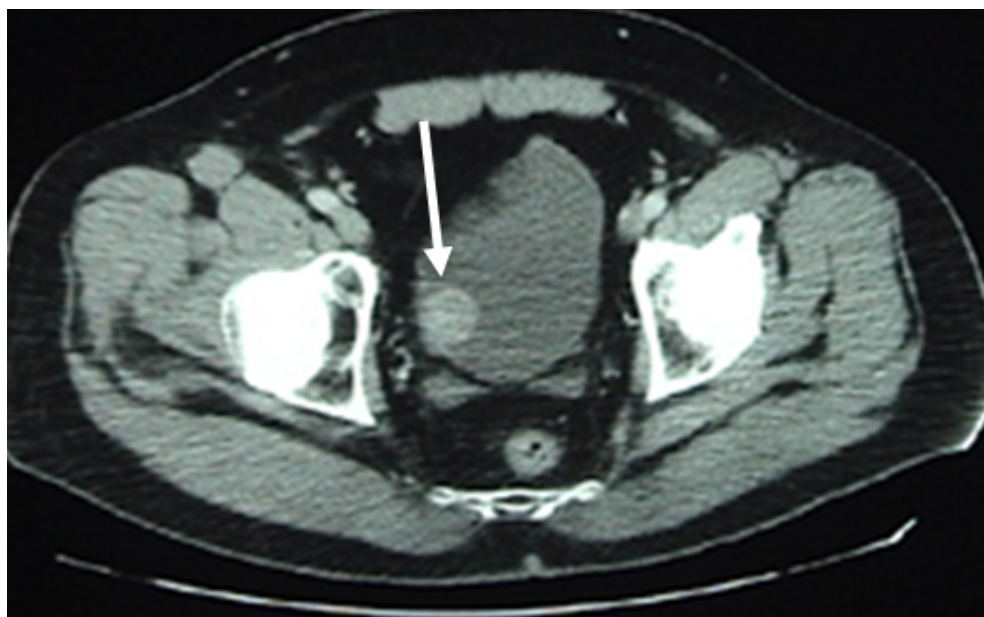


Figure 48: Enhanced pelvic CT showing a well circumscribed enhancing bladder tumor (arrow)

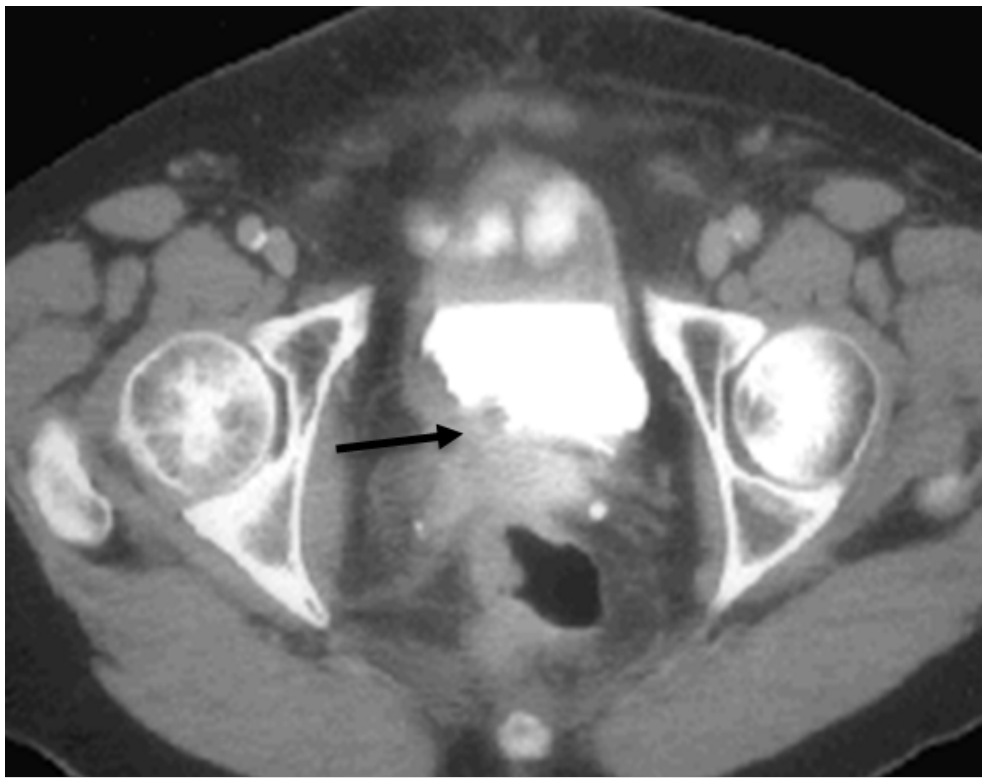


Figure 49: Delayed pelvic CT with bladder partially filled with contrast showing irregular right posterior bladder tumor with thickened bladder wall (arrow) and probable extension outside of bladder.

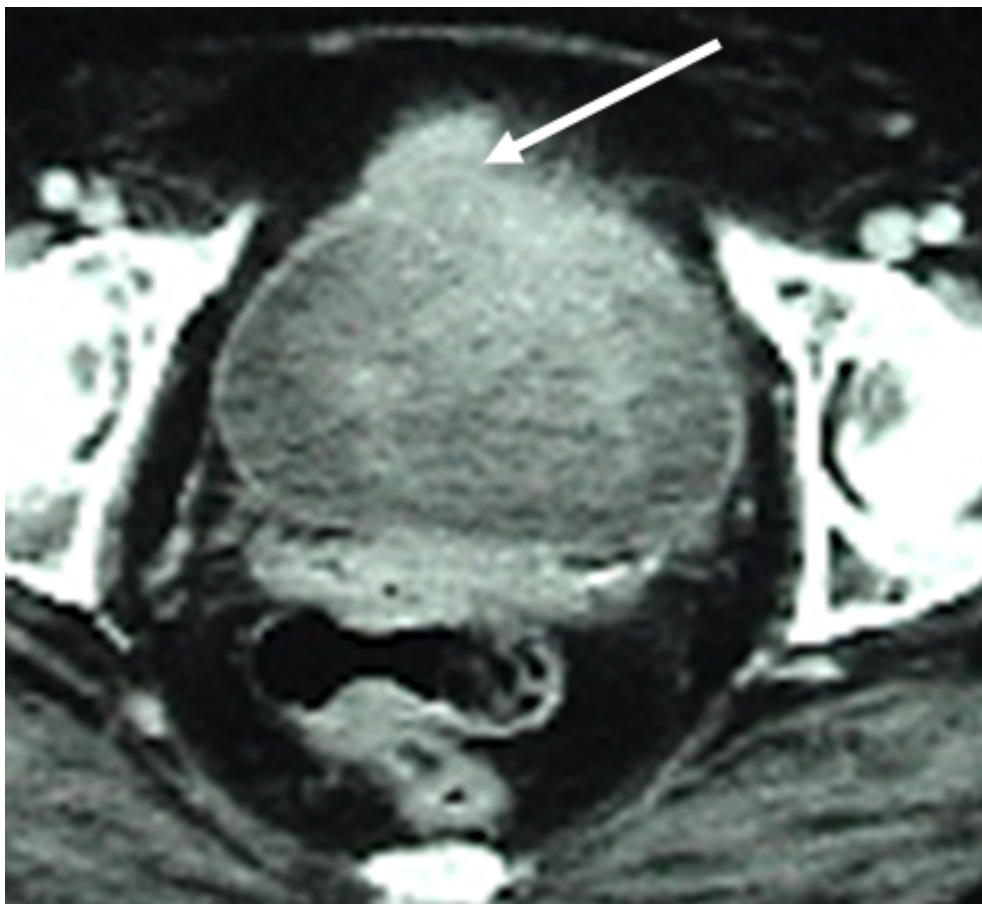


Figure 50: Solid enhancing bladder mass involving the anterior bladder in the midline and extending outside the bladder wall. Lesion does not significantly extend along the course of the urachus, but was surgically proven to be urachal carcinoma

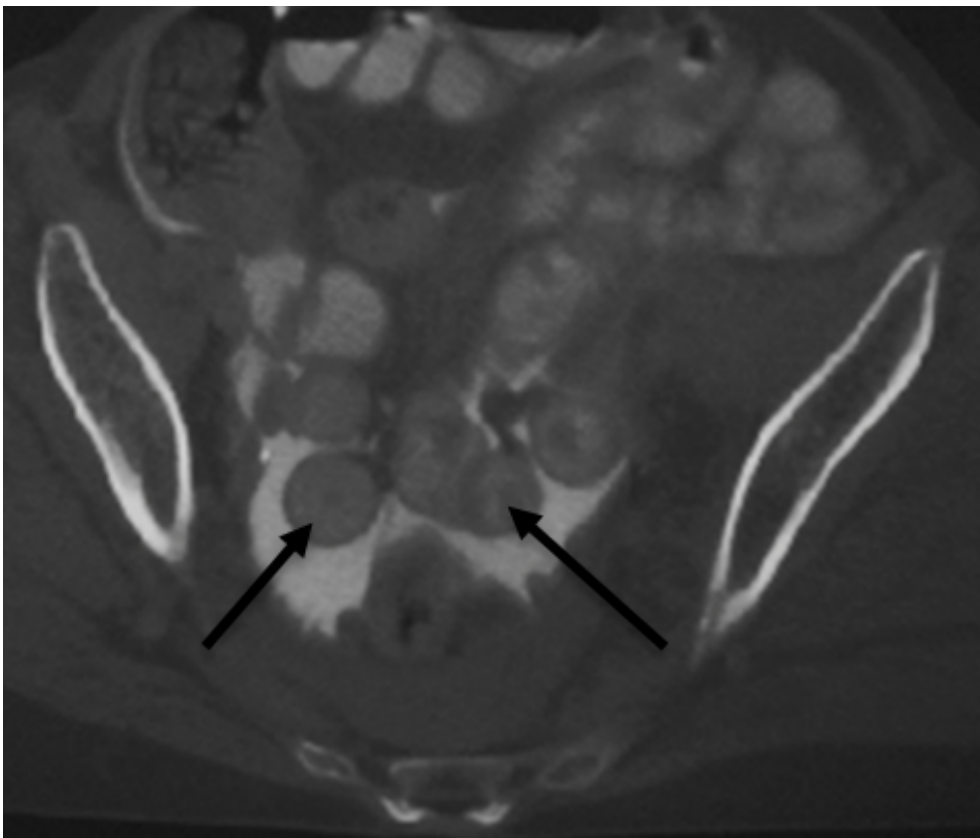


Figure 51: Pelvic CT following cystography showing contrast (white) surrounding bowel loops (arrows) and indicating intraperitoneal bladder injury

8.2.4 Bladder Trauma

Trauma of the bladder may be secondary to blunt or sharp injury. CT cystography is commonly used to evaluate bladder injuries. Excreted contrast from the ureters is not sufficient to evaluate bladder injuries and thus contrast must be injected in a retrograde fashion. It is not sufficient to clamp the catheter and wait for filling of the bladder with contrast. Contrast should be diluted to approximately 3% (6:1 with saline) to allow for adequate visualization. When adequately performed, CT cystography is nearly 100% sensitive for the detection of bladder rupture. Intraperitoneal injury will reveal the presence of contrast in the paracolic gutters or outlining the bowel wall. Contrast is seen limited to the extravesical space in extraperitoneal injury although it may track down fascial layers into the thigh, scrotum, penis, or perineum (**Figure 51**).^{132,141}

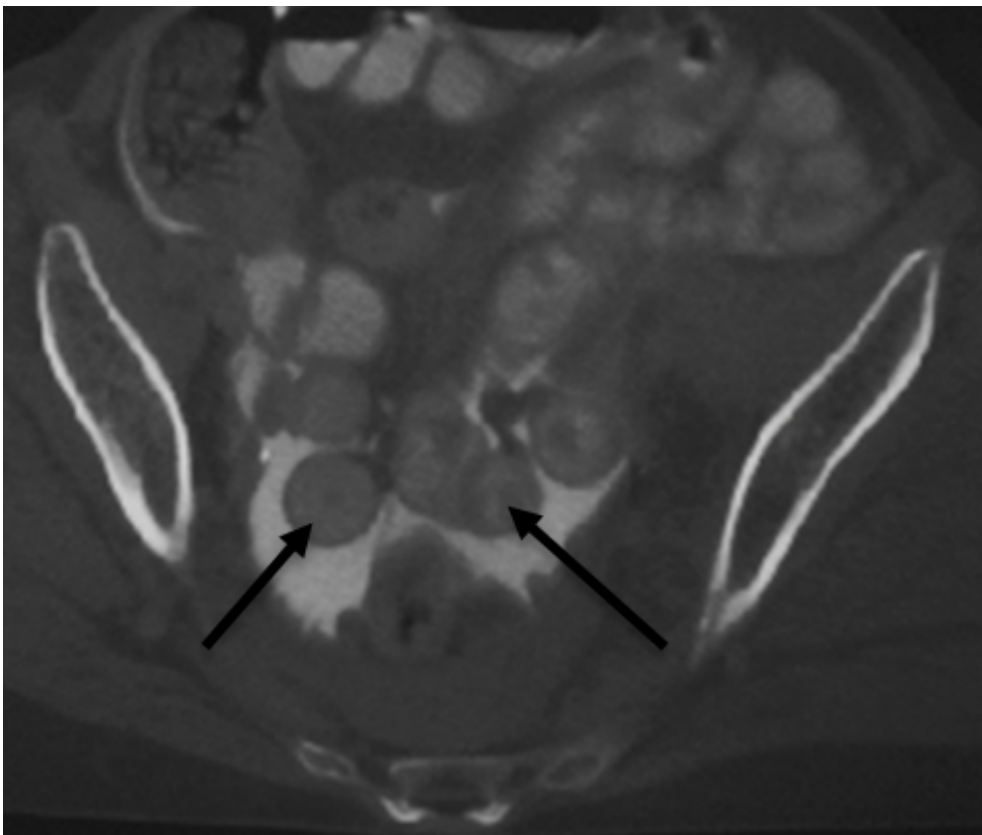


Figure 51: Pelvic CT following cystography showing contrast {white} surrounding bowel loops (arrows) and indicating intraperitoneal bladder injury

9. Prostate

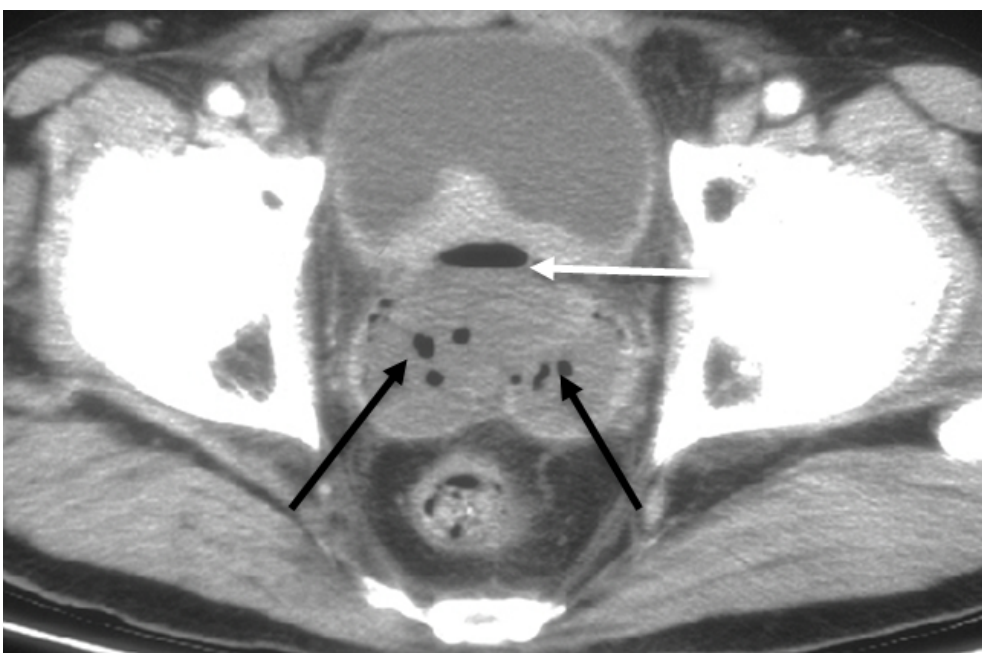


Figure 52: Prostatic abscess containing focal air (black arrows) and air-fluid level (white arrow) Soft tissue thickening at base of bladder is also present.

9.1 Benign Prostatic Hyperplasia (BPH)

Prostate ultrasound is typically the radiologic modality utilized to assess benign prostatic hyperplasia (BPH). For uncomplicated BPH, CT scan should not play a role in evaluation, treatment and management. BPH is more frequently an incidental finding noted on CT scan of the pelvis obtained for other indications. On axial imaging, extension of the prostate gland above the symphysis pubis can be a marker of enlarged prostate size, but volume acquisition using axial/coronal/sagittal reformatting should allow for measurement of prostate size. **Overestimation** of prostate volume on CT (up to 30-50% compared to transrectal ultrasound) is relatively common due to limited soft tissue contrast so that differentiation of the prostate from the bladder wall or levator ani muscles is not easily performed.¹⁴²

9.2 Acute and Chronic Prostatitis

Diagnosis of acute and chronic prostatitis is typically made based on history, physical examination, and urinary studies. Radiographic imaging is **not** routinely part of the evaluation of these conditions.¹⁴³ However, if a patient with suspected acute prostatitis either does not demonstrate improvement on appropriate antibiotic therapy or an examination reveals a soft, tender prostate concerning for abscess, a CT scan is recommended.¹⁴⁴ On CT, acute prostatitis will appear as a diffusely enlarged, edematous gland with predilection for peripheral zone involvement. Chronic prostatitis may appear as an area of hypoattenuation in the prostate on CT, although this may also be present in prostatic abscess, cystic masses of the prostate (e.g. Mullerian Duct cyst) or prostatic tuberculosis. In this latter condition, CT may demonstrate focal hypoattenuating areas in the outer gland.

9.3 Prostatic Abscess

Contrast enhanced CT is the best imaging tool if abscess suspected. When an abscess is present it is seen as a nonenhancing fluid-density collection with rim-enhancement (**Figure 52**).¹⁴⁵ This lesion can be a unilocular or multilocular hypodensity in the peripheral zone. Central zone involvement is encountered in post transurethral resection of prostate procedure. The abscess can extend through the pelvic diaphragm into the base of the penis.

9.4 Prostatic Infarct

Little data exists regarding the utility of CT for evaluation and management of prostatic infarction. Radiographic appearance of prostatic infarct varies based on the chronicity of the event with the timing of imaging. Initially in the natural history of this condition, prostate tissue swells and hypodensity may not be as prominent due to adjacent inflammation and reaction. However, after 48-72 hours, a defined hypodensity may be visible in the area of affected tissue.

9.5 Prostatic Cyst

Cystic lesions of the prostate are most commonly identified on ultrasound or MRI but may be visible

on CT as **sharply marginated, homogeneously hypodense thick walled cystic lesions** within the prostate.¹⁴⁶ They are incidentally observed in 0.5-7.9% of patients.¹⁴⁷ These may represent a variety of etiologies, including prostatic utricle cyst, Mullerian duct cysts, ejaculatory duct cysts, prostatic retention cysts, infectious/inflammatory/parasitic cysts and cystic degeneration associated with BPH or cancer.^{148,149}

9.6 Prostatic Calculi

CT has great sensitivity in identifying the one to hundreds of prostatic calculi that are often found in the prostate gland. On axial imaging, they are commonly located at the apical margin of the prostatic adenoma within the cleavage line between nodular hyperplasia and the surgical capsule.^{150,151} While they are thought to be formed under inflammatory conditions, many men with these stones presents are symptomatic. **However, as the majority of calculi are discovered incidentally, the significance of this finding is often unclear.**

9.7 Prostate Malignancies

9.7.1 Adenocarcinoma of the Prostate

Role of CT in the evaluation and staging of prostate cancer

The utility of CT scan for management of prostate cancer is less than in other genitourinary malignancies. In the absence of contrast, the prostate has uniform density (40-65 HU), similar to skeletal muscle. With contrast, the peripheral zone may appear relatively hypoattenuating. In general, CT is **inadequate** to evaluate the prostate gland itself, but rather may provide detail regarding gross extracapsular disease (including seminal vesicle invasion) and nodal or visceral metastatic disease. As such, this modality should only be used in selected patients for initial staging. These include patients with T3 or T4 disease or those with >10% probability of lymph node involvement.¹⁵²

The primary role of CT in prostate cancer diagnosis is size determination, assessment of nodal metastases in the pelvis and treatment planning for radiation therapy. **CT demonstrates a 32% increase in prostate volume compared with MRI**,¹⁵³ with the primary discrepancy arising from differences in measurement of the prostatic apex, neurovascular bundles and posterior aspect of the gland. CT lacks the resolution of MRI to detect intraprostatic disease, extracapsular extension, or seminal vesical involvement. Given the relative infrequency of positive lymph nodes in newly diagnosed prostate cancer in the PSA screening era and the poor correlation between nodal size and metastatic involvement,¹⁵⁴ **CT plays a limited role unless the PSA level is greater than >20 ng/dL**.¹⁵⁵

9.7.2 Tumors Invading the Prostate (colon, bladder)

As CT imaging is the mainstay for radiographic imaging for both gastrointestinal and bladder cancers, the initial suggestion of local invasion of the prostate is typically first seen on CT scan. The involvement of bladder cancer into the prostate is difficult to assess radiographically due to lack the

distinction between the two soft tissue structures on CT and is best characterized through transurethral resection and histologic evaluation. **Involvement of colon cancer** with the bladder can be assessed as violation of the perivesical fat surrounding the bladder is an ominous sign and is well characterized on contrasted CT scan. A contiguous mass between an irregularly thickened bladder wall and colon wall on CT with follow-up cystoscopy has been shown to predict up to 80% of urinary bladder invasion with colorectal carcinomas.¹⁵⁶ CT was shown to predict both macroscopic invasion and pathologic involvement with high specificity, but did not discriminate between pathologic invasion and inflammatory adhesion.

10. Seminal Vesicles

10.1 Congenital Absence of Seminal Vesicles

There are two subsets of patients with seminal vesicle agenesis. The first have an embryologic insult to the mesonephric duct with associated ipsilateral absence of the vas deferens and kidney.^{157,158} The second have agenesis of the vas deferens secondary to a mutation in the cystic fibrosis transmembrane conductance regulator gene CFTR but the kidneys are normal.¹⁵⁹ As the seminal vesicles are well visualized on CT scan, their absence is easily detectable and would prompt abdominal CT for characterization of the kidneys.¹⁶⁰

10.2 Seminal Vesicle Dilatation/Cyst

Ejaculatory duct obstruction is typically identified as part of an azoospermia workup and is defined as dilated seminal vesicles with an anterior-posterior length greater than 1.5 cm or ejaculatory ducts with a diameter greater than 2.3 mm.¹⁶¹ As previously mentioned, the resolution of CT is limited in evaluating the ejaculatory ducts and surrounding structures and this diagnosis is most commonly made by transrectal ultrasound. Congenital cysts of the seminal vesicle can be isolated in nature or associated with upper urinary tract anomalies (such as ipsilateral renal agenesis or dysplasia, seen in two thirds of patients or autosomal dominant polycystic kidney disease).¹⁶¹ This association occurs secondary to maldevelopment of the distal mesonephric duct and faulty ureteral budding and atresia of the ejaculatory duct.¹⁶² Cysts in the seminal vesicles are often discovered incidentally in the second to third decade of life.¹⁶³ However, if very large, they may be associated with voiding difficulties.

These cysts are visualized on CT as **a clearly marginated mass with attenuation consistent with water (> 40 HU) that arises from the seminal vesicle cephalad to the prostate gland behind the bladder**.¹⁶⁴ Reported variations on CT include irregularity of the cystic wall to obstruction and dilation of the ipsilateral seminal vesicle.¹⁶⁵ Rarely, cystic dilation of the seminal vesicle occurs secondary to ectopic ureteral insertion into the seminal vesicle, but CT is inferior to MRI to demonstrating the connection between the two structures.^{166,167,168}

10.3 Inflammation

Seminal vesicle hydatid cysts are a rare cause of inflammation, but CT is a useful modality to assess

for these.¹⁶⁹ **Cysts are typically thin walled with water density, and daughter cysts may be visible.**¹⁷⁰ These cysts can evolve into abscesses and require percutaneous drainage.

11. Scrotum

The most commonly utilized modality to detect scrotal and intrascrotal anatomy and pathology is color Doppler ultrasonography. For reasons of radioprotection, CT is not indicated for the routine evaluation of the anatomy of these organs. As such, CT should not be a primarily modality for evaluation of the scrotum and its contents, although it can serve to identify hernias into the scrotum and undescended testes in the inguinal canals. **For primary testicular malignancies, CT is the mainstay for staging of intraabdominal, mediastinal and pulmonary metastatic disease.** MRI, which can provide much higher quality images of the scrotum and intrascrotal contents, rarely yields additional information beyond that obtained by ultrasound. Therefore, tests such as nuclear testicular scans, CT or MRI have essentially no role in the contemporary management of the acute scrotum.

11.1 Extratesticular Conditions

11.1.1 Benign extratesticular lesions: hydrocele, spermatocele, varicocele, epididymal cysts

For all four benign conditions listed above, ultrasound remains a very reliable means of evaluation and is a relatively quick, noninvasive and inexpensive test. **Very few indications exist for additional imaging including CT scan for any of the above conditions.** For hydrocele, an avascular mass with fluid attenuation extending through the inguinal canal may represent an abdominoscrotal hydrocele which may be confused with an abdominal mass.¹⁷¹ Spermatocele may demonstrate a fluid collection of greater density than simple fluid, which may aid in the differentiation between spermatocele and other extratesticular fluid collections.¹⁷² CT scanning with increased intra-abdominal pressure can detect varicocele and demonstrate the proximal extension of this lesion. Classically, unilateral right-sided varicoceles are rare and should prompt the urologist to consider pathologies that cause inferior vena cava obstruction such as right-sided renal cell carcinoma or lymphoma.¹⁷³ However, the sudden onset of a non-reducing left-sided varicocele may also represent obstruction of the testicular vein due to involvement of the left renal vein.¹⁷⁴ **While CT has no standard role in the evaluation of epididymal cysts, the presence of these lesions with other pathology findings on CT (retinal angiomas, pheochromocytomas, hemangioblastomas of the cerebellum and spinal cord, and renal cell carcinomas as well as angiomatous or cystic lesions of the kidneys and pancreas) may suggest a complete workup and investigation for von Hippel-Lindau disease.**¹⁷⁵

11.1.2 Hernia

While hernia is often a clinical diagnosis based on history and physical examination, CT can serve as a useful **adjunct** to further characterize the etiology. If the hernia contains fat, it can be identified by either ultrasound or CT, although CT may provide greater resolution regarding whether a spermatic cord lipoma is present. Bowel loops within the hernia can easily be identified by the presence of air

or administered oral contrast. If there is concern regarding herniation of the ureter or bladder, CT is the optimal study as urography can opacify the intrascrotal component and the bladder or ureter can be traced back to the intraabdominal component of the organ.

11.1.3 Epididymitis/Orchitis

As the clinical presentation for epididymitis or orchitis can mimic testicular torsion, distinguishing these two etiologies (infarction from infection/inflammation) is critical. Because of the incorporation of color Doppler, ultrasound is the primary modality to identify decreased flow in torsion compared with increased flow in epididymitis/orchitis. In most circumstances, there is no role for CT in the evaluation of these conditions. Emphysematous epididymo-orchitis is a rare entity which may occasionally not be fully characterized on clinical exam and **CT may be needed to identify gas in the scrotum**.¹⁷⁶

11.1.4 Fournier's Gangrene

The diagnosis of Fournier's gangrene is typically made based on clinical symptoms and history, including urinary tract infection, recent urologic instrumentation or peri-rectal or colonic disease. Delay of management with antibiotics and surgery should not occur in order to obtain radiographic imaging.¹⁷⁷ However, if the patient is clinically stable, CT may aid in the extent and involvement of **disease (and therefore guide the surgical plan and potentially decrease unnecessary surgical intervention in unclear cases) by identifying subcutaneous emphysema in involved tissues**.

While plain radiography and ultrasound may also demonstrate these findings, CT has greater specificity than either of these modalities to assess the etiology of the disease, the anatomic pathways of spread, and the presence of fluid collections or abscess.^{178,179} It is estimated that at least 1/5 of patients with clinical manifestations of necrotizing fasciitis did not have evidence of necrotizing fasciitis during surgical exploration.^{180,181}

Furthermore, emerging evidence now supports routine use of CT prior to surgical intervention. In a 2010 study, 67 patients had a CT scan prior to intervention due to suspicion of necrotizing fasciitis, the sensitivity of CT to identify necrotizing infections was 100% and the positive predictive value was 76% and negative predictive value was 100%.¹⁸¹

CT findings in Fournier's gangrene include asymmetric fascial thickening, fat stranding around the involved structures, fluid collection or abscess, and subcutaneous emphysema secondary to gas-forming bacteria which may extend from the scrotum to the inguinal area, thighs, abdominal wall and retroperitoneum. Following treatment, CT can be utilized to assess for response to therapy.

11.1.5 Scrotal Abscess

Scrotal abscess and Fournier's gangrene may appear in the differential diagnosis of infection-related genitourinary pathology, but can be distinguished both on physical exam and on imaging. Again, ultrasound is the modality of choice due to superior imaging characteristics in the scrotum. On CT, a rim-enhancing fluid collection involving the scrotal sac is typically seen without significant changes in the scrotal skin, although non-specific thickening may be noted. This collection may contain

septations, debris or even multiple pockets of gas. Urogenital tuberculosis may originate in the prostate (granulomatous prostatitis) and descend to involve the epididymis; this condition is more often seen in immunocompromised men and those with HIV infection.

11.2 Intratesticular Conditions

11.2.1 Testicular Tumor

CT is **inferior** to color Doppler ultrasound for evaluation of intratesticular masses due to the ability to demonstrate increased flow to large tumors (and decreased flow to small tumors) and to display the contrast between normal testicular parenchymal tissue and the lesion. MRI can be used for initial diagnosis as well, but rarely adds additional information beyond ultrasound.

CT is the cornerstone of surveillance for testicular cancer following orchectomy and determination of histologic type.¹⁸² As the risk of retroperitoneal nodal recurrence and metastasis vary by histology, staging and treatment, the use of CT for testicular tumors varies as described below. For either pure seminoma or nonseminoma, the staging workup following inguinal orchectomy entails CT scan of the abdomen and pelvis to assess for retroperitoneal nodal metastases¹⁸³ and a chest CT if the abdominal CT is positive or a chest x-ray is abnormal. CT scan of the chest remains an ideal modality to assess for tumor involvement of thoracic, mediastinal and supraclavicular nodes.¹⁸⁴

11.2.2 Scrotal Trauma

Scrotal trauma may be detected on CT as part of a trauma workup, but diagnosis and etiology are typically made by clinical history, physical examination and ultrasound findings.¹³³ Very few papers discuss the role of CT in the rapid diagnosis of penoscrotal trauma.¹⁸⁵ If ultrasound findings are equivocal, typically surgical exploration is favored over additional imaging due to the relatively emergent conditions of testicular rupture and tunica albuginea fracture.¹⁸⁶

11.2.3 Testicular Torsion

Color Doppler ultrasonography has a superior sensitivity (97%), specificity (98%), positive predictive value (92%), and negative predictive value (99%) for testicular torsion compared with CT and MRI.¹⁸⁷ MRI with contrast enhancement is highly sensitive for testicular torsion,¹⁸⁸ but the limited availability, duration of study and cost make it an unfavorable first-line option for imaging. **Perfusion CT**, which is an indirect evaluation of tissue metabolic activity, has been studied in animal models¹⁸⁹ but caution should be placed on adding CT scans to the workup of pediatric patients given the associated radiation and costs of this technique.¹⁹⁰

11.2.4 Cryptorchidism

The preferred modality for a cryptorchid testis is ultrasound. Three-quarters of these will be in the inguinal canal below the internal inguinal ring and are easily accessible by this technique.¹⁹¹ **However, if the testis is not visible on ultrasound, either CT or MRI is the next option to identify an intra-abdominal testis.**¹⁹² Both techniques have their benefits and limitations; CT

requires radiation and does not have multiplanar capability, whereas MRI has superior soft-tissue contrast and multiplanar capability but loses discrimination when the testis is higher in the abdomen near loops of bowel. On CT, the cryptorchid testis is an oval soft-tissue mass which enhances homogenously with IV contrast and can be differentiated from a lymph node by the absence of a fatty hilum.

12. PENIS AND URETHRA

The penis and urethra are structures best imaged by modalities other than computed tomography.¹⁹³ For intraluminal urethral lesions, retrograde urethrography and voiding cystourethrogram (in conjunction with urethroscopy) are the optimal studies to assess for traumatic injuries, inflammatory conditions, malignancy and stricture disease. Periurethral lesions can be assessed by cross-sectional imaging including CT, but ultrasonography (for assessment of the extent of urethral stricture disease) and MRI (for evaluation of urethral and periurethral soft tissue lesions) are often preferred.

At axial CT, the UGD is seen in contiguity with the prostatic apex. The prostatic urethra is typically not seen on axial CT. The UGD surrounds the membranous urethra and is mainly formed by the deep perineal muscles, including the transverse perinei profundi and the sphincter urethrae. At axial CT, the bulbocavernosus muscle is seen as a small U-shaped muscle that surrounds the bulb of the penis, which is an enlargement of the proximal corpus spongiosum. At the medial aspect of the ischiopubic ramus, the penile crura are seen with the ischiocavernosus muscle, which originates from the medial aspect of the ischial tuberosity and inserts on the ramus, covering the crus of the penis. Distally, the muscle merges with the corpus cavernosum.

12.1 Urethral Injury

While retrograde urography is the traditional method for diagnosing urethral injury from blunt trauma, CT is typically utilized for global assessment of the injured patient. However, The CT findings of elevation of the prostatic apex, extravasation of urinary tract contrast material above the urogenital diaphragm (UGD), and extravasation of urinary tract contrast material below the UGD were specific for type I, II, and III urethral injuries, respectively . If extraperitoneal bladder rupture is present along with periurethral extravasation of contrast material, the possibility of type IV and IVA urethral injuries should be considered. In addition, the CT findings of distortion or obscuration of the UGD fat plane, hematoma of the ischiocavernosus muscle, distortion or obscuration of the prostatic contour, distortion or obscuration of the bulbocavernosus muscle, and hematoma of the obturator internus muscle were more common in patients with pelvic fractures and associated urethral injuries than in patients with uncomplicated pelvic fractures. ¹⁹⁴ (see **Table 3**)¹⁹⁵

Table 3 CT Findings in Pelvic Fractures and Associated Urethral Injuries

Injury Type	Findings
I	The posterior urethra is stretched and elongated but intact. The prostate and bladder apex are displaced superiorly due to disruption of the puboprostatic ligaments and resulting hematoma.
II	Disruption of the urethra occurs above the urogenital diaphragm (UGD) in the prostatic segment. The membranous urethra is intact.
III	The membranous urethra is disrupted with extension of injury to the proximal
IV	Bladder neck injury with extension into the proximal urethra.
IVA	Injury of the base of the bladder with periurethral extravasation simulating a true type IV urethral injury.
V	Partial or complete pure anterior urethral injury.

12.2 Urethral Stricture

CT is **rarely** used to study the urethra, but can be helpful for the evaluation of inflammatory fluid collections or the identification of gas formed during necrosis or trauma.¹⁹⁶ Some centers have begun to use CT voiding urethrography to assess the urethra for urethral pathology.¹⁹⁷ This protocol involves thinly collimated transverse images (0.75 mm collimation) which may provide high quality of the reformatted images. The authors note the ability to compare luminal size and stricture length and distance from the urethral meatus as well as the fact that voiding urethrography is more physiologic than retrograde urethrography, which involves forceful injection of contrast medium which may overcome the resistance of a stricture. However, this technique is used in a limited number of locations and should not yet be considered an alternative to traditional retrograde techniques.

12.3 Penile Cancer

For the majority of men with a primary penile cancer, a clinical examination with examination of the penis and inguinal region is indicated for men treated with local therapy alone (topical, laser, radiation, wide local excision, partial penectomy or total penectomy) or in men who were N0 or N1 at the time of ilioinguinal lymph node dissection.¹⁹⁸ Patients without nodal involvement have a regional recurrence rate of 2%, and more than 90% will be detected within 5 years of primary treatment.¹⁹⁹ If a patient has an abnormal exam or has had prior inguinal surgery or obesity that limits the ability to perform a satisfactory examination, then **CT of the pelvis can be considered to better characterize the inguinal region.**²⁰⁰

12.4 Urethral Cancer

MRI is the preferred method for evaluating urethral neoplasms secondary to the superior soft-tissue resolution and improved anatomic detailed compared with CT scanning.²⁰¹ However, MRI is not as commonly available as CT and requires specialized personnel to acquire optimal images and interpret them. Staging of urethral cancer is typically performed with CT of the chest, abdomen, pelvis and perineum.

13. SURVEILLANCE OF UROLOGICAL CONDITIONS

CT remains the **mainstay** for evaluation and surveillance of the majority of urologic malignancies. Its availability, speed and consistency make computerized tomography a highly reliable and accurate tool in the surveillance of both benign and malignant urologic conditions.

13.1 Adrenal

The use of follow-up imaging in adrenal tumors is based on tumor size and predicted histology based on CT characteristics. If the primary lesion is **≤ 10 HU** on unenhanced imaging, the tumor is likely benign whereas when the lesion is **> 10 HU** on unenhanced imaging, additional evaluation of the enhanced images with associated washout.²⁰² If there is **> 60%** washout of contrast in 15 minutes following uptake, the lesion is likely to be benign whereas if it is below this threshold, the tumor may be

malignant. For benign-appearing adenomas < 4cm on CT scan or myelolipoma of any size by radiographic features, **repeat imaging is recommended in 6 to 12 months by NCCN guidelines.**²⁰³ If the primary lesion is unchanged, no further imaging is needed; alternatively, if the primary lesion has enlarged > 1cm in 12 months, either adrenalectomy or short-interval follow-up is recommended. For benign-appearing adenomas of intermediate size (4-6cm), **repeat CT is recommended in 3 to 6 months.** If the size of the mass is unchanged, repeat imaging is recommended in 6 to 12 months, whereas adrenalectomy is recommended if the tumor enlarges more than >1 cm in 1 year due to increased suspicion for carcinoma. For adrenal tumors that are suspected carcinomas, imaging of the chest, abdomen and pelvis is recommended to evaluate for local extension and metastasis prior to adrenalectomy. For patients with localized disease, follow-up with CT or MRI is recommended every 3 to 12 months for up to 5 years to evaluate for recurrence. If disease is metastatic, the interval for imaging should be 3 months with consideration of metastatectomy (if > 90% of the tumor volume is removable) or systemic therapy.

13.2 Renal

Active surveillance for small **renal masses** has increased in utilization.²⁰⁴ It appears that eventual management of these masses, if followed appropriately, do not compromise oncologic outcome.²⁰⁵ For patients who have undergone treatment (radical or partial nephrectomy, ablative techniques), NCCN guidelines recommend customized follow-up based on patient and tumor characteristics following an initial evaluation of chest and abdominal/pelvic imaging at 2 to 6 months after treatment.¹⁸² For Stage I-III tumors, the median time to relapse after surgery is 12 to 24 months after surgery and 20-30% of patients will have relapse with the lung being the most common site of metastasis.²⁰⁶ Therefore, the NCCN Kidney Cancer Panel recommends that patients have abdominal (+/- pelvic) and chest imaging every 6 months for the first two years after surgery and annually thereafter.¹⁸²

For patients with urothelial carcinomas of the renal pelvis or ureter, following treatment, imaging of the upper tract collecting system is recommended at 3 to 12 month intervals

13.3 Testis

CT is the cornerstone of surveillance for **testicular cancer** following orchiectomy and determination of histologic type.¹⁸² As the risk of retroperitoneal nodal recurrence and metastasis vary by histology, staging and treatment, the use of CT for testicular tumors varies as described below.

For pure seminoma, the post-diagnostic workup entails CT scan of the abdomen and pelvis to assess for retroperitoneal nodal metastases¹⁸³ and a chest CT if the abdominal CT is positive or a chest x-ray is abnormal. CT scan of the chest remains an ideal modality to assess for tumor involvement of thoracic, mediastinal and supraclavicular nodes.¹⁸⁴

Patients with stage IA and IB pure seminoma are offered surveillance (preferred option), chemotherapy or radiotherapy as standard treatment options after initial orchiectomy. As the risk of recurrence for stage I seminoma patients is highest in the first two years,²⁰⁷ for patient on

surveillance, an abdominopelvic CT scan should be obtained every six months for years 1 and 2, every 6-12 months for year three and annually for years 4 and 5 (7 to 8 CT scans total), with chest x-rays performed instead of chest CT as the common initial site of relapse will be in the retroperitoneum. Clinical trials are underway to determine if reduced intensity of CT imaging is safe in the surveillance of stage I seminoma.²⁰⁸ For patients who received adjuvant therapy with carboplatin or radiation therapy, the standard recommendation is for an annual abdominal and pelvic CT for the first three years after therapy, as late relapse after 3 years occurs in only 0.2% of patients.²⁰⁹ Follow-up thereafter is recommended for up to 10 years with history and physical with tumor markers alone. Patients with stage IS pure seminoma (a rare condition) are generally treated with radiation and have similar follow-up recommendations.

For patients with stage IIA/B pure seminoma, radiation is typically the standard treatment.²¹⁰ Following radiotherapy, an abdominal CT is recommended every 6 months in years 1 and 2 and annually in year 3. For those patients who have undergone retroperitoneal lymph node dissection (RPLND), only an initial abdominal CT scan is recommended at 3 to 6 months following surgery and then as indicated.²¹⁰ For pure seminoma stage IIC and stage III, following chemotherapy, patients are initially evaluated with a CT scan of the chest, abdomen and pelvis. If disease has resolved (or a residual mass is less than 3cm) and markers are normal, they can be followed with CT as clinically indicated. If PET scan demonstrates residual active tumor, RPLND may be considered if technically feasible and a CT scan should be performed at 3 to 6 months following surgery and then as clinically indicated.²¹¹

Management of non-seminoma of the testis following orchietomy is **similar** to management of seminoma, with CT of the abdomen and pelvis performed for staging. CT of the chest should be obtained if the CXR is abnormal. Primary treatment of nonseminoma stage IA disease is either surveillance or RPLND, whereas RPLND or chemotherapy (and surveillance in selected patients) is traditionally used to treat stage IB disease; the post-treatment frequency of imaging varies based on treatment decision. For stage IA/B patients on surveillance, abdominal/pelvic CT scan should be obtained every 3-4 months in year 1, 4-6 months in year 2, 6-12 months in years 3 and 4, 12 months in year 5 and then every 12-24 months after this period. If RPLND is performed, a CT is obtained following surgery to establish a baseline and then no additional studies are mandated unless clinically indicated. For nonseminoma stage IS and good risk patients with stage IIA/B/C or IIIA, abdominopelvic CT scan is recommended every 6 months in year 1, 6-12 months in year 2, every 12 months in years 3 to 5, and then as clinically indicated thereafter if there is a complete response to chemotherapy ± RPLND.

13.4 Bladder

All patients with newly diagnosed bladder cancer should have **imaging of the upper tract collecting system (IVP, CT urography, renal ultrasound with retrograde pyelogram, ureteroscopy, or MRI urogram) as well as a pelvic CT** if the prior study does not include imaging of the pelvis. Once clinical staging has been confirmed, upper tract collecting system imaging should be considered

every 1-2 years with one of the modalities as specified above for patients with T1 or high grade **non-muscle invasive** cancer.²¹² For patients with **muscle invasive** or selected patient with metastatic disease treated with curative intent, imaging of the chest, upper tracts, abdomen and pelvis should be performed every 3 to 12 months for two years, and then as clinically indicated.²¹³

13.5 Prostate

The utility of CT scan for management of **prostate cancer** is less involved than in other genitourinary malignancies. In general, CT is **inadequate** to evaluate the prostate gland itself, but rather may provide detail regarding gross extracapsular disease (including seminal vesicle invasion) and nodal or visceral metastatic disease. As such, this modality should only be used in selected patients for initial staging. These include patients with T3 or T4 disease or those with >10% probability of lymph node involvement.¹⁵² For patients with PSA persistence (failure to fall to undetectable levels) or recurrence following radical prostatectomy, a CT scan (or MRI) may be indicated based on risk category, Gleason grade and stage, PSA and PSA doubling time. For patients with biochemical failure or a positive DRE following radiation therapy, CT of the abdominal and pelvis may also be indicated. Low and intermediate risk groups with low serum PSAs postoperatively have a very low risk of positive CT scan. PET/CT is not routinely used in men with prostate cancer and data regarding its utility are limited.

13.6 Penile

For the majority of men with a primary **penile cancer**, a clinical examination with examination of the penis and inguinal region is indicated for men treated with local therapy alone (topical, laser, radiation, wide local excision, partial penectomy or total penectomy) or in men who were N0 or N1 at the time of ilioinguinal lymph node dissection. Patients without nodal involvement have a regional recurrence rate of 2%, and more than 90% will be detected within 5 years of primary treatment.¹⁹⁹ If a patient has an abnormal exam or has had prior inguinal surgery or obesity that limits the ability to perform a satisfactory examination, then CT of the pelvis can be considered to better characterize the inguinal region. For men with N2 or N3 disease, an abdominopelvic CT scan (or MRI) is recommended every 3 months in year 1 and then every 6 months in year 2.

13.7 After urinary diversion

Excretory urography and fluoroscopic retrograde contrast injections of the urethra, loop, pouch or neobladder are traditionally the methods for evaluating the urinary diversion. These techniques, though useful to identify issues such **as leak, obstruction and stricture, are limited in assessing tumor recurrence**. There is no strong consensus about the role of CT scan in routine follow-up of patients with urinary diversions. After urinary diversion excluding the urethra, recurrent cancer is identified in 6-10% of patients.²¹⁴ CT scan is limited except for the most proximal areas of the urethra, and intraoperative frozen section should be performed to ensure that disease is not present at the prostatic apex. The recommended schedule of imaging for muscle-invasive bladder cancer (CT scan every 3 to 12 months for the first two years) will allow for early detection of recurrence but

longer-term imaging may be needed to detect the complications of urinary diversion, such as urolithiasis, inadequate drainage of continent reservoirs or hydronephrosis due to benign etiologies. Some authors recommend CT scan of the abdomen and pelvis with urography every 2 years following the initial intensive period of cancer surveillance to assess the urinary diversion.

CT can also address benign complications such as alterations in bowel motility, calculi, ureteral strictures, anastomotic leaks, fluid collections (urinoma, abscess, lymphocele, and hematoma), fistulas, and peristomal herniation.²¹⁵ Multidetector CT allows visualization of the anastomosis of the ureters to the urinary diversion as well as the entero-enteric anastomosis (which can be identified by the staple line).

Videos

Presentation Video 1

Presentations

Computed Tomography Presentation 1

References

- 1 Hounsfield GN. Computerized transverse axial scanning (tomography). 1. Description of system. *The British journal of radiology*. 1973;46(552):1016-22.
- 2 Beckmann EC. CT scanning the early days. *The British journal of radiology*. 2006;79(937):5-8.
- 3 Brant WE, Helms CA. Fundamentals of diagnostic radiology. 4th ed. Philadelphia: Wolters Kluwer/Lippincott Williams & Wilkins Health; 2012. p. p.
- 4 Joudi FN, Kuehn DM, Williams RD. Maximizing clinical information obtained by CT. *The Urologic clinics of North America*. 2006;33(3):287-300.
- 5 Erkonen WE, Smith WL. Radiology 101 : the basics and fundamentals of imaging. 3rd ed. Philadelphia: Wolters Kluwer/Lippincott Williams & Wilkins; 2010. vi, 376 p. p.
- 6 Goldman LW. Principles of CT and CT technology. *Journal of nuclear medicine technology*. 2007;35(3):115-28; quiz 29-30.
- 7 Wein AJ, Kavoussi LR, Campbell MF. Campbell-Walsh urology / editor-in-chief, Alan J. Wein ; [editors, Louis R. Kavoussi ... et al.]. 10th ed. Philadelphia, PA: Elsevier Saunders; 2012.

- 8 Madsen MT. The AAPM/RSNA physics tutorial for residents. Introduction to emission CT. Radiographics : a review publication of the Radiological Society of North America, Inc. 1995;15(4):975-91.
- 9 Wang G, Vannier MW. Optimal pitch in spiral computed tomography. Medical physics. 1997;24(10):1635-9.
- 10 Maher MM, Kalra MK, Sahani DV, Perumpillichira JJ, Rizzo S, Saini S, et al. Techniques, clinical applications and limitations of 3D reconstruction in CT of the abdomen. Korean journal of radiology : official journal of the Korean Radiological Society. 2004;5(1):55-67.
- 11 Cody DD. AAPM/RSNA physics tutorial for residents: topics in CT. Image processing in CT. Radiographics : a review publication of the Radiological Society of North America, Inc. 2002;22(5):1255-68.
- 12 Bhalla M, Naidich DP, McGuinness G, Gruden JF, Leitman BS, McCauley DI. Diffuse lung disease: assessment with helical CT--preliminary observations of the role of maximum and minimum intensity projection images. Radiology. 1996;200(2):341-7.
- 13 Coll DM, Herts BR, Davros WJ, Uzzo RG, Novick AC. Preoperative use of 3D volume rendering to demonstrate renal tumors and renal anatomy. Radiographics : a review publication of the Radiological Society of North America, Inc. 2000;20(2):431-8.
- 14 ☆ El Fettouh HA, Herts BR, Nimeh T, Wirth SL, Caplin A, Sands M, et al. Prospective comparison of 3-dimensional volume rendered computerized tomography and conventional renal arteriography for surgical planning in patients undergoing laparoscopic donor nephrectomy. The Journal of urology. 2003;170(1):57-60
- 15 Picchio M, Briganti A, Fanti S, Heidenreich A, Krause BJ, Messa C, et al. The role of choline positron emission tomography/computed tomography in the management of patients with prostate-specific antigen progression after radical treatment of prostate cancer. European urology. 2011;59(1):51-60.
- 16 Bushberg JT. The essential physics of medical imaging. 3rd ed. Philadelphia: Wolters Kluwer Health/Lippincott Williams & Wilkins; 2012. xii, 1030 p. p.
- 17 Al-Shakhrah I A-OT. Common artifacts in computerized tomography: A review. Applied Radiology. 2003;32(8):25-30.
- 18 Barrett JF, Keat N. Artifacts in CT: recognition and avoidance. Radiographics : a review publication of the Radiological Society of North America, Inc. 2004;24(6):1679-91.
- 19 Webb WR, Brant WE, Helms CA. Fundamentals of body CT. 2nd ed. Philadelphia: Saunders; 1998. xii, 363 p. p.

- 20 The 2007 Recommendations of the International Commission on Radiological Protection.
ICRP publication 103. *Annals of the ICRP*. 2007;37(2-4):1-332.
- 21 Brenner DJ, Hall EJ. Computed tomography--an increasing source of radiation exposure. *The New England journal of medicine*. 2007;357(22):2277-84.
- 22 Finnerty M, Brennan PC. Protective aprons in imaging departments: manufacturer stated lead equivalence values require validation. *European radiology*. 2005;15(7):1477-84.
- 23 Lambert K, McKeon T. Inspection of lead aprons: criteria for rejection. *Health physics*. 2001;80(5 Suppl):S67-9.
- 24 Friedman AA, Ghani KR, Peabody JO, Jackson A, Trinh QD, Elder JS. Radiation safety knowledge and practices among urology residents and fellows: results of a nationwide survey. *Journal of surgical education*. 2013;70(2):224-31.
- 25 Cruz-Suarez R, Nosske D, Souza-Santos D. Radiation protection for pregnant workers and their offspring: a recommended approach for monitoring. *Radiation protection dosimetry*. 2011;144(1-4):80-4.
- 26 Brateman L. Radiation safety considerations for diagnostic radiology personnel. *Radiographics : a review publication of the Radiological Society of North America, Inc.* 1999;19(4):1037-55.
- 27 Wagner LK, Lester RG, Saldana LR. Exposure of the pregnant patient to diagnostic radiations : a guide to medical management. 2nd ed. Madison, Wis.: Medical Physics Pub.; 1997. xix, 259 p. p.
- 28 Marx MV, Niklason L, Mauger EA. Occupational radiation exposure to interventional radiologists: a prospective study. *Journal of vascular and interventional radiology : JVIR*. 1992;3(4):597-606.
- 29 Blake ME, Oates ME, Applegate K, Kuligowska E, American Association for Women R, Association of Program Directors in R. Proposed program guidelines for pregnant radiology residents: a project supported by the American Association for Women Radiologists and the Association of Program Directors in Radiology. *Academic radiology*. 2006;13(3):391-401.
- 30 Practice ACoO. ACOG Committee Opinion. Number 299, September 2004. Guidelines for diagnostic imaging during pregnancy. *Obstetrics and gynecology*. 2004;104(3):647-51.
- 31 Kal HB, Struikmans H. [Pregnancy and medical irradiation; summary and conclusions from the International Commission on Radiological Protection, Publication 84]. *Nederlands tijdschrift voor geneeskunde*. 2002;146(7):299-303.
- 32 Osei EK, Faulkner K. Fetal doses from radiological examinations. *The British journal of radiology*. 1999;72(860):773-80.

- 33 Wang PI, Chong ST, Kielar AZ, Kelly AM, Knoepp UD, Mazza MB, et al. Imaging of pregnant and lactating patients: part 1, evidence-based review and recommendations. *AJR American journal of roentgenology*. 2012;198(4):778-84.
- 34 Wagner LK, Applegate KE. Re: More cautions on imaging of pregnant patients. *Radiographics : a review publication of the Radiological Society of North America, Inc.* 2011;31(3):891; author reply -2.
- 35 National Research Council (U.S.). Committee to Assess Health Risks from Exposure to Low Level of Ionizing Radiation. *Health risks from exposure to low levels of ionizing radiation : BEIR VII Phase 2*. Washington, D.C.: National Academies Press; 2006. xvi, 406 p. p.
- 36 Patel SJ, Reede DL, Katz DS, Subramaniam R, Amorosa JK. Imaging the pregnant patient for nonobstetric conditions: algorithms and radiation dose considerations. *Radiographics : a review publication of the Radiological Society of North America, Inc.* 2007;27(6):1705-22.
- 37 Goldberg-Stein S, Liu B, Hahn PF, Lee SI. Body CT during pregnancy: utilization trends, examination indications, and fetal radiation doses. *AJR American journal of roentgenology*. 2011;196(1):146-51.
- 38 Lazarus E, Debenedictis C, North D, Spencer PK, Mayo-Smith WW. Utilization of imaging in pregnant patients: 10-year review of 5270 examinations in 3285 patients--1997-2006. *Radiology*. 2009;251(2):517-24.
- 39 McCollough CH, Schueler BA, Atwell TD, Braun NN, Regner DM, Brown DL, et al. Radiation exposure and pregnancy: when should we be concerned? *Radiographics : a review publication of the Radiological Society of North America, Inc.* 2007;27(4):909-17; discussion 17-8.
- 40 Committee Opinion No. 723: Guidelines for Diagnostic Imaging During Pregnancy and Lactation [published correction appears in *Obstet Gynecol*. 2018 Sep;132(3):786]. *Obstet Gynecol*. 2017;130(4):e210-e216. doi:10.1097/AOG.0000000000002355
- 41 Miglioretti DL, Johnson E, Williams A, Greenlee RT, Weinmann S, Solberg LI, et al. The use of computed tomography in pediatrics and the associated radiation exposure and estimated cancer risk. *JAMA pediatrics*. 2013;167(8):700-7.
- 42 Brenner D, Elliston C, Hall E, Berdon W. Estimated risks of radiation-induced fatal cancer from pediatric CT. *AJR American journal of roentgenology*. 2001;176(2):289-96.
- 43 Frush DP, Donnelly LF, Rosen NS. Computed tomography and radiation risks: what pediatric health care providers should know. *Pediatrics*. 2003;112(4):951-7.
- 44 Slovis TL. Children, computed tomography radiation dose, and the As Low As Reasonably Achievable (ALARA) concept. *Pediatrics*. 2003;112(4):971-2.

- 45 Loughlin KR, Hawtrey CE. Moses Swick, the father of intravenous urography. *Urology*. 2003;62(2):385-9.
- 46 Pasternak JJ, Williamson EE. Clinical pharmacology, uses, and adverse reactions of iodinated contrast agents: a primer for the non-radiologist. *Mayo Clinic proceedings*. 2012;87(4):390-402.
- 47 Brinker JA. Gadzooks, noniodinated contrast? *Catheterization and cardiovascular interventions : official journal of the Society for Cardiac Angiography & Interventions*. 2001;54(1):70-1.
- 48 Spinoza DJ, Angle JF, Hagspiel KD, Hartwell GD, Jenkins AD, Matsumoto AH. Interventional uroradiologic procedures performed using gadodiamide as an alternative to iodinated contrast material. *Cardiovascular and interventional radiology*. 2000;23(1):72-5.
- 49 Sarkis A, Badaoui G, Azar R, Sleilaty G, Bassil R, Jebara VA. Gadolinium-enhanced coronary angiography in patients with impaired renal function. *The American journal of cardiology*. 2003;91(8):974-5, A4.
- 50 Dickinson MC, Kam PC. Intravascular iodinated contrast media and the anaesthetist. *Anaesthesia*. 2008;63(6):626-34.
- 51 Morcos SK, Thomsen HS. Adverse reactions to iodinated contrast media. *European radiology*. 2001;11(7):1267-75.
- 52 Schabelman E, Witting M. The relationship of radiocontrast, iodine, and seafood allergies: a medical myth exposed. *The Journal of emergency medicine*. 2010;39(5):701-7.
- 53 Leung NY, Wai CY, Shu S, Wang J, Kenny TP, Chu KH, et al. Current Immunological and Molecular Biological Perspectives on Seafood Allergy: A Comprehensive Review. *Clinical reviews in allergy & immunology*. 2012.
- 54 Katayama H, Yamaguchi K, Kozuka T, Takashima T, Seez P, Matsuura K. Adverse reactions to ionic and nonionic contrast media. A report from the Japanese Committee on the Safety of Contrast Media. *Radiology*. 1990;175(3):621-8.
- 55 Hartman GW, Hattery RR, Witten DM, Williamson B, Jr. Mortality during excretory urography: Mayo Clinic experience. *AJR American journal of roentgenology*. 1982;139(5):919-22.
- 56 Weese DL, Greenberg HM, Zimmern PE. Contrast media reactions during voiding cystourethrography or retrograde pyelography. *Urology*. 1993;41(1):81-4.
- 57 Kemp SF, Lockey RF, Simons FE, World Allergy Organization ad hoc Committee on Epinephrine in A. Epinephrine: the drug of choice for anaphylaxis. A statement of the World Allergy Organization. *Allergy*. 2008;63(8):1061-70.

- 58 Lasser EC, Berry CC, Talner LB, Santini LC, Lang EK, Gerber FH, et al. Pretreatment with corticosteroids to alleviate reactions to intravenous contrast material. *The New England journal of medicine*. 1987;317(14):845-9.
- 59 Lasser EC, Berry CC, Mishkin MM, Williamson B, Zheutlin N, Silverman JM. Pretreatment with corticosteroids to prevent adverse reactions to nonionic contrast media. *AJR American journal of roentgenology*. 1994;162(3):523-6.
- 60 Greenberger PA, Patterson R. The prevention of immediate generalized reactions to radiocontrast media in high-risk patients. *The Journal of allergy and clinical immunology*. 1991;87(4):867-72.
- 61 Loh S, Bagheri S, Katzberg RW, Fung MA, Li CS. Delayed adverse reaction to contrast-enhanced CT: a prospective single-center study comparison to control group without enhancement. *Radiology*. 2010;255(3):764-71.
- 62 Sutton AG, Finn P, Grech ED, Hall JA, Stewart MJ, Davies A, et al. Early and late reactions after the use of iopamidol 340, ioxaglate 320, and iodixanol 320 in cardiac catheterization. *American heart journal*. 2001;141(4):677-83.
- 63 Mikkonen R, Vehmas T, Granlund H, Kivisaari L. Seasonal variation in the occurrence of late adverse skin reactions to iodine-based contrast media. *Acta radiologica*. 2000;41(4):390-3.
- 64 Hall KA, Wong RW, Hunter GC, Camazine BM, Rappaport WA, Smyth SH, et al. Contrast-induced nephrotoxicity: the effects of vasodilator therapy. *The Journal of surgical research*. 1992;53(4):317-20.
- 65 Goldenberg I, Matetzky S. Nephropathy induced by contrast media: pathogenesis, risk factors and preventive strategies. *CMAJ : Canadian Medical Association journal = journal de l'Association medicale canadienne*. 2005;172(11):1461-71.
- 66 Morcos SK. Contrast-induced nephropathy: are there differences between low osmolar and iso-osmolar iodinated contrast media? *Clinical radiology*. 2009;64(5):468-72.
- 67 Freeman RV, O'Donnell M, Share D, Meengs WL, Kline-Rogers E, Clark VL, et al. Nephropathy requiring dialysis after percutaneous coronary intervention and the critical role of an adjusted contrast dose. *The American journal of cardiology*. 2002;90(10):1068-73.
- 68 Rihal CS, Textor SC, Grill DE, Berger PB, Ting HH, Best PJ, et al. Incidence and prognostic importance of acute renal failure after percutaneous coronary intervention. *Circulation*. 2002;105(19):2259-64.
- 69 Rao QA, Newhouse JH. Risk of nephropathy after intravenous administration of contrast material: a critical literature analysis. *Radiology*. 2006;239(2):392-7.

- 70 Nijssen EC, Rennenberg RJ, Nelemans PJ, et al. Prophylactic hydration to protect renal function from intravascular iodinated contrast material in patients at high risk of contrast-induced nephropathy (AMACING): a prospective, randomised, phase 3, controlled, open-label, non-inferiority trial. Lancet. 2017;389(10076):1312-1322.
doi:10.1016/S0140-6736(17)30057-0
- 71 Kooiman J, Sijpkens YW, van Buren M, et al. Randomised trial of no hydration vs. sodium bicarbonate hydration in patients with chronic kidney disease undergoing acute computed tomography-pulmonary angiography. J Thromb Haemost. 2014;12(10):1658-1666.
doi:10.1111/jth.12701
- 72 Fishbane S. N-acetylcysteine in the prevention of contrast-induced nephropathy. Clinical journal of the American Society of Nephrology : CJASN. 2008;3(1):281-7.
- 73 Kshirsagar AV, Poole C, Mottl A, Shoham D, Franceschini N, Tudor G, et al. N-acetylcysteine for the prevention of radiocontrast induced nephropathy: a meta-analysis of prospective controlled trials. Journal of the American Society of Nephrology : JASN. 2004;15(3):761-9.
- 74 Trivedi H, Daram S, Szabo A, Bartorelli AL, Marenzi G. High-dose N-acetylcysteine for the prevention of contrast-induced nephropathy. The American journal of medicine. 2009;122(9):874 e9-15.
- 75 McDougal WS. Campbell-Walsh urology tenth edition review. Philadelphia, PA: Elsevier/Saunders; 2012. xxxii, 667 p. p.
- 76 Matsuura T, Takase K, Ota H, Yamada T, Sato A, Satoh F, et al. Radiologic anatomy of the right adrenal vein: preliminary experience with MDCT. AJR American journal of roentgenology. 2008;191(2):402-8.
- 77 Ozisik G, Achermann JC, Meeks JJ, Jameson JL. SF1 in the development of the adrenal gland and gonads. Hormone research. 2003;59 Suppl 1:94-8.
- 78 Bernard P, Ludbrook L, Queipo G, Dinulos MB, Kletter GB, Zhang YH, et al. A familial missense mutation in the hinge region of DAX1 associated with late-onset AHC in a prepubertal female. Molecular genetics and metabolism. 2006;88(3):272-9.
- 79 Fu Y, Nie M, Xia WB, Lu L, Mao JF, Pan H, et al. [Clinical features of 9 patients with X-linked adrenal hypoplasia congenita caused by DAX1/NR0B1 gene mutations]. Zhonghua yi xue za zhi. 2010;90(30):2119-22.
- 80 Vachharajani A, Bethin K, Mouillet JF, Sadovsky Y, Saunders S. The rare occurrence of absent adrenals in a term infant: a case report and review of the literature. American journal of perinatology. 2006;23(2):111-4.

- 81 Harinarayana CV, Renu G, Ammini AC, Khurana ML, Ved P, Karmarkar MG, et al. Computed tomography in untreated congenital adrenal hyperplasia. *Pediatric radiology*. 1991;21(2):103-5.
- 82 Falke TH, van Seters AP, Schaberg A, Moolenaar AJ. Computed tomography in untreated adults with virilizing congenital adrenal cortical hyperplasia. *Clinical radiology*. 1986;37(2):155-60.
- 83 Roman S. Adrenocortical carcinoma. *Current opinion in oncology*. 2006;18(1):36-42.
- 84 Ng L, Libertino JM. Adrenocortical carcinoma: diagnosis, evaluation and treatment. *The Journal of urology*. 2003;169(1):5-11.
- 85 Scott DJ, Wallace WH, Hendry GM. With advances in medical imaging can the radiologist reliably diagnose Wilms' tumours? *Clinical radiology*. 1999;54(5):321-7.
- 86 Albregts AE, Cohen MD, Galliani CA. Neuroblastoma invading the kidney. *Journal of pediatric surgery*. 1994;29(7):930-3.
- 87 Dickson PV, Sims TL, Streck CJ, McCarville MB, Santana VM, McGregor LM, et al. Avoiding misdiagnosing neuroblastoma as Wilms tumor. *Journal of pediatric surgery*. 2008;43(6):1159-63.
- 88 Brodeur AE, Brodeur GM. Abdominal masses in children: neuroblastoma, Wilms tumor, and other considerations. *Pediatrics in review / American Academy of Pediatrics*. 1991;12(7):196-207.
- 89 Pizzo PA, Poplack DG. Principles and practice of pediatric oncology. 6th ed. Philadelphia, PA: Wolters Kluwer/Lippincott Williams & Wilkins Health; 2011. xx, 1531 p. p.
- 90 Kloos RT, Gross MD, Francis IR, Korobkin M, Shapiro B. Incidentally discovered adrenal masses. *Endocrine reviews*. 1995;16(4):460-84.
- 91 Young WF, Jr. Clinical practice. The incidentally discovered adrenal mass. *The New England journal of medicine*. 2007;356(6):601-10.
- 92 Dluhy RG. Pheochromocytoma--death of an axiom. *The New England journal of medicine*. 2002;346(19):1486-8.
- 93 Neumann HP, Bausch B, McWhinney SR, Bender BU, Gimm O, Franke G, et al. Germ-line mutations in nonsyndromic pheochromocytoma. *The New England journal of medicine*. 2002;346(19):1459-66.
- 94 Bausch B, Wellner U, Bausch D, Schiavi F, Barontini M, Sanso G, et al. Long-term prognosis of patients with pediatric pheochromocytoma. *Endocrine-related cancer*. 2014;21(1):17-25.

- 95 Motta-Ramirez GA, Remer EM, Herts BR, Gill IS, Hamrahian AH. Comparison of CT findings in symptomatic and incidentally discovered pheochromocytomas. *AJR American journal of roentgenology*. 2005;185(3):684-8.
- 96 Patel J, Davenport MS, Cohan RH, Caoili EM. Can established CT attenuation and washout criteria for adrenal adenoma accurately exclude pheochromocytoma? *AJR American journal of roentgenology*. 2013;201(1):122-7.
- 97 Shawa H, Elsayes KM, Javadi S, Morani A, Williams MD, Lee JE, et al. Adrenal ganglioneuroma: features and outcomes of 27 cases at a referral cancer centre. *Clinical endocrinology*. 2014;80(3):342-7.
- 98 Song JH, Chaudhry FS, Mayo-Smith WW. The incidental adrenal mass on CT: prevalence of adrenal disease in 1,049 consecutive adrenal masses in patients with no known malignancy. *AJR American journal of roentgenology*. 2008;190(5):1163-8.
- 99 Johnson PT, Horton KM, Fishman EK. Adrenal imaging with MDCT: Nonneoplastic disease. *AJR American journal of roentgenology*. 2009;193(4):1128-35.
- 100 Yang ZG, Guo YK, Li Y, Min PQ, Yu JQ, Ma ES. Differentiation between tuberculosis and primary tumors in the adrenal gland: evaluation with contrast-enhanced CT. *European radiology*. 2006;16(9):2031-6.
- 101 Guo YK, Yang ZG, Li Y, Deng YP, Ma ES, Min PQ, et al. Uncommon adrenal masses: CT and MRI features with histopathologic correlation. *European journal of radiology*. 2007;62(3):359-70.
- 102 ☆ Day K, Nikolaidis P, Casalino DD. Adrenal tuberculosis. *The Journal of urology*. 2012;187(1):285-6.
- 103 Ozdemir D, Dagdelen S, Erbas T. Endocrine involvement in systemic amyloidosis. *Endocrine practice : official journal of the American College of Endocrinology and the American Association of Clinical Endocrinologists*. 2010;16(6):1056-63.
- 104 Lachmann HJ, Goodman HJ, Gilbertson JA, Gallimore JR, Sabin CA, Gillmore JD, et al. Natural history and outcome in systemic AA amyloidosis. *The New England journal of medicine*. 2007;356(23):2361-71.
- 105 Delanaye P, Krzesinski JM. Massive renal and adrenal calcifications in a young dialysis patient with familial Mediterranean fever. *Nephrology, dialysis, transplantation : official publication of the European Dialysis and Transplant Association - European Renal Association*. 2005;20(1):238.

- 106 Koene RJ, Catanese J, Sarosi GA. Adrenal hypofunction from histoplasmosis: a literature review from 1971 to 2012. *Infection*. 2013;41(4):757-9.
- 107 Matsuda Y, Kawate H, Okishige Y, Abe I, Adachi M, Ohnaka K, et al. Successful management of cryptococcosis of the bilateral adrenal glands and liver by unilateral adrenalectomy with antifungal agents: a case report. *BMC infectious diseases*. 2011;11:340.
- 108 Jordan E, Poder L, Courtier J, Sai V, Jung A, Coakley FV. Imaging of nontraumatic adrenal hemorrhage. *AJR American journal of roentgenology*. 2012;199(1):W91-8.
- 109 Lau H, Lo CY, Lam KY. Surgical implications of underestimation of adrenal tumour size by computed tomography. *The British journal of surgery*. 1999;86(3):385-7.
- 110 Bulow B, Jansson S, Juhlin C, Steen L, Thoren M, Wahrenberg H, et al. Adrenal incidentaloma - follow-up results from a Swedish prospective study. *European journal of endocrinology / European Federation of Endocrine Societies*. 2006;154(3):419-23.
- 111 Grumbach MM, Biller BM, Braunstein GD, Campbell KK, Carney JA, Godley PA, et al. Management of the clinically inapparent adrenal mass ("incidentaloma"). *Annals of internal medicine*. 2003;138(5):424-9.
- 112 Hamrahan AH, Ioachimescu AG, Remer EM, Motta-Ramirez G, Bogabathina H, Levin HS, et al. Clinical utility of noncontrast computed tomography attenuation value (hounsfield units) to differentiate adrenal adenomas/hyperplasias from nonadenomas: Cleveland Clinic experience. *The Journal of clinical endocrinology and metabolism*. 2005;90(2):871-7.
- 113 Korobkin M, Brodeur FJ, Francis IR, Quint LE, Dunnick NR, Lonyd F. CT time-attenuation washout curves of adrenal adenomas and nonadenomas. *AJR American journal of roentgenology*. 1998;170(3):747-52.
- 114 Pena CS, Boland GW, Hahn PF, Lee MJ, Mueller PR. Characterization of indeterminate (lipid-poor) adrenal masses: use of washout characteristics at contrast-enhanced CT. *Radiology*. 2000;217(3):798-802.
- 115 Boland GW, Lee MJ, Gazelle GS, Halpern EF, McNicholas MM, Mueller PR. Characterization of adrenal masses using unenhanced CT: an analysis of the CT literature. *AJR American journal of roentgenology*. 1998;171(1):201-4.
- 116 Low G, Dhliwayo H, Lomas DJ. Adrenal neoplasms. *Clinical radiology*. 2012;67(10):988-1000.
- 117 Quayle FJ, Spitzer JA, Pierce RA, Lairmore TC, Moley JF, Brunt LM. Needle biopsy of incidentally discovered adrenal masses is rarely informative and potentially hazardous. *Surgery*. 2007;142(4):497-502; discussion -4.

- 118 Mazzaglia PJ, Monchik JM. Limited value of adrenal biopsy in the evaluation of adrenal neoplasm: a decade of experience. *Archives of surgery*. 2009;144(5):465-70.
- 119 Dunnick NR. Renal transplantation. *Textbook of Uroradiology*. 4th ed. Philadelphia, PA: Lippincott Williams & Wilkins; 2008. p. 229-45.
- 120 S R. Renal parenchymal disease, including renal failure, renovascular disease, and transplantation. *Grainger & Allison's Diagnostic Radiology*. 2. 5 ed2008.
- 121 Singh AK, Sahani DV. Imaging of the renal donor and transplant recipient. *Radiologic clinics of North America*. 2008;46(1):79-93, vi.
- 122 Dunnick NR. Vascular diseases. *Textbook of Uroradiology*. 4th ed. Philadelphia, PA: Lippincott Williams & Wilkins; 2008. p. p.186-202.
- 123 Dunnick NR. Congenital anomalies. *Textbook of Uroradiology*. 4th ed. Philadelphia, PA: Lippincott Williams & Wilkins; 2008. p. p.14-29.
- 124 Dunnick NR. Renal cystic disease. *Textbook of Uroradiology*. 4th ed. Philadelphia, PA: Lippincott Williams & Wilkins; 2008. p. p.113-33.
- 125 Bosniak MA. Diagnosis and management of patients with complicated cystic lesions of the kidney. *AJR American journal of roentgenology*. 1997;169(3):819-21.
- 126 Israel GM, Bosniak MA. An update of the Bosniak renal cyst classification system. *Urology*. 2005;66(3):484-8.
- 127 ☆ Campbell S, Uzzo RG, Allaf ME et al: Renal mass and localized renal cancer: AUA guideline. *J Urol* 2017; 198: 520.
- 128 Rottenberg S RS. Renal masses. *Grainger & Allison's Diagnostic Radiology*. 1. 5 ed2008.
- 129 Ananthakrishnan L HB, Simmons MN, Campbell SC Imaging of the common benign disorders of the urinary tract: urolithiasis and renal infections. *AUA Update Series*. 262007. p. 396-8.
- 130 Rottenberg S SS. Radiology of the upper urinary tract. *Grainger & Allison's Diagnostic Radiology*. 1. 5 ed2008.
- 131 Dunnick NR. Renal inflammatory disease. *Textbook of Uroradiology*. 4th ed. Philadelphia, PA: Lippincott Williams & Wilkins; 2008. p. p.165-85.
- 132 Dunnick NR. Urinary tract trauma. *Textbook of Uroradiology*. 4th ed. Philadelphia, PA: Lippincott Williams & Wilkins; 2008. p. 382-93.

- 133 Jankowski JT, Spirnak JP. Current recommendations for imaging in the management of urologic traumas. *The Urologic clinics of North America*. 2006;33(3):365-76.
- 134 Grosjean R, Daudon M, Chammas MF, Jr., Claudon M, Eschwege P, Felblinger J, et al. Pitfalls in urinary stone identification using CT attenuation values: are we getting the same information on different scanner models? *European journal of radiology*. 2013;82(8):1201-6.
- 135 Kenney PJ. CT evaluation of urinary lithiasis. *Radiologic clinics of North America*. 2003;41(5):979-99.
- 136 Park S, Pearle MS. Imaging for percutaneous renal access and management of renal calculi. *The Urologic clinics of North America*. 2006;33(3):353-64.
- 137 Hong SH, Kim KA, Woo OH, Park CM, Kim CH, Kim MJ, et al. Dedifferentiated liposarcoma of retroperitoneum: spectrum of imaging findings in 15 patients. *Clinical imaging*. 2010;34(3):203-10.
- 138 Eken A, Alma E. Emphysematous cystitis: The role of CT imaging and appropriate treatment. *Canadian Urological Association journal = Journal de l'Association des urologues du Canada*. 2013;7(11-12):E754-6.
- 139 Chang SD HH. Radiological evaluation of the urinary bladder, prostate and urethra. *Grainger & Allison's Diagnostic Radiology*. 1. 5 ed2008.
- 140 Hafeez S, Huddart R. Advances in bladder cancer imaging. *BMC medicine*. 2013;11:104.
- 141 Ishak C, Kanth N. Bladder trauma: multidetector computed tomography cystography. *Emergency radiology*. 2011;18(4):321-7.
- 142 Hoffelt SC, Marshall LM, Garzotto M, Hung A, Holland J, Beer TM. A comparison of CT scan to transrectal ultrasound-measured prostate volume in untreated prostate cancer. *International journal of radiation oncology, biology, physics*. 2003;57(1):29-32.
- 143 Sharp VJ, Takacs EB, Powell CR. Prostatitis: diagnosis and treatment. *American family physician*. 2010;82(4):397-406.
- 144 Chia JK, Longfield RN, Cook DH, Flax BL. Computed axial tomography in the early diagnosis of prostatic abscess. *The American journal of medicine*. 1986;81(5):942-4.
- 145 Thornhill BA, Morehouse HT, Coleman P, Hoffman-Tretin JC. Prostatic abscess: CT and sonographic findings. *AJR American journal of roentgenology*. 1987;148(5):899-900.
- 146 Schwartz JM, Bosniak MA, Hulnick DH, Megibow AJ, Raghavendra BN. Computed tomography of midline cysts of the prostate. *Journal of computer assisted tomography*. 1988;12(2):215-8.

- 147 ☆ Galosi AB, Montironi R, Fabiani A, Lacetera V, Galle G, Muzzonigro G. Cystic lesions of the prostate gland: an ultrasound classification with pathological correlation. *The Journal of urology*. 2009;181(2):647-57.
- 148 Lee JY, Kang DH, Park HY, Park JS, Son YW, Moon HS, et al. An anteriorly positioned midline prostatic cyst resulting in lower urinary tract symptoms. *International neurourology journal*. 2010;14(2):125-9.
- 149 Curran S, Akin O, Agildere AM, Zhang J, Hricak H, Rademaker J. Endorectal MRI of prostatic and periprostatic cystic lesions and their mimics. *AJR American journal of roentgenology*. 2007;188(5):1373-9.
- 150 Godara R, Garg P, Karwasra RK. Prostatic calculi--a diagnostic dilemma. *Tropical doctor*. 2003;33(2):105.
- 151 Sfanos KS, Wilson BA, De Marzo AM, Isaacs WB. Acute inflammatory proteins constitute the organic matrix of prostatic corpora amylacea and calculi in men with prostate cancer. *Proceedings of the National Academy of Sciences of the United States of America*. 2009;106(9):3443-8.
- 152 ☆ Wolf JS, Jr., Cher M, Dall'era M, Presti JC, Jr., Hricak H, Carroll PR. The use and accuracy of cross-sectional imaging and fine needle aspiration cytology for detection of pelvic lymph node metastases before radical prostatectomy. *The Journal of urology*. 1995;153(3 Pt 2):993-9.
- 153 Roach M, 3rd, Faillace-Akazawa P, Malfatti C, Holland J, Hricak H. Prostate volumes defined by magnetic resonance imaging and computerized tomographic scans for three-dimensional conformal radiotherapy. *International journal of radiation oncology, biology, physics*. 1996;35(5):1011-8.
- 154 ☆ Albertsen PC, Hanley JA, Harlan LC, Gilliland FD, Hamilton A, Liff JM, et al. The positive yield of imaging studies in the evaluation of men with newly diagnosed prostate cancer: a population based analysis. *The Journal of urology*. 2000;163(4):1138-43.
- 155 Mohler, J. L., E. S. Antonarakis, A. J. Armstrong, A. V. D'Amico, B. J. Davis, T. Dorff, et al. 2019. 'Prostate Cancer, Version 2.2019, NCCN Clinical Practice Guidelines in Oncology', *J Natl Compr Canc Netw*, 17: 479-505.
- 156 Kobayashi T, Kamoto T, Sugino Y, Takeuchi H, Habuchi T, Ogawa O. High incidence of urinary bladder involvement in carcinomas of the sigmoid and rectum: a retrospective review of 580 patients with colorectal carcinoma. *Journal of surgical oncology*. 2003;84(4):209-14.

- 157 McCallum T, Milunsky J, Munarriz R, Carson R, Sadeghi-Nejad H, Oates R. Unilateral renal agenesis associated with congenital bilateral absence of the vas deferens: phenotypic findings and genetic considerations. *Hum Reprod.* 2001;16(2):282-8.
- 158 Wu HF, Qiao D, Qian LX, Song NH, Feng NH, Hua LX, et al. Congenital agenesis of seminal vesicle. *Asian journal of andrology.* 2005;7(4):449-52.
- 159 Dohle GR, Veeze HJ, Overbeek SE, van den Ouweleen AM, Halley DJ, Weber RF, et al. The complex relationships between cystic fibrosis and congenital bilateral absence of the vas deferens: clinical, electrophysiological and genetic data. *Hum Reprod.* 1999;14(2):371-4.
- 160 Kenney PJ, Leeson MD. Congenital anomalies of the seminal vesicles: spectrum of computed tomographic findings. *Radiology.* 1983;149(1):247-51.
- 161 Arora SS, Breiman RS, Webb EM, Westphalen AC, Yeh BM, Coakley FV. CT and MRI of congenital anomalies of the seminal vesicles. *AJR American journal of roentgenology.* 2007;189(1):130-5.
- 162 ☆ Beeby DI. Seminal vesicle cyst associated with ipsilateral renal agenesis: case report and review of literature. *The Journal of urology.* 1974;112(1):120-2.
- 163 Rappe BJ, Meuleman EJ, Debruyne FM. Seminal vesicle cyst with ipsilateral renal agenesis. *Urologia internationalis.* 1993;50(1):54-6.
- 164 Livingston L, Larsen CR. Seminal vesicle cyst with ipsilateral renal agenesis. *AJR American journal of roentgenology.* 2000;175(1):177-80.
- 165 Vohra S, Morgentaler A. Congenital anomalies of the vas deferens, epididymis, and seminal vesicles. *Urology.* 1997;49(3):313-21.
- 166 Matsuki M, Matsuo M, Kaji Y, Okada N. Ectopic ureter draining into seminal vesicle cyst: usefulness of MRI. *Radiation medicine.* 1998;16(4):309-11.
- 167 Steffens J, Oberschulte-Beckmann D, Siller V, Rottger P, Polsky MS. Ectopic refluxing ureter entering a seminal vesicle cyst associated with ipsilateral renal dysplasia. *World journal of urology.* 2000;18(3):232-4.
- 168 Schwartz ML, Kenney PJ, Bueschen AJ. Computed tomographic diagnosis of ectopic ureter with seminal vesicle cyst. *Urology.* 1988;31(1):55-6.
- 169 Papathanasiou A, Voulgaris S, Salpiggidis G, Charalabous S, Fatles G, Rombis V. Hydatid cyst of the seminal vesicle. *International journal of urology : official journal of the Japanese Urological Association.* 2006;13(3):308-10.

- 170 Passomenos D, Dalamarinis C, Antonopoulos P, Sklavos H. Seminal vesicle hydatid cysts: CT features in two patients. *AJR American journal of roentgenology*. 2004;182(4):1089-90.
- 171 Fenton LZ, McCabe KJ. Giant unilateral abdominoscrotal hydrocele. *Pediatric radiology*. 2002;32(12):882-4.
- 172 Osband AJ, Laskow DA. Spermatocele following kidney transplant. *American journal of transplantation : official journal of the American Society of Transplantation and the American Society of Transplant Surgeons*. 2012;12(7):1936-7.
- 173 Skinner DG, Pritchett TR, Lieskovsky G, Boyd SD, Stiles QR. Vena caval involvement by renal cell carcinoma. Surgical resection provides meaningful long-term survival. *Annals of surgery*. 1989;210(3):387-92; discussion 92-4.
- 174 Ljungberg B, Cowan NC, Hanbury DC, Hora M, Kuczyk MA, Merseburger AS, et al. EAU guidelines on renal cell carcinoma: the 2010 update. *Eur Urol*. 2010;58(3):398-406.
- 175 Lonser RR, Glenn GM, Walther M, Chew EY, Libutti SK, Linehan WM, et al. von Hippel-Lindau disease. *Lancet*. 2003;361(9374):2059-67.
- 176 Mathur A, Manish A, Maletha M, Luthra NB. Emphysematous epididymo-orchitis: A rare entity. *Indian journal of urology : IJU : journal of the Urological Society of India*. 2011;27(3):399-400.
- 177 Levenson RB, Singh AK, Novelline RA. Fournier gangrene: role of imaging. *Radiographics : a review publication of the Radiological Society of North America, Inc*. 2008;28(2):519-28.
- 178 Amendola MA, Casillas J, Joseph R, Antun R, Galindez O. Fournier's gangrene: CT findings. *Abdominal imaging*. 1994;19(5):471-4.
- 179 Rajan DK, Scharer KA. Radiology of Fournier's gangrene. *AJR American journal of roentgenology*. 1998;170(1):163-8.
- 180 Howell EC, Keeley JA, Kaji AH, Deane MR, Kim DY, Putnam B, Lee SL, Woods AL, Neville AL. Chance to cut: defining a negative exploration rate in patients with suspected necrotizing soft tissue infection. *Trauma Surg Acute Care Open*. 2019 Feb 27;4(1):e000264. doi: 10.1136/tsaco-2018-000264. PMID: 30899795; PMCID: PMC6407535.
- 181 Zacharias N, Velmahos GC, Salama A, et al. Diagnosis of Necrotizing Soft Tissue Infections by Computed Tomography. *Arch Surg*. 2010;145(5):452–455. doi:10.1001/archsurg.2010.50
- 182 Motzer RJ, Agarwal N, Beard C, Bolger GB, Boston B, Carducci MA, et al. NCCN clinical practice guidelines in oncology: kidney cancer. *Journal of the National Comprehensive Cancer Network : JNCCN*. 2009;7(6):618-30.

- 183 Leibovitch L, Foster RS, Kopecky KK, Donohue JP. Improved accuracy of computerized tomography based clinical staging in low stage nonseminomatous germ cell cancer using size criteria of retroperitoneal lymph nodes. *The Journal of urology*. 1995;154(5):1759-63.
- 184 ☆ See WA, Hoxie L. Chest staging in testis cancer patients: imaging modality selection based upon risk assessment as determined by abdominal computerized tomography scan results. *The Journal of urology*. 1993;150(3):874-8.
- 185 Ezra N, Afari A, Wong J. Pelvic and scrotal trauma: CT and triage of patients. *Abdominal imaging*. 2009;34(4):541-4.
- 186 Ko SF, Ng SH, Wan YL, Huang CC, Lee TY, Kung CT, et al. Testicular dislocation: an uncommon and easily overlooked complication of blunt abdominal trauma. *Annals of emergency medicine*. 2004;43(3):371-5.
- 187 Waldert M, Klatte T, Schmidbauer J, Remzi M, Lackner J, Marberger M. Color Doppler sonography reliably identifies testicular torsion in boys. *Urology*. 2010;75(5):1170-4.
- 188 Watanabe Y, Dohke M, Ohkubo K, Ishimori T, Amoh Y, Okumura A, et al. Scrotal disorders: evaluation of testicular enhancement patterns at dynamic contrast-enhanced subtraction MR imaging. *Radiology*. 2000;217(1):219-27.
- 189 Ovali GY, Yilmaz O, Tarhan S, Genc A, Demireli P, Tuncyurek O, et al. Perfusion CT evaluation in experimentally induced testicular torsion. *Canadian Urological Association journal = Journal de l'Association des urologues du Canada*. 2009;3(5):383-6.
- 190 Farhat WA. Perfusion CT evaluation in experimentally induced testicular torsion: proceed with caution. *Canadian Urological Association journal = Journal de l'Association des urologues du Canada*. 2009;3(5):387.
- 191 D'Andrea A, Coppolino F, Cesarano E, Russo A, Cappabianca S, Genovese EA, et al. US in the assessment of acute scrotum. *Critical ultrasound journal*. 2013;5 Suppl 1:S8.
- 192 Wolverson MK, Houttuin E, Heiberg E, Sundaram M, Shields JB. Comparison of computed tomography with high-resolution real-time ultrasound in the localization of the impalpable undescended testis. *Radiology*. 1983;146(1):133-6.
- 193 Kawashima A, Sandler CM, Wasserman NF, LeRoy AJ, King BF, Jr., Goldman SM. Imaging of urethral disease: a pictorial review. *Radiographics : a review publication of the Radiological Society of North America, Inc*. 2004;24 Suppl 1:S195-216.
- 194 Ali M, Safriel Y, Sclafani SJ, Schulze R. CT signs of urethral injury. *Radiographics : a review publication of the Radiological Society of North America, Inc*. 2003;23(4):951-63; discussion 63-6.

- 195 ☆ Goldman SM, Sandler CM, Corriere JN, Jr., McGuire EJ. Blunt urethral trauma: a unified, anatomical mechanical classification. *The Journal of urology*. 1997;157(1):85-9.
- 196 Pavlica P, Menchi I, Barozzi L. New imaging of the anterior male urethra. *Abdominal imaging*. 2003;28(2):180-6.
- 197 Chou CP, Huang JS, Wu MT, Pan HB, Huang FD, Yu CC, et al. CT voiding urethrography and virtual urethroscopy: preliminary study with 16-MDCT. *AJR American journal of roentgenology*. 2005;184(6):1882-8.
- 198 Clark PE, Spiess PE, Agarwal N, Biagioli MC, Eisenberger MA, Greenberg RE, et al. Penile cancer: Clinical Practice Guidelines in Oncology. *Journal of the National Comprehensive Cancer Network : JNCCN*. 2013;11(5):594-615.
- 199 Leijte JA, Kirrander P, Antonini N, Windahl T, Horenblas S. Recurrence patterns of squamous cell carcinoma of the penis: recommendations for follow-up based on a two-centre analysis of 700 patients. *European urology*. 2008;54(1):161-8.
- 200 Spiess PE. New treatment guidelines for penile cancer. *Journal of the National Comprehensive Cancer Network : JNCCN*. 2013;11(5 Suppl):659-62.
- 201 Gakis G, Witjes JA, Comperat E, Cowan NC, De Santis M, Lebret T, et al. EAU guidelines on primary urethral carcinoma. *European urology*. 2013;64(5):823-30.
- 202 Caoili EM, Korobkin M, Francis IR, Cohan RH, Platt JF, Dunnick NR, et al. Adrenal masses: characterization with combined unenhanced and delayed enhanced CT. *Radiology*. 2002;222(3):629-33.
- 203 Clark OH, Benson AB, 3rd, Berlin JD, Choti MA, Doherty GM, Engstrom PF, et al. NCCN Clinical Practice Guidelines in Oncology: neuroendocrine tumors. *Journal of the National Comprehensive Cancer Network : JNCCN*. 2009;7(7):712-47.
- 204 Hollingsworth JM, Miller DC, Daignault S, Hollenbeck BK. Rising incidence of small renal masses: a need to reassess treatment effect. *J Natl Cancer Inst*. 2006;98(18):1331-4.
- 205 Rais-Bahrami S, Guzzo TJ, Jarrett TW, Kavoussi LR, Allaf ME. Incidentally discovered renal masses: oncological and perioperative outcomes in patients with delayed surgical intervention. *BJU international*. 2009;103(10):1355-8.
- 206 Eggner SE, Yossepowitch O, Pettus JA, Snyder ME, Motzer RJ, Russo P. Renal cell carcinoma recurrence after nephrectomy for localized disease: predicting survival from time of recurrence. *Journal of clinical oncology : official journal of the American Society of Clinical Oncology*. 2006;24(19):3101-6.

- 207 Martin JM, Panzarella T, Zwahlen DR, Chung P, Warde P. Evidence-based guidelines for following stage 1 seminoma. *Cancer*. 2007;109(11):2248-56.
- 208 Cafferty FH, Gabe R, Huddart RA, Rustin G, Williams MP, Stenning SP, et al. UK management practices in stage I seminoma and the Medical Research Council Trial of Imaging and Schedule in Seminoma Testis managed with surveillance. *Clin Oncol (R Coll Radiol)*. 2012;24(1):25-9.
- 209 Mead GM, Fossa SD, Oliver RT, Joffe JK, Huddart RA, Roberts JT, et al. Randomized trials in 2466 patients with stage I seminoma: patterns of relapse and follow-up. *Journal of the National Cancer Institute*. 2011;103(3):241-9.
- 210 Classen J, Schmidberger H, Meisner C, Souchon R, Sautter-Bihl ML, Sauer R, et al. Radiotherapy for stages IIA/B testicular seminoma: final report of a prospective multicenter clinical trial. *Journal of clinical oncology : official journal of the American Society of Clinical Oncology*. 2003;21(6):1101-6.
- 211 Oldenburg J, Fossa SD, Nuver J, Heidenreich A, Schmoll HJ, Bokemeyer C, et al. Testicular seminoma and non-seminoma: ESMO Clinical Practice Guidelines for diagnosis, treatment and follow-up. *Annals of oncology : official journal of the European Society for Medical Oncology / ESMO*. 2013;24 Suppl 6:vi125-32.
- 212 ☆ Brausi M, Witjes JA, Lamm D, Persad R, Palou J, Colombel M, et al. A review of current guidelines and best practice recommendations for the management of nonmuscle invasive bladder cancer by the International Bladder Cancer Group. *The Journal of urology*. 2011;186(6):2158-67.
- 213 Witjes JA, Comperat E, Cowan NC, De Santis M, Gakis G, Lebret T, et al. EAU Guidelines on Muscle-invasive and Metastatic Bladder Cancer: Summary of the 2013 Guidelines. *European urology*. 2013.
- 214 Cagiannos I, Morash C. Surveillance strategies after definitive therapy of invasive bladder cancer. *Canadian Urological Association journal = Journal de l'Association des urologues du Canada*. 2009;3(6 Suppl 4):S237-42.
- 215 Catala V, Sola M, Samaniego J, Marti T, Huguet J, Palou J, et al. CT findings in urinary diversion after radical cystectomy: postsurgical anatomy and complications. *Radiographics : a review publication of the Radiological Society of North America, Inc.* 2009;29(2):461-76.